Luminophores based on 2*H*-1,2,3-triazoles: synthesis, photophysical properties, and application prospects

Igor A. Lavrinchenko,[a] ● **Timofey D. Moseev,**[a] ● **Mikhail V. Varaksin,**[a,b]* ●
Valery N. Charushin,[a,b]* ● **Oleg N. Chupakhin**[a,b] ●
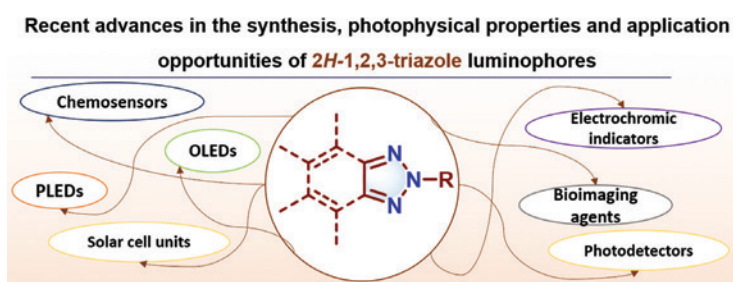
[a] *Ural Federal University named after the First President of Russia B.N.Yeltsin,*
 620062 Ekaterinburg, Russia
[b] *I.Ya.Postovsky Institute of Organic Synthesis, Ural Branch of the Russian Academy of Sciences,*
 620990 Ekaterinburg, Russia

The review systematizes the data on the synthesis of 2*H*-1,2,3-triazole-based luminophores published between 2005 and the beginning of 2024. The benefits and limitations of the described synthetic strategies are revealed. The possibilities and prospects for the practical applications of these molecular systems as chemosensors for pH and metal ion determination, bioimaging agents, and working elements of molecular electronic devices (organic light emitting diodes, organic field-effect transistors, *etc*.) are discussed. The bibliography includes 84 references.

The bibliography includes 84 references.

Keywords: triazoles, luminophores, photodetectors, organic light-emitting diodes, chemosensors, bioimaging.

Recent advances in the synthesis, photophysical properties and application opportunities of 2,3-triazole luminophores

Contents

1. Introduction

Today, the development of optical functional materials is a rapidly upcoming area of modern organic chemistry and related fields of science. Photoactive molecular systems are used as chemosensors, compounds for bioimaging and photodynamic therapy, organic light emitting diodes (OLEDs), organic field-effect transistors (OFETs), organic semiconductors, and other materials for molecular electronics.[1–5]

Compounds that possess promising photophysical properties can be obtained from either acenes (naphthalene, pyrene, *etc*.) or heterocyclic systems (azoles, azines, thiophenes, *etc*.).

I.A.Lavrinchenko. Post-graduate Student, Research Engineer at the Department of Organic and Biomolecular Chemistry of the Institute of Chemical Engineering, UrFU.
E-mail*:* Igor.lavrinchenko@urfu.ru
Current research interests: heterocyclic compounds, fluorophores, organic electronics, chemosensors, bioimaging.
T.D.Moseev. PhD, Associate Professor at the Scientific, Education, and Innovation Centre for Chemical and Pharmaceutical Technologies of the Institute of Chemical Engineering, UrFU.
E-mail: timofey.moseev@urfu.ru
Current research interests: C–H-functionalization, green chemistry, organofluorine compounds, fluorophores, organic electronics.
M.V.Varaksin. Doctor of Chemical Sciences, Professor of the Department of Organic and Biomolecular Chemistry, Director of the Institute of Chemical Engineering, UrFU, Researcher at the Laboratory of Coordination Compounds of IOS UB RAS.
E-mail: m.v.varaksin@urfu.ru
Current research interests: C–H-functionalization, green chemistry, heterocyclic compounds, functional materials, organic electronics, medicinal chemistry.

V.N.Charushin. Academician of RAS, Doctor of Chemical Sciences, Professor at the Department of Organic and Biomolecular Chemistry of the Institute of Chemical Engineering, UrFU, Chief Researcher at IOS UB RAS. E-mail: charushin@ios.uran.ru
Current research interests: C–H-functionalization of (hetero)arenes free from metal catalysts, PASE methods in the synthesis of aza-heterocycles, biologically active compounds, medicinal chemistry, luminophores.
O.N.Chupakhin. Academician of RAS, Doctor of Chemical Sciences, Professor at the Department of Organic and Biomolecular Chemistry of the Institute of Chemical Engineering, UrFU, Head of the Laboratory of Coordination Compounds of IOS UB RAS.
E-mail: o.n.chupakhin@urfu.ru
Current research interests: nucleophilic substitution of hydrogen, C–H-functionalization of (hetero)arenes free from metal catalysts, one-step regioselective methods for the construction of complex heterocyclic structures, chemistry of fluorine-containing compounds, chemical aspects of environmental protection, biologically active compounds, medicinal chemistry.
Translation: Z.P.Svitanko

Heterocyclic compounds are of particular interest for the development of novel materials, since the introduction of heteroatoms affects the electronic structure of the molecule and crystal packing; this may give rise to valuable properties, and, hence, to expand the scope of practical applicability. In addition, in most cases, heterocyclic moieties increase the affinity of compounds to biological targets and also open wide possibilities for further modification.[6,7]

1,2,3-Triazoles are photoactive compounds that give rise to two types of structures, namely, 1*H*- and 2*H*-functionalized 1,2,3-triazoles. 2*H*-1,2,3-Triazoles are used most often for the design of advanced materials, owing to their linear structure and conjugation, while 1*H*-triazoles are more popular as biologically active compounds.[8,9]

The first mention[10] on the synthesis of 2*H*-1,2,3-triazoles dates back to 1921 (Fig. 1); however, their photophysical properties were described only 84 years later (see below). Since 2008, studies of luminescent chemosensors based on 2*H*-1,2,3-triazoles for detection of cations, anions, and nitroarenes have been rapidly developing. Further insight into this class of compounds resulted in the design of the first organic (OLEDs) and polymer (PLEDs) light-emitting diodes. By the end of the second decade of the 21st century and until now, 2*H*-1,2,3-triazoles have been widely used for bioimaging and photodynamic therapy, and as active elements of photodetectors.

Figure 2 shows examples of functional materials containing a 2*H*-functionalized 1,2,3-triazole moiety that are now actively studied as chemosensors for fluorescent pH determination,[11] reagents for metal ion detection,[12] OLED components,[13] medications for the treatment of various diseases,[14,15] or diagnostic agents for bioimaging of cancer cells, fatty degeneration of cells, heart contraction, *etc*.

Diverse 2*H*-1,2,3-triazoles are synthesized using reactions of hydrazines with nitrogen-containing compounds, reactions of aromatic substrates with diazonium salts, arylation, cyclization of substituted alkynes with azides, and various types of cross-coupling. There are a few reviews[16-21] addressing the synthesis and biological properties of 2*H*-functionalized 1,2,3-triazoles, but they do not include data on the methods for the synthesis of these compounds for the use as functional optical materials. The present review summarizes the data published in the period from 2005 to the beginning of 2024 describing the known methods for the synthesis of luminophores based on 2*H*-1,2,3-triazoles, in particular 2*H*-aryl-substituted, benzo- and heteroannulated derivatives, their luminescent properties, and prospects for practical application.

## 2. Features of the electronic structure of 2*H*-1,2,3-triazoles

1,2,3-Triazole, a five-membered heterocycle composed of three nitrogen atoms and two carbon atoms, has a ring system of 6π-electrons and two multiple bonds in the molecule. Two triazole nitrogen atoms can be referred to the pyridine type and the third nitrogen can be classified as a pyrrole type. All 1,2,3-triazole atoms are sp²-hybridized, with π-electrons being in conjugation; therefore, the heterocycle is aromatic. There can be 2*H*-, 4*H*-, and 1*H*-1,2,3-triazoles, which are tautomers. 2*H*-1,2,3-Triazoles are used most widely for the design of functional optical materials (Fig. 3). Meanwhile, 1*H*-1,2,3-triazoles possess various types of biological activity and have found use as antifungal, antiviral, and other agents. Finally, 4*H*-1,2,3-triazole is not aromatic and has no stable forms.[22]

The pyridine type nitrogens are highlighted in red and pyrrole nitrogens are blue.

Among five-membered nitrogen-containing heterocycles, 1,2,3-triazole has one of the highest ionization energies, which vary in the following series: imidazole (8.78 eV), pyrazole (9.15 eV), 1,2,4-triazole (10.00 eV), 1,2,3-triazole (10.06 eV), and tetrazole (11.30 eV). In addition, 1,2,3-triazole has clear-cut acidic properties (pK_a = 9.4), especially in comparison with
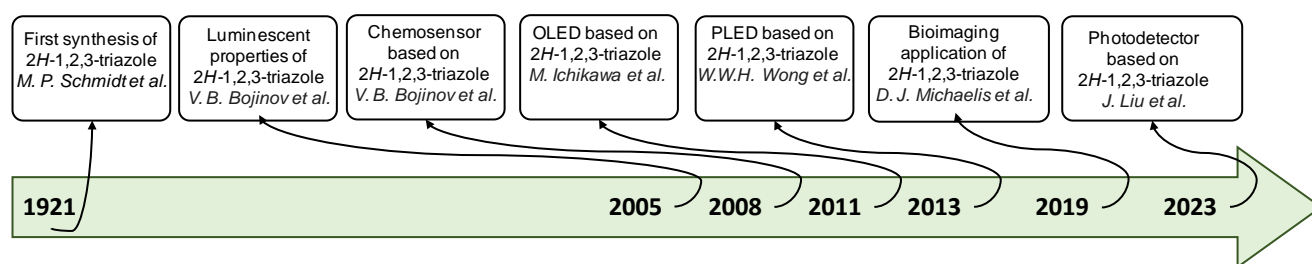
Figure 1. Retrospective of the stages of appearance of functional materials based on 2*H*-1,2,3-triazoles.
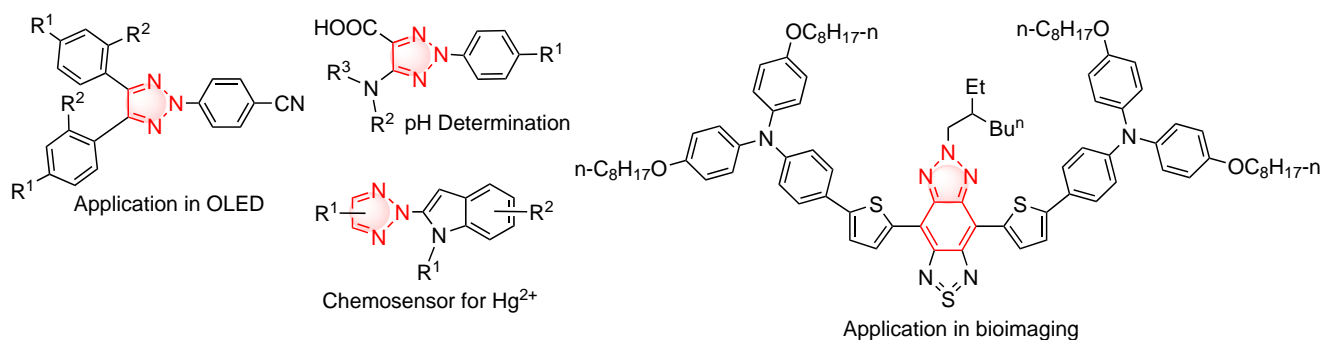
Figure 2. Structures of compounds containing a 2*H*-functionalized 1,2,3-triazole moiety used to design functional materials for various purposes.

I.A.Lavrinchenko, T.D.Moseev, M.V.Varaksin, V.N.Charushin, O.N.Chupakhin
Russ. Chem. Rev., 2024, **93** (10) RCR5130

3 of 34
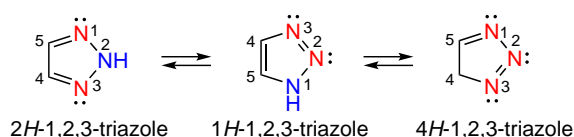
**Figure 3.** Structures of 2*H*-, 1*H*-, and 4*H*-1,2,3-triazoles.

1,2,4-triazole, pyrazole, or imidazole, the pK_a values of which are 10.3, 11.5, and 14.9.[23]

3. 2*H*-Aryl-1,2,3-triazoles

This Section addresses the key preparation methods and properties of 2*H*-substituted 1,2,3-triazoles containing different functional groups at carbon atoms in positions 4 and 5.

Benassi, Belskaya, and co-workers[24] developed a series of 5-amino-2-aryl-1,2,3-triazole derivatives. The target fluorophores **4** were prepared by the reaction of secondary amines **2** with arylhydrazononitriles **1** followed by cyclization of intermediates **3** in the presence of copper acetate [Scheme 1; the maximum absorption (λ_{abs}) and emission (λ_{em}) wavelengths in the electronic spectra and the quantum yields (QY) are given below the structures].[†] These fluorophores show emission in the 410 to 446 nm range with Stokes shift ranging from 2494 to 9461 cm^{-1} and quantum yields of 4 to 99%. It is worth noting that electron-withdrawing substituents induce a red shift in the absorption and emission spectra.

In another study, the same authors[25] proposed a procedure for the preparation of a number of 2*H*-aryl-1,2,3-triazole-4-carboxylic acids. The starting triazoles **4** were obtained by a one-pot process, similar to that depicted in Scheme 1. The subsequent hydrolysis of the nitrile group was carried out under alkaline conditions using excess NaOH in a mixture of solvents (EtOH and H$_2$O) with heating. In the presence of hydrochloric
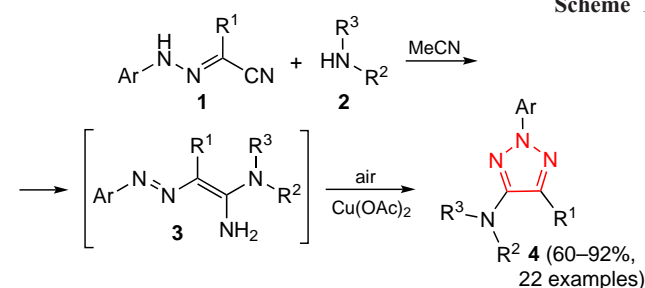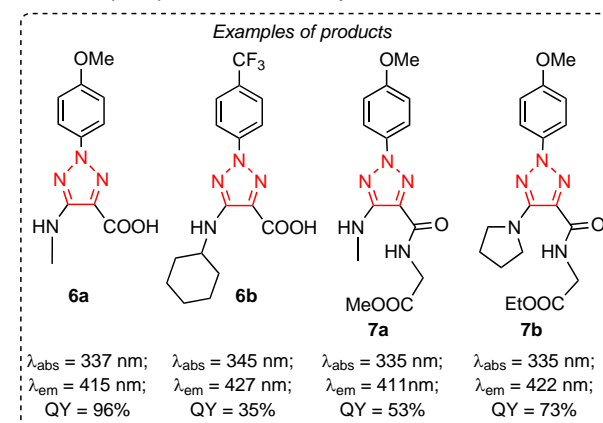
**Scheme 1**
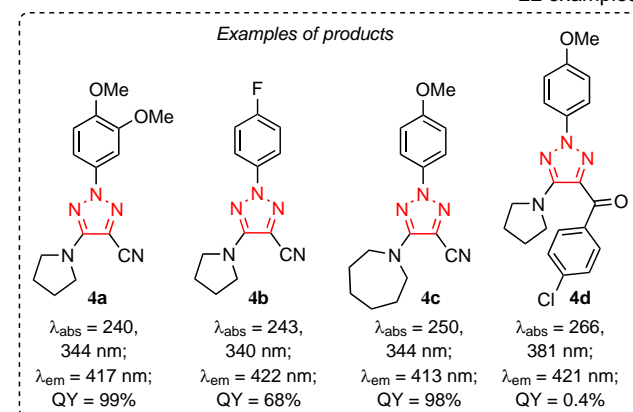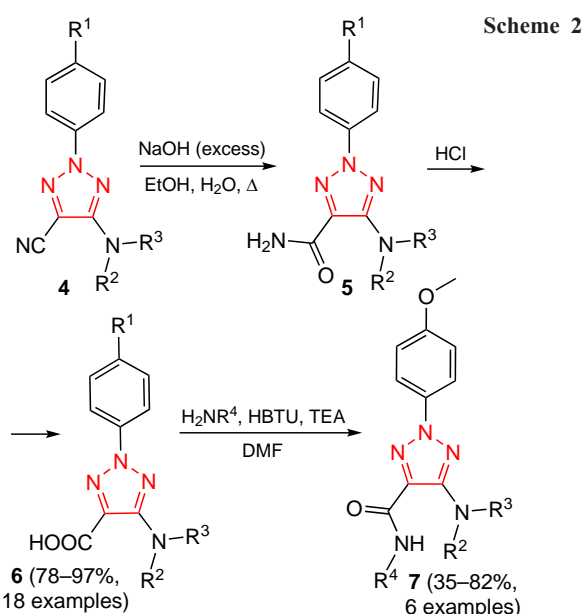
Scheme 2

HBTU is *N,N,N′,N′*-tetramethyl-*O*-(1*H*-benzotriazol-1-yl)uronium hexafluorophosphate, TEA is triethylamine

acid, amides **5** were converted to carboxylic acids **6** (Scheme 2). Fluorophores **6** showed a bright blue fluorescence in the range from 410 to 435 nm with quantum yields of up to 96%. It is noteworthy that the quantum yields varied depending on the pH, but the effect of compound structure on this characteristic could not be identified. Safronov *et al.*[26] described a number of sodium salts of carboxylic acids **6**, which had similar properties, but were better soluble in organic solvents. Further modification of the products afforded a series of substituted amides **7** in moderate to high yields.[27] Some compounds exhibited the aggregation-induced emission (AIE) effect. In particular, in the case of compound **7a**, the quantum yields varied depending on the DMSO to H$_2$O ratio: for $f_w = 90\%$, the quantum yield can reach 99% (f_w is the fraction of water).

A popular method for the synthesis of 1,2,3-triazoles is the cycloaddition of azides to alkynes; for the selective formation of 2*H*-derivatives, disubstituted alkynes must be used in this reaction. A study on the design of blue-green fluorophores based on 1,2,3-triazole was performed by the research group headed by Hong and Lee.[28] As the starting compound, the authors used 4,4′-dibromotolane **8a** or its dimethyl derivative **8b**, which was subjected to 1,3-dipolar cycloaddition with sodium azide, resulting in the formation of intermediate triazoles **9a,b** in moderate yields. The subsequent nucleophilic aromatic substitution (S$_N^{Ar}$) involving 4-fluorobenzonitrile yielded

Scheme 3
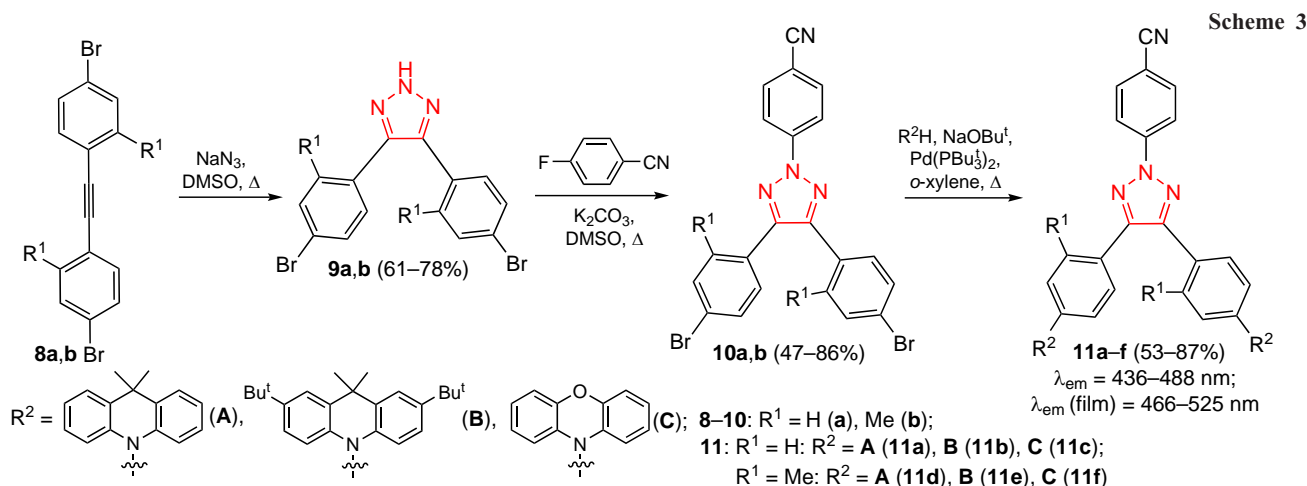
2*H*-functionalized 1,2,3-triazoles **10a,b**. The final step was the Buchwald–Hartwig reaction with acridine derivatives, 9,9-dimethyl-9,10-dihydroacridine (**A**), 2,7-di-*tert*-butyl-9,9-dimethyl-9,10-dihydroacridine (**B**), or phenoxazine (**C**), giving rise to target products **11a–f** (Scheme 3).

The products showed emission in the 464−524 nm range; the presence of a methyl group in the benzene ring induced a blue shift, while unsubstituted compounds (with R^1 = H) showed red fluorescence. The authors also fabricated experimental OLEDs, which were characterized by electroluminescence in the blue to green spectral range (Fig. 4).

The research groups headed by Shi,[29–31] Tabolin,[32] Huszthy,[33] and Fu[34] developed similar methods for the synthesis of 2*H*-functionalized 1,2,3-triazole derivatives, consisting in the *N*-arylation of a triazole nitrogen atom (Scheme 4). In the first

step, alkyne **12** reacted with sodium azide to give triazole **13**. This product was either *N*-arylated according to the Chan–Lam coupling reaction (with boronic acids), or subjected to Cu^I-catalyzed C–X/N–H coupling (X = Br, I), or reacted with indole in the presence of *N*-iodosuccinimide. The yields of the resulting triazoles **14** varied from moderate to high.

Products **14** showed emission in the range from 329 to 550 nm, with the quantum yields being 30 to 99% for solutions and up to 46% for powders. In addition, depending on the nature of aromatic substituent, the Stokes shift changed from 522 to 14 219 cm^{-1}. Compound **14d** was found to exhibit chemosensory properties suitable for the recognition of enantiomeric 1-phenylethylamine (PEA) perchlorates, 1-(1-naphthyl)-ethylamine, phenylglycine and phenylalanine methyl esters; some of these analytes are regulated precursors and, hence, they
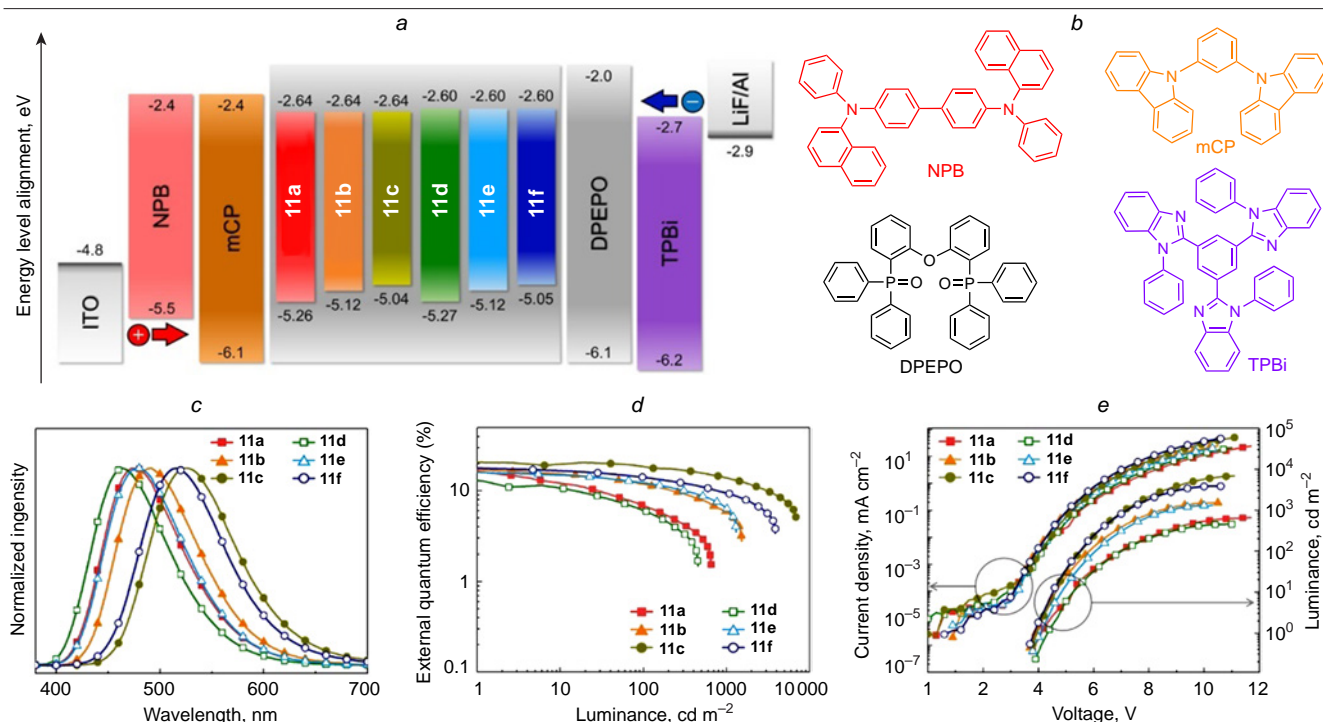
Figure 4. Diagram of the device and comparison of LUMO and HOMO energies of the components (*a*) and chemical formulas of some of the used compounds (*b*); electroluminescence spectra (*c*) and external quantum efficiency (EQE) *vs*. luminance (*d*); current density and luminance *vs*. voltage (*e*). Reproduced from Lee and co-workers[28] with permission from the American Chemical Society. (ITO is indium tin oxide, LUMO is the lowest unoccupied molecular orbital, HOMO is the highest occupied molecular orbital).

I.A.Lavrinchenko, T.D.Moseev, M.V.Varaksin, V.N.Charushin, O.N.Chupakhin
Russ. Chem. Rev., 2024, **93** (10) RCR5130

5 of 34

Scheme 4

(*a*) for **14a**: R³B(OH)₂, Cu(OAc)₂, Py, THF, O₂, 63 °C;[29]
(*b*) for **14b**: R³B(OH)₂, Cu(OAc)₂·H₂O, DMSO, O₂ (1 atm), 100 °C, 2 h;[32]
(*c*) for **14c**: NIS, K₂CO₃, 1,4-dioxane, indole;[34]
(*d*) for **14d**: ArI, CuCl, K₂CO₃, DMSO, proline, 85–110 °C;[33]
(*e*) for **15a**: R³Br, K₂CO₃, LiAlH₄, THF, PCC, DCM; or LiAlH₄, THF, I₂, TBSCl, DMF or ArI, CuI, proline, TBAF, THF, PCC, DCM (see [30])

12 NaN₃, DMSO, Δ → **13** (74–99%) → *a*, or *b*, or *c*, or *d*, or *e* → **14** (37–93%, 60 examples) → EtOH, Δ → **15** (67–92%, 11 examples)

Examples of products

14a
λ_abs = 369 nm;
λ_em = 533 nm;
QY = 52%

14b
λ_abs = 308 nm;
λ_em = 464 nm;
QY = 62%

14c
λ_abs = 310 nm;
λ_em = 437 nm;
QY = 90%

14d
λ_abs = 312 nm;
λ_em = 379 nm;
QY = 93 %

15a
λ_abs = 293 nm;
λ_em = 329 nm;
QY = 86%

Py is pyridine,
TMS is trimethylsilyl,
NIS is *N*-iodosuccinimide,
PCC is pyridinium chlorochromate,
DCM is dichloromethane,
TBS is *tert*-buthyldimethylsilyl,
TBA is tetrabuthylammonium

---

are subject to strict control. This chemosensor provides rapid detection of these compounds in the samples. As a rule, the emission intensity decreased two- to eight-fold in the presence of an analyte in the system; in the case of (*S*)-PEA, a threefold decrease in the emission intensity at 400 nm and appearance of new peaks at 600 nm were detected. Meanwhile, compound **14c** containing an indole moiety in the molecule proved to form complexes with Pd, which can serve as the basis for effective catalysts of organic reactions.

Shi and co-workers[30] did not study the optical properties of the obtained triazoles, but used them as intermediates for condensation with *o*-phenylenediamine to give conjugates **15** with benzimidazole. These compounds exhibit chemosensory properties for the detection of silver ions; in the presence of the analyte, the emission intensity decreased 10-fold; the limit of detection (LOD) was 10^{-9} M.
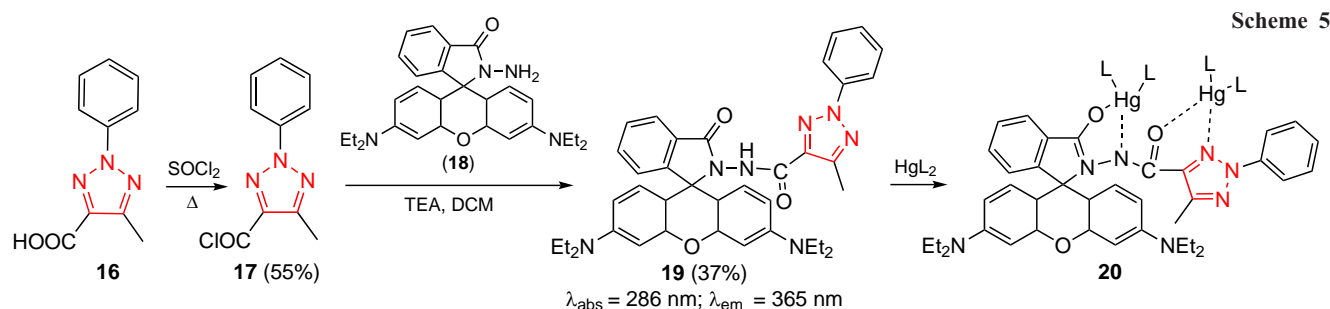
The research group headed by Feng and He[35] proposed a synthesis of fluorescent 2*H*-phenyl-1,2,3-triazole derivative meant for the detection of Hg²⁺ ions (Scheme 5).
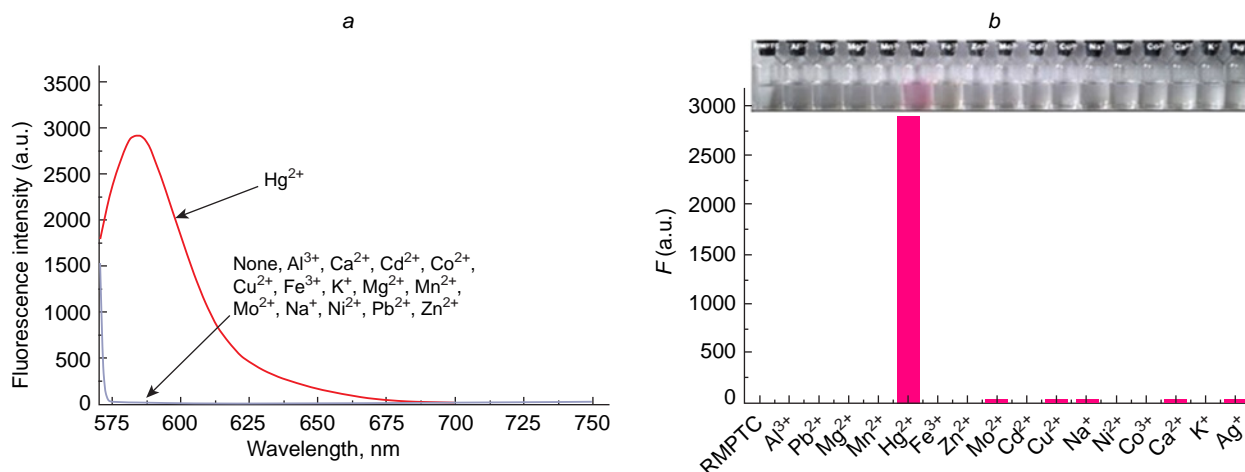
In the first step, the reaction of compound **16** with thionyl chloride yielded acid chloride **17**, which then reacted with fluorescein derivative **18** to give product **19** in a moderate yield. This fluorophore has an emission maximum at 365 nm and selective response to Hg²⁺ ions; the addition of an analytical sample induced the appearance of an absorption peak at 563 nm and an emission peak at 577 nm. When mercury ions are present

in the mixture, complex **20** is formed, and the solution becomes pink; this allows for naked-eye detection of the metal (Fig. 5).
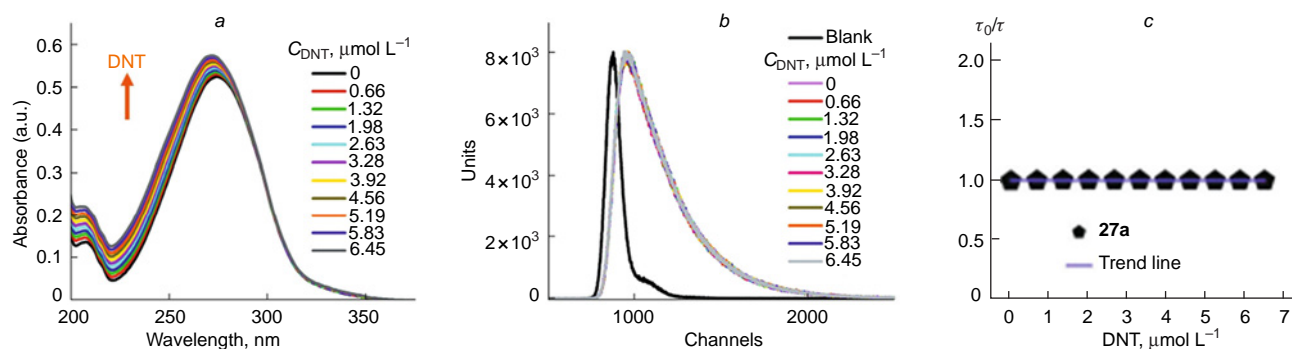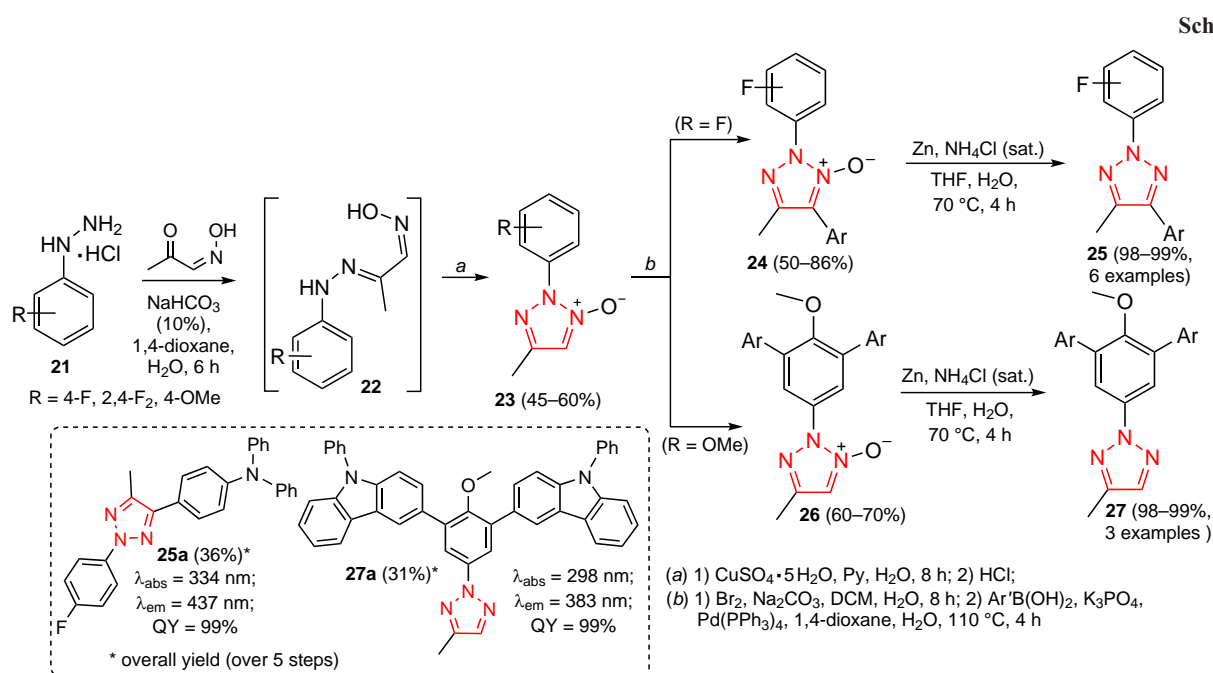
A five-step method for the synthesis of push–pull fluorophores based on 2*H*-aryl-1,2,3-triazoles (Scheme 6) was developed by our group.[36,37] First, hydrazine **21** was subjected to condensation with oxopropanal oxime to give hydrazone **22**, which cyclized in the presence of copper sulfate to give triazole *N*-oxide **23** in a moderate yield. The subsequent bromination and the Suzuki–Miyaura reaction with boronic acids gave triazole *N*-oxides **24** and **25**. It should be noted that in the presence of electron-donating substituents in the benzene ring, bromination occurs into the *ortho*-position relative to these groups, while in the presence of electron-withdrawing substituents, bromination is directed to the triazole ring. The *N*-oxide group was removed by reduction with zinc dust in a supersaturated solution of ammonium chloride, which gave fluorophores **26** and **27**, for example compound **27a**, in almost quantitative yields. This method is suitable for the synthesis of linear or Y-shaped fluorescent systems. These molecules have absorption peaks between 290 and 340 nm and emission peaks up to 470 nm and show quantum yields of up to 99%. Branched fluorophores **27** were found to exhibit chemosensory properties for the detection of nitroaromatic explosives [*e.g.*, 2,4-dinitrotoluene (DNT)] with LOD of 278 ppm (Fig. 6).

Thus, in this Section, we considered methods for the synthesis of 2*H*-aryl-1,2,3-triazole derivatives containing different

Scheme 5

16 (HOOC) → SOCl₂, Δ → **17** (ClOC) (55%) → (**18**), TEA, DCM → **19** (37%) λ_abs = 286 nm; λ_em = 365 nm → HgL₂ → **20**

Figure 5. Fluorescence spectra (*a*) and fluorescence intensity (*F*) (*b*) of compound **19** in a DMF — water (1:1 v/v) mixture and tris(hydromethyl)aminomethane hydrochloride (Tris-HCl) at pH 7.4 in the presence of various cations (40 μM concentration; excitation wavelength λ_{ex} = 563 nm); the upper part shows photographs of solutions of compound **19** in the presence of Hg^{2+} and other metal ions. Reproduced from He and co-workers[35] with permission from Elsevier.

Scheme 6

(*a*) 1) $CuSO_4 \cdot 5H_2O$, Py, H_2O, 8 h; 2) HCl;
(*b*) 1) Br_2, Na_2CO_3, DCM, H_2O, 8 h; 2) Ar'B(OH)$_2$, K_3PO_4, Pd(PPh$_3$)$_4$, 1,4-dioxane, H_2O, 110 °C, 4 h

Figure 6. Photometric titration involving DNT (*a*), two-dimensional fluorescence attenuation profiles (*b*), and results of time correlated single photon counting (TCSPC) determination of fluorescence quenching of compound **27a** upon the addition of DNT recorded at λ_{em} = 369 nm (*c*). Reproduced from Lavrinchenko *et al.*[37] with permission from Springer Nature.

Scheme 7
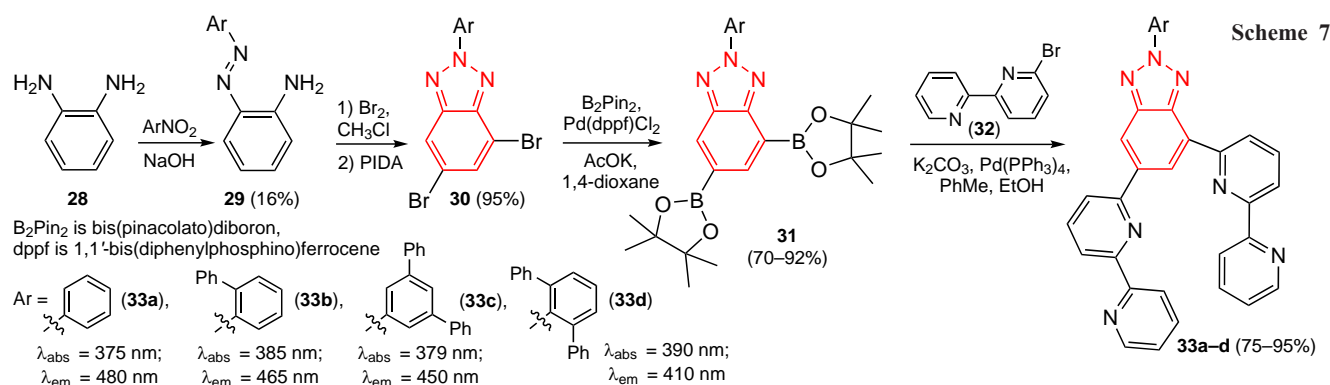
functional groups in the molecule at C(4) and C(5) atoms. Currently, there are several approaches to the preparation of this type of compounds such as azide–alkyne cycloaddition, arylation of 2*H*-1,2,3-triazoles, and cyclization of hydrazones. *N*-Arylation is most convenient from the synthetic standpoint; it can provide fine tuning of the physicochemical properties of functional materials prepared from such molecular blocks. Fluorophores of this type emit in the range below 500 nm with quantum yields of up to 99%; they are used as chemosensors and working elements of organic light-emitting diodes. It is noteworthy that the investigation for 2*H*-functionalized 1,2,3-triazoles exhibiting emission properties in the solid state is considered to be a promising line of research, as only one such example has been described so far.

4. Benzannulated 2*H*-1,2,3-triazoles

Below we consider the synthesis and luminescent properties of annulated 1,2,3-triazoles. The most common methods for the preparation of these compounds include cyclization of *o*-phenylenediamines followed by functionalization, (hetero) arylation of 2*H*-benzotriazoles, and Stille, Suzuki–Miyaura, and other cross-couplings

Ichikawa *et al*.[38] proposed a method for the synthesis of new fluorophores based on benzotriazole and 2,2′-bipyridine (Scheme 7). In the first step, *o*-phenylenediamine **28** was treated
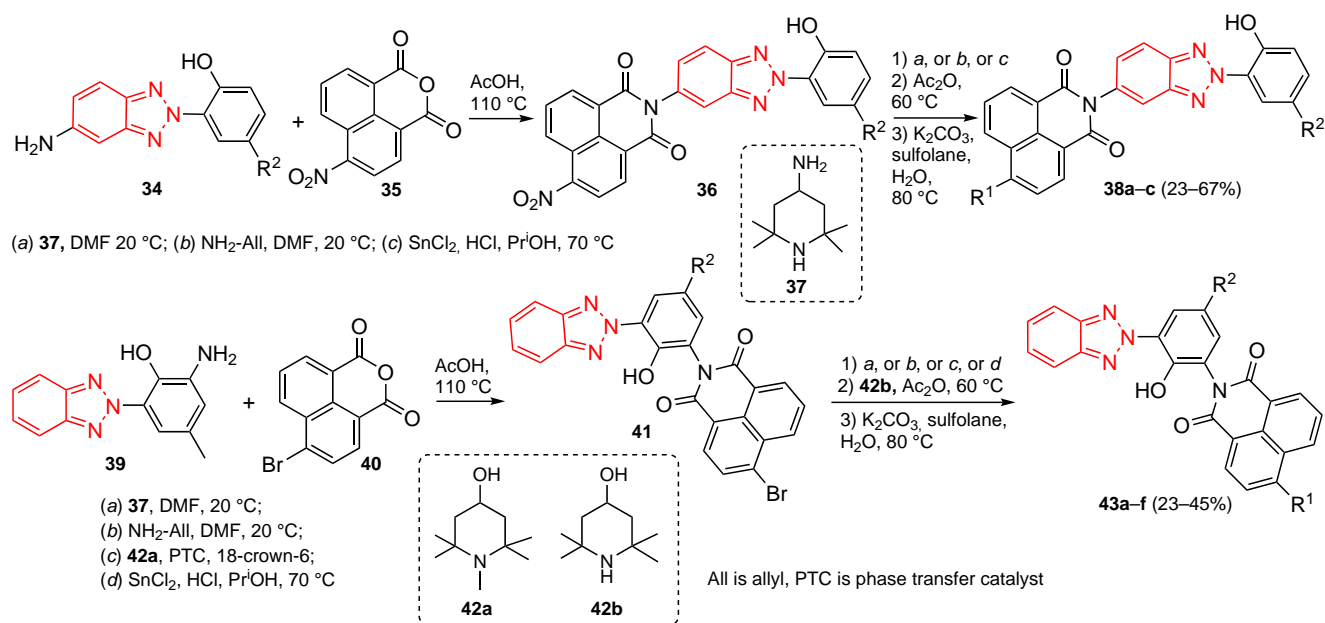
with aromatic nitro compounds in the presence of NaOH to give various diazo compounds **29**, which were brominated and then subjected to oxidative cyclization induced by di(acetoxy) iodobenzene (PIDA) to form benzotriazoles **30**. It is worth noting that this synthetic approach (diazotization and cyclization) is one of the most popular for the synthesis of 2*H*-functionalized 1,2,3-benzotriazoles. Substrates **30** were converted to boronic acids **31**, which were allowed to react with 6-bromo-2,2′-bipyridine **32** to give the target compounds **33** in high yields. These luminophores are characterized by light absorption in the 375 to 390 nm range and emission in the 410 to 480 nm range. The synthesized fluorophores exhibited electroluminescence; they also had high thermal stability: their decomposition temperature (T_{dec}) was > 410 °C, *i.e.*, it was higher than that for tris(8-quinolinolato)aluminium, which is widely used in light-blue OLEDs. In addition, this characteristic directly affects the decrease in the operating voltage of the devices. Thus, the obtained ensembles represent promising working components of organic light-emitting diodes (Fig. 7).

Bojinov *et al*.[39−41] and Uesaka *et al*.[42] reported the preparation of 1,8-naphthalimide benzotriazole derivatives (Scheme 8). First, benzotriazoles **34**, **39** were allowed to react with 4-substituted 1,8-naphthalic anhydrides **35**, **40** in acetic acid, which gave the corresponding 1,8-naphthalimide derivatives. Then the nitro group in compounds **36** and **41** was substituted for the piperidine (**37** and **42**) or prop-2-enylamine moiety in
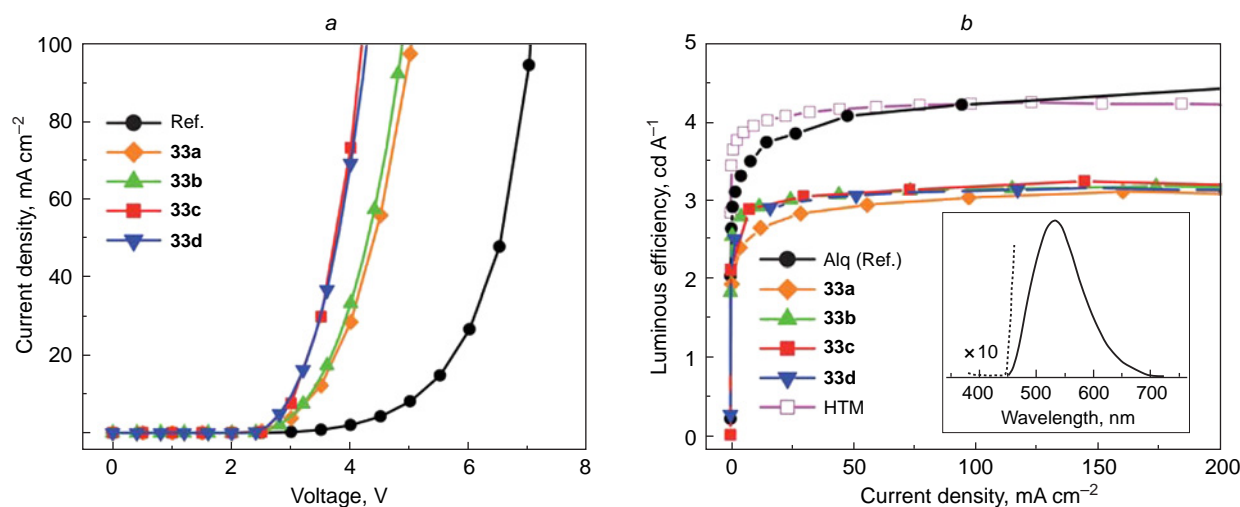
Figure 7. Current density vs. voltage (*a*) and luminous efficiency *vs.* current density (*b*) for compounds **33a−d**. The inset shows the electroluminescence spectra of compound **33b**: experimental curve (solid line) and 10-fold magnification (dashed line). The curve Ref. shows analogous dependences for the device without the test fluorophores; the HTM curve refers to hole-transporting materials. Reproduced from Icihikwa *et al*.[38] with permission from the Royal Society of Chemistry.

I.A.Lavrinchenko, T.D.Moseev, M.V.Varaksin, V.N.Charushin, O.N.Chupakhin

Scheme 8

(*a*) **37**, DMF 20 °C; (*b*) NH$_2$-All, DMF, 20 °C; (*c*) SnCl$_2$, HCl, Pr^{i}OH, 70 °C

(*a*) **37**, DMF, 20 °C;
(*b*) NH$_2$-All, DMF, 20 °C;
(*c*) **42a**, PTC, 18-crown-6;
(*d*) SnCl$_2$, HCl, Pr^{i}OH, 70 °C

All is allyl, PTC is phase transfer catalyst

45–72% yields. It is noteworthy that in the presence of amino group in the γ-position (conditions *b*), this group can be acylated to give compounds **38c**, **43d–e** (Table 1). These fluorophores absorb in the 330–440 nm range and emit in the 460–570 nm range, with the quantum yields being up to 66%. Compound **43a** was found to possess chemosensory properties for determination

Table 1. Photophysical properties of 1,8-naphthalimide benzotriazole derivatives.

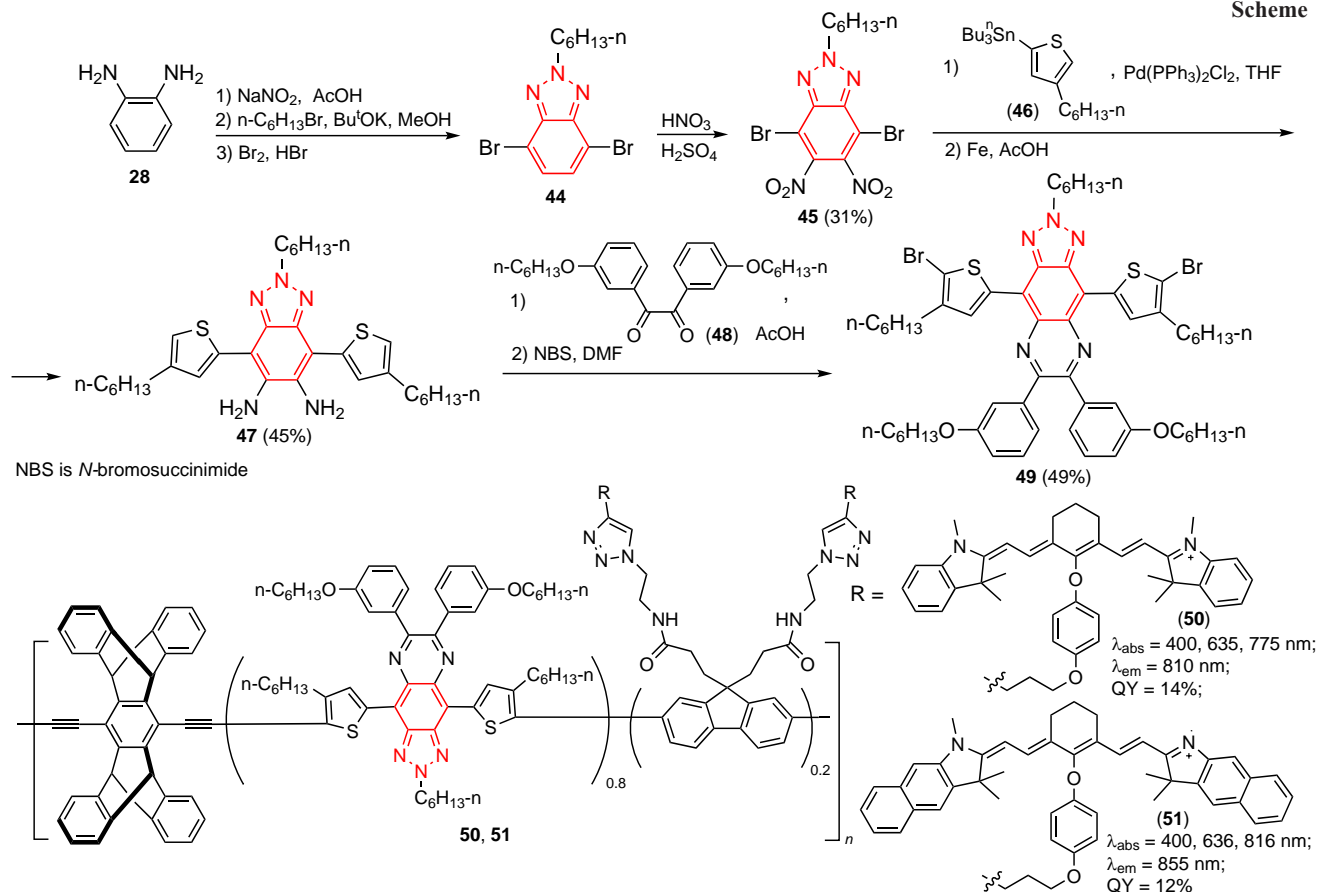| Com-pound	R^1	R^2	λ_{abs}, nm	λ_{em}, nm	QY (%)	Ref.
38a	(4-amino-2,2,6,6-tetramethylpiperidine)	H	434	520	42	39
38b	NHAll	H	338, 424	516	62	39
38c	NHAc	Bu^t	356	466	42	42
43a	(4-amino-2,2,6,6-tetramethylpiperidine)	Me	434	519	46	39
43b	NHAll	Me	336, 422	512	66	40
43c	(4-oxy-2,2,6,6-tetramethylpiperidine)	Me	434	519	46	41
43d	NHAc	Me	337	466	56	42
43e	NHAc	CMe$_2$CH$_2$Bu^t	442	568	8	42
43f	(4-oxy-N-methyl-2,2,6,6-tetramethylpiperidine)	Me	368	440	9	41

of Cu^{2+} ions; the formation of the copper complex increased the emission intensity four-fold. Compounds **38b** and **43b** proved to be capable of detecting Zn^{2+} ions: the addition of the analyte resulted in an up to eight-fold increase in the emission intensity, depending on the concentration of the metal ions in solution. This behaviour may imply the possible use of these fluorophores as fluorescent detectors for metal ions. Thus, a versatile analytical platform for the design of selective fluorescent chemosensors for the determination of various divalent metal cations has been developed. Further studies in this area could be aimed at the design of devices with these compounds as working elements or at expansion of the range of analytes.

Chan's research group[43] synthesized fluorophores based on triazoloquinoxalines. For this purpose, *o*-phenylenediamine **28** was first cyclized with sodium nitrite in acetic acid to give benzotriazole. The subsequent arylation and bromination gave product **44**, the nitration of which led to dinitrobenzotriazole **45**. This product was subjected to the Stille cross-coupling with stannane **46** and then the nitro group was reduced. The cyclization of the resulting diamine **47** with diketone **48** followed by one more bromination of the intermediate afforded the target compound **49**, which was then co-polymerized with fluorene and pentiptycene derivatives (Scheme 9). Polymers **50** and **51** exhibit emission in the near-IR region (λ > 900 nm) with quantum yields of up to 14%. The authors revealed low toxicity of these fluorophores in 2 nM concentration against human ovarian cancer cells (SKOV-3). It was also shown that these products can be used to diagnose ovarian cancer in a laboratory mouse model. The quantum yields and fluorescence brightness of this polymer were 30 times as high as those for known[44] indocyanine green (ICG) and Alexa Fluor 790 dyes.

Wong and co-workers[45] developed a method for the synthesis of polymers containing a benzotriazole moiety (Scheme 10). The sequence of transformations included the Suzuki and Stille cross-coupling reactions involving aryl bromides **53**–**55** and **60** and also benzotriazole derivatives **52** and **59**. This gave four polymers (**56**–**58** and **61**) with molecular weights from 3000 to 151 000 a.m.u in 73–98% yields. These fluorophores emit in the 486–708 nm range with quantum yields of up to 90%. Prototypes of PLED devices exhibiting electroluminescent properties

I.A.Lavrinchenko, T.D.Moseev, M.V.Varaksin, V.N.Charushin, O.N.Chupakhin
Russ. Chem. Rev., 2024, **93** (10) RCR5130

9 of 34

Scheme 9

NBS is *N*-bromosuccinimide

λ_{abs} = 400, 635, 775 nm;
λ_{em} = 810 nm;
QY = 14%;
(50)

λ_{abs} = 400, 636, 816 nm;
λ_{em} = 855 nm;
QY = 12%
(51)

Scheme 10

MW is microwave irradiation

(*a*) Pd(PPh$_3$)$_4$, PhMe,
Et$_4$NOH, LiOH, 90 °C, 24 h

56	57	58	61
λ_{abs} = 474 nm;	λ_{abs} = 500 nm;	λ_{abs} = 396 nm;	λ_{abs} = 356 nm,
λ_{em} = 541 nm;	λ_{em} = 604 nm;	λ_{em} = 487 nm;	604 nm;
QY = 90%	QY = 83%	QY = 63%	λ_{em} = 708 nm
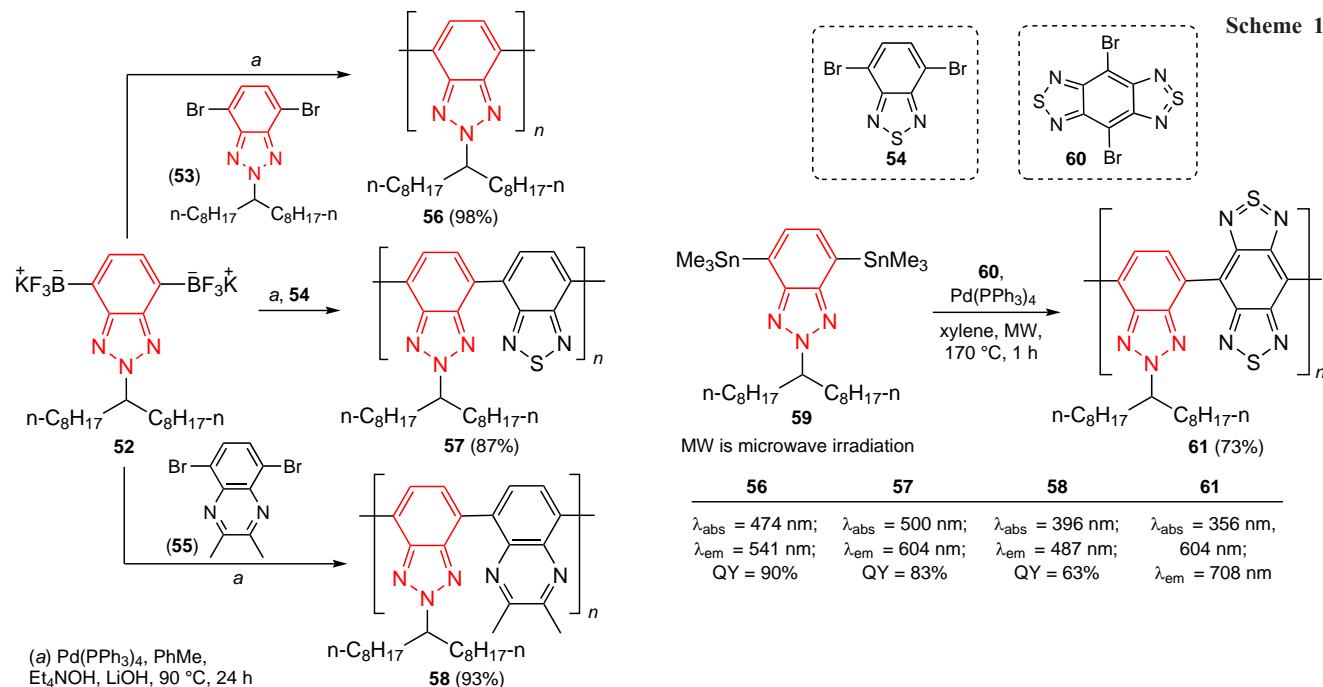
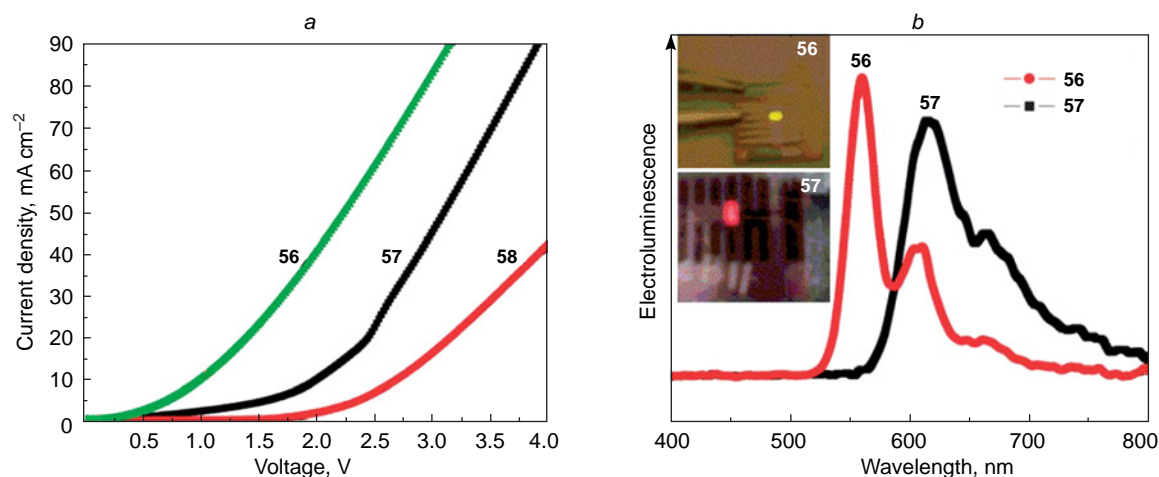(PV$_{fill\ factor}$ = 43, PCE = 0.4%) at V = 1.6 and 2.4 V were designed on the basis of polymers **57**, **58**, and **61** (Fig. 8). (PV$_{fill\ factor}$ is the fill factor for organic photovoltaics; PCE is the power conversion efficiency; V is the voltage). In addition, it was found that these compounds can be used in the acceptor layer in solar panel.

Pan *et al*.[46] proposed a method for the synthesis of polymeric benzotriazole-containing fluorophores (Scheme 11). The target compounds were obtained by six successive reactions. The benzotriazole ring was assembled by diazotization and cyclization of the starting compound **62**; the subsequent alkylation and iodination resulted in 2-γ-vinylalkyl-1,2,3-benzotriazole **63**. The next steps included silylation with reagent **64** in the presence of the Karstedt catalyst (**65**), cross-coupling with (2-thienyl)stannane, and bromination and produced the key triazole **67**. This product was co-polymerized with heterocycle

I.A.Lavrinchenko, T.D.Moseev, M.V.Varaksin, V.N.Charushin, O.N.Chupakhin
Russ. Chem. Rev., 2024, **93** (10) RCR5130

Figure 8. Current density *vs*. voltage for PLED devices with polymers **56**–**58**, respectively (*a*) and electroluminescence spectra of PLEDs based on compounds **56** and **57** (*b*). Reproduced from Wong and co-workers[45] with permission from the Royal Society of Chemistry.

Scheme 11
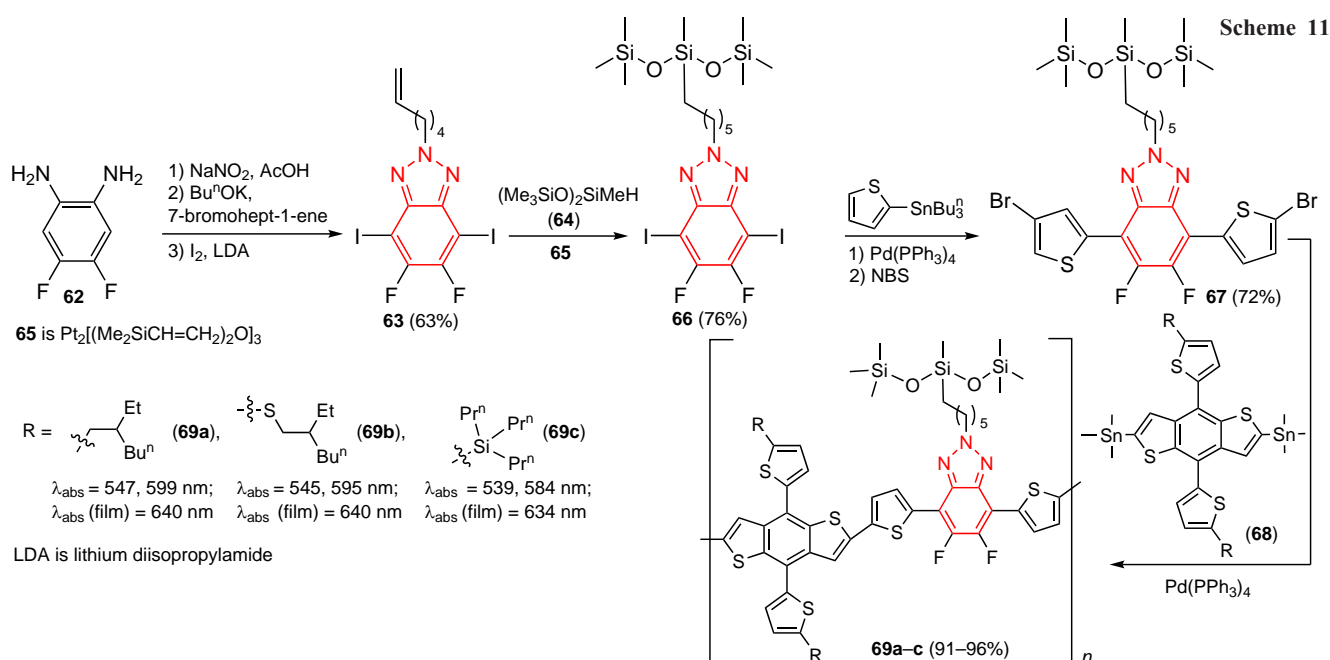
68 in the presence of Pd(PPh$_3$)$_4$ to give polymers **69** with molecular masses from 4600 to 7900 a.m.u. Solutions of these polymeric fluorophores absorb in the 538–598 nm range, while the absorption of films occurs in the range from 400 to 800 nm. The authors measured the quantum efficiency of fluorescence,[‡] which reached 66%. Quantum efficiency is a key characteristic for photosensitive devices. In addition, the open-circuit voltage (V_{oc}) was 0.94. Thus, compounds with the indicated properties can be used in the design of energy-efficient solar panels.
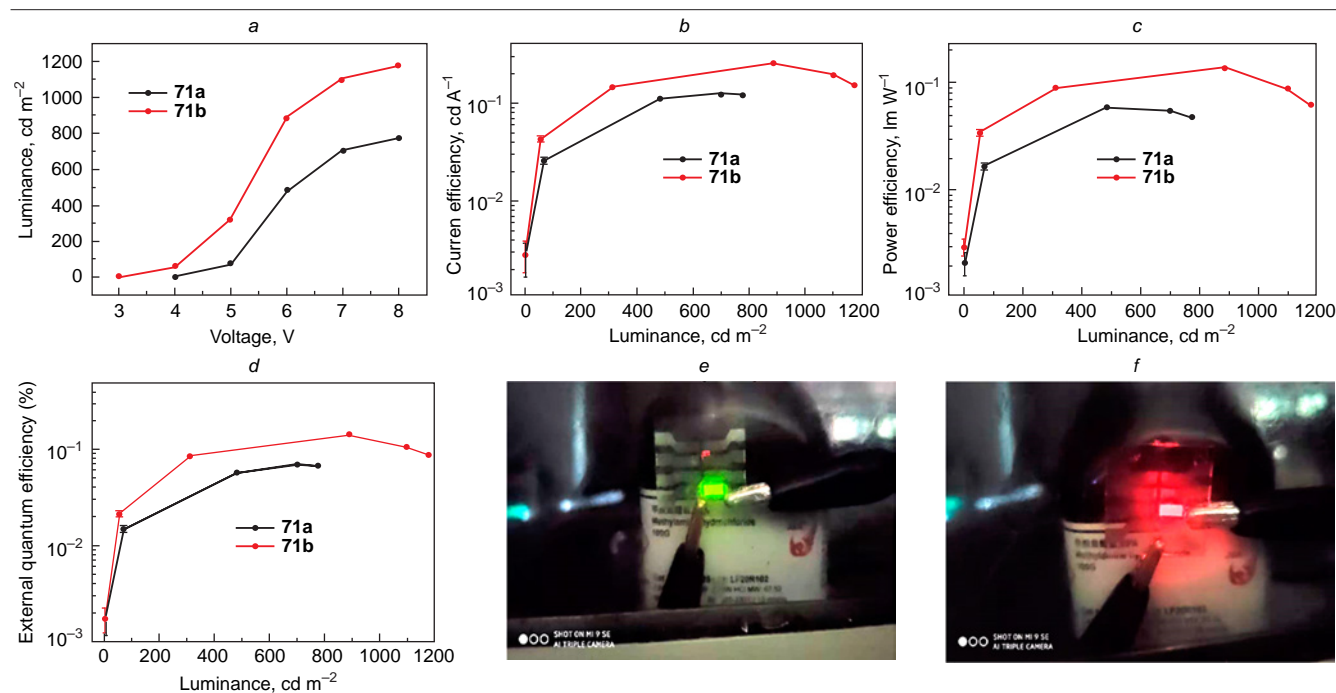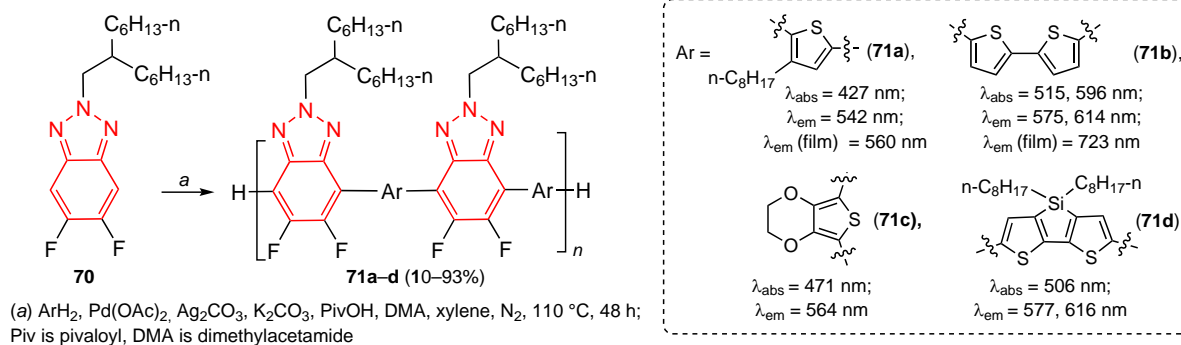
Lu and co-workers[47] prepared polymers based on difluorobenzotriazole (Scheme 12). The method for the synthesis of these compounds included the palladium-catalyzed C−H/C−H couplings of 5,6-difluorobenzotriazole (**70**) with thiophene derivatives. Four polymers **71a–d** with molecular weights of up to 41 000 a.m.u. were isolated in yields varying over a wide range. These compounds exhibited green and orange

emission in the 540–620 nm range. OLED prototypes with quantum yields of 0.07 and 0.14% at a voltage of 3 to 4 V were designed on the basis of polymers **71a,b** (Fig. 9). The maximum current efficiency for these devices was 0.25 cd A^{-1}; the power efficiency ranged from 0.059 to 0.13 lm W^{-1}.

The research group headed by Liu[48] proposed a method for the synthesis of polymers based on benzotriazole and benzimidazole conjugates (Scheme 13). A three-step process was used to form a polymer chain unit. Unsubstituted benzotriazole **72**, used as the starting compound, was alkylated with 1,6-dibromohexane and brominated to give compound **73** in a relatively low yield; this product reacted with substituted benzimidazole **74** to give monomer **75**. The Suzuki–Miyaura reaction was chosen for the polymerization, with the product yield being moderate. Polymer **76** had a molecular weight of 10089 a.m.u., and its electronic spectrum exhibited two absorption peaks in the ranges of 290–320 and 330–480 nm and one emission maximum in the 471–483 nm range, with the quantum yield being up to 76%. In addition, this compound exhibited chemosensory properties for the detection of I$^-$ anion

---

[‡] The ratio of the number of photons the absorption of which causes the formation of quasi-particles to the total number of absorbed photons.

Scheme 12

(*a*) ArH$_2$, Pd(OAc)$_2$, Ag$_2$CO$_3$, K$_2$CO$_3$, PivOH, DMA, xylene, N$_2$, 110 °C, 48 h; Piv is pivaloyl, DMA is dimethylacetamide

Figure 9. Luminance *vs.* voltage (*a*) and current efficiency (*b*), power efficiency (*c*), and external quantum efficiency (*d*) *vs.* luminance of PLEDs based on compound **71a**,**b**; and photographs of devices based on polymer **71a** with green emission (*e*) and polymer **71b** with red emission at a voltage of 8 V. Reproduced from Lu and co-workers[47] with permission from MDPI.

[LOD of 10^{-4} M for **71b** (**P2**)]; Fe^{3+}, Cu^{2+}, and Ag$^+$ cations (LOD ≈ 10^{-5} M), and cysteine (Fig. 10). In another study of the same authors,[49] further modification of substrate **73** afforded two new polymers **80** and **79** with molecular masses of 32865 and 5096 a.m.u., respectively, in moderate yields. Both polymers absorbed in the 420–470 nm range, with their emission being in the 460–530 nm range; and the quantum yields were 45–57%. Like fluorophores described above, compounds **79** and **80** showed a similar chemosensory response for the detection of Fe^{3+} and Cu^{2+} cations [binding constant (K) ≈ 10^{-4} M^{-1}], while iron(III) complex of compounds **79**, **80** showed a response to PO$_4^-$ ions (LOD ≈ 10^{-3} M) (Fig. 11, 12).
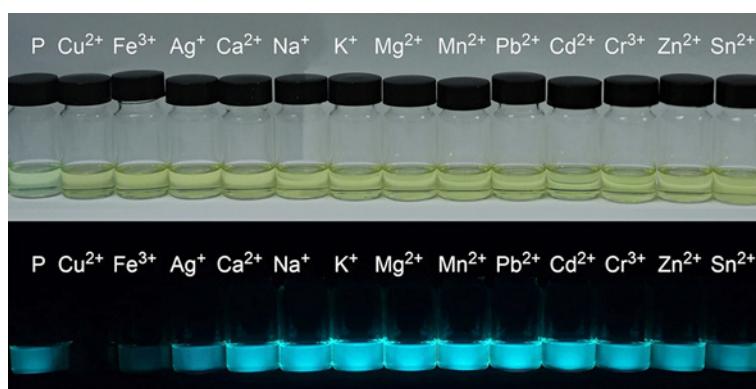
Figure 10. Photographs showing the emission of polymer **79** in the presence of metal cations under daylight (*above*) and under UV light (*below*). Reproduced from Liu and co-workers[48] with permission from Springer Link.

Scheme 13

R is the corresponding aryl; Cy is cyclohexyl; Aq336 is methyltrioctylammonium chloride

(*a*) 1) Pd(OAc)$_2$, PCy$_3$, RB(OH)$_2$, Aq336, K$_2$CO$_3$, PhMe; 2) NBS, AcOH, CH$_3$Cl

79 (41%)
λ_{abs} = 420 nm;
λ_{em} = 464 nm;
QY = 45%

80 (54%)
λ_{abs} = 467 nm;
λ_{em} = 529 nm;
QY = 57%

76 (59%)
λ_{abs} = 290–320 nm,
λ_{em} = 330–480 nm,
QY = 76%
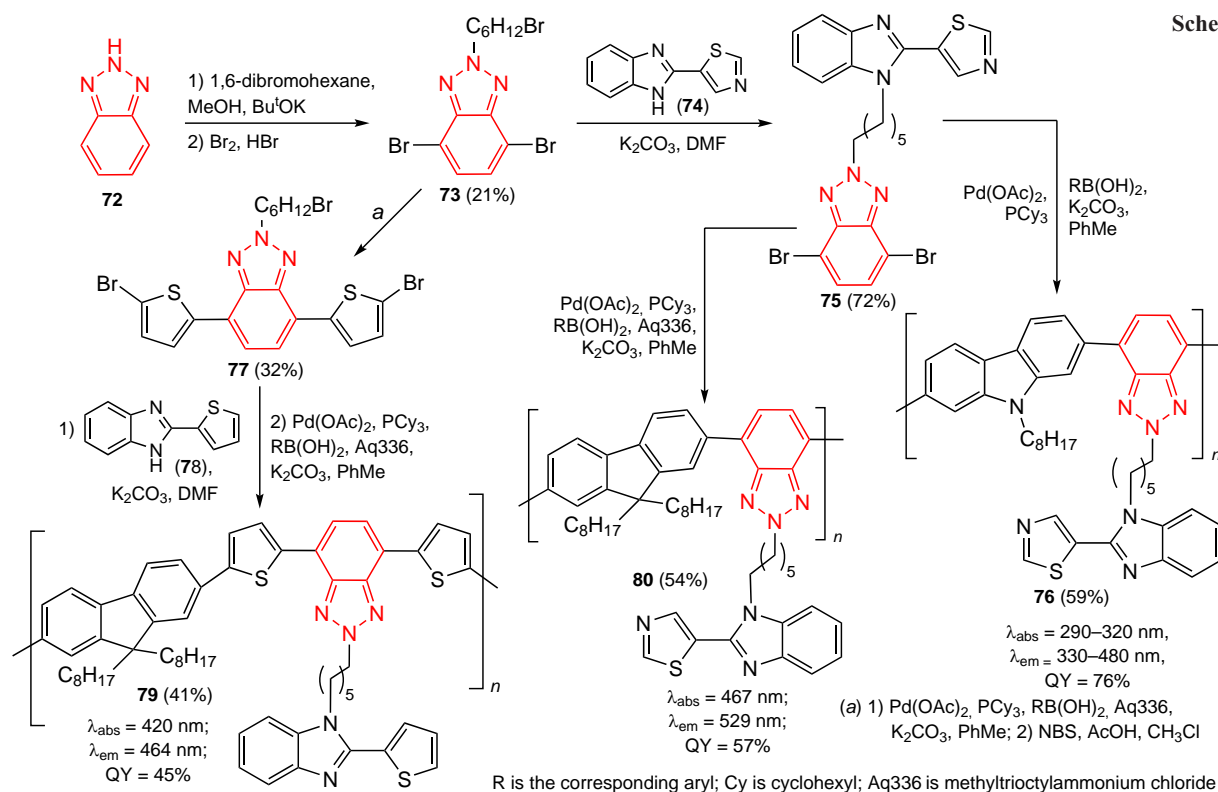
Figure 11. Photographs showing the emission of complex [**79**-Fe^{3+}] with anions under daylight (*above*) and under UV light (*below*). Reproduced from Liu and co-workers[48] with permission from Wiley.
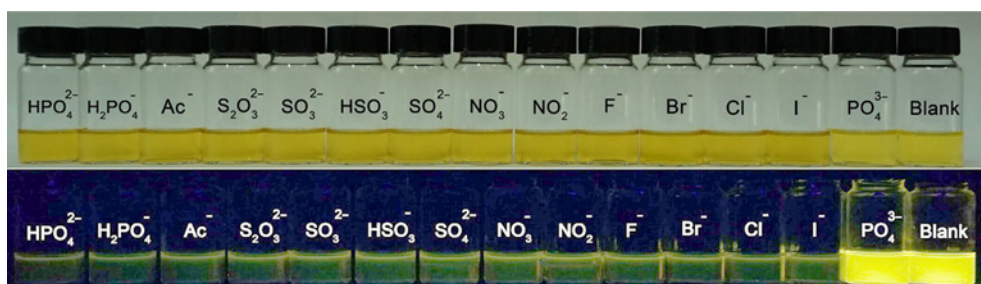
Figure 12. Photographs showing the emission of complex [**80**-Fe^{3+}] with anions under daylight (*above*) and UV light (*below*). Reproduced from Liu and co-workers[49] with permission from Wiley.

Tang and co-workers[50] and Wu and co-workers[51] described the synthesis of fluorophores with the D−π-A−π-D structure (D is donor, A is acceptor) including triazolobenzothiadiazole or its selenium analogue (Scheme 14). Tetraphenylet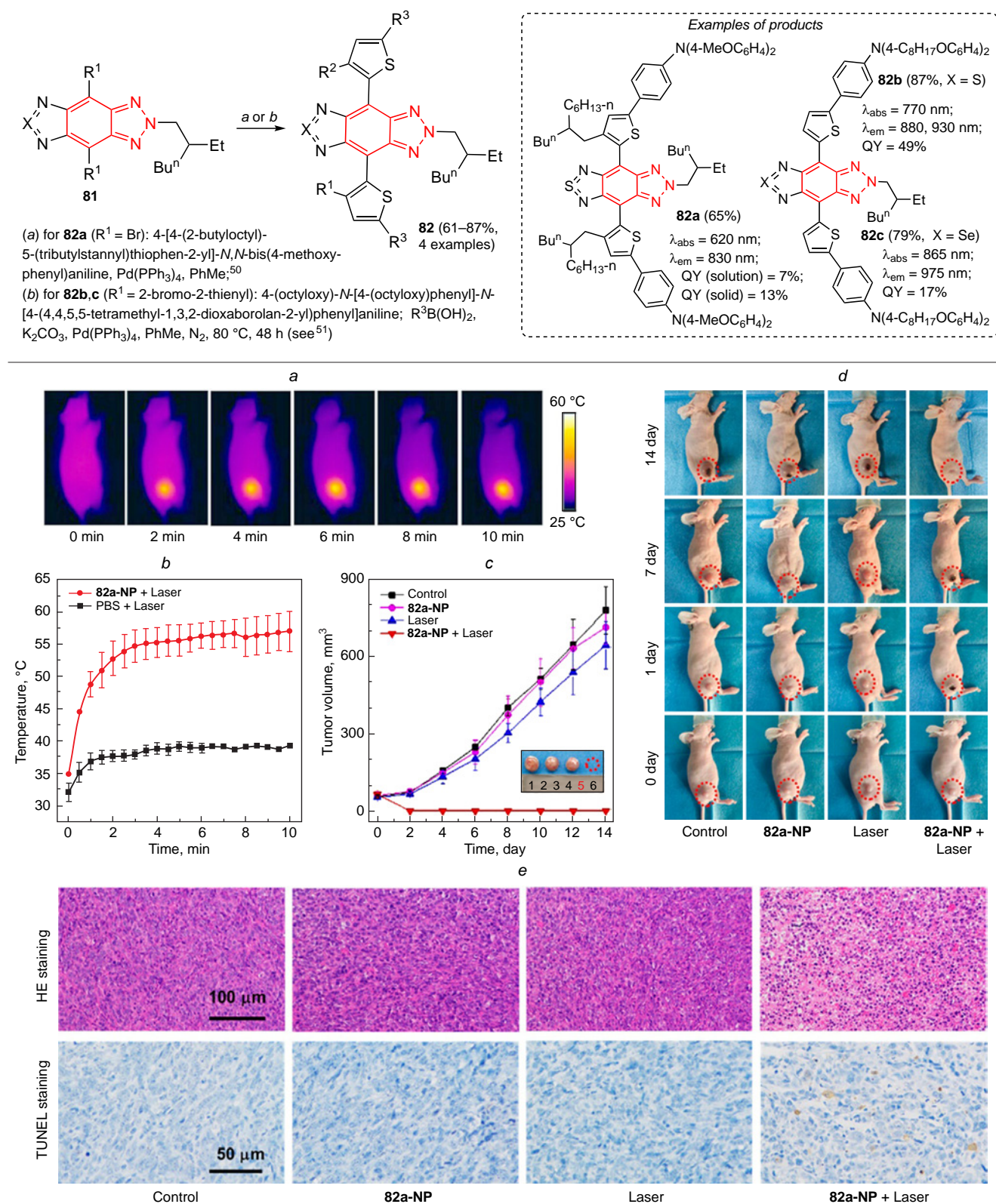hylene and triphenylamine moieties served as the electron-donating groups, while thiophenes acted as π-linkers. These photoactive compounds were prepared using a two-step method starting with the Stille cross-coupling reaction involving aryl bromides and (2-thienyl)stannane. This gave intermediate compounds, which were functionalized with an aza-heterocyclic moiety *via* an analogous reaction to give products **82a**,**b** in up to 65% yields. Alternatively, the same compounds were obtained by the

Miyaura borylation of triarylamine followed by Suzuki−Miyaura cross-coupling, which afforded the corresponding products in up to 87% yields. The products absorbed at 582–620 nm and emitted in the 750–930 nm range, which corresponds to the near-IR region. The quantum yields in solutions ranged from 17 to 49%. These compounds showed AIE effects at f_w > 50%; in the case of compound **82a**, a three-fold enhancement of the emission was observed. Furthermore, fluorophores **82a**,**b** had low cytotoxicity (IC$_{50}$ > 1000). Nanoparticles (NPs) of compound **82a** were tested as agents for phototherapy of cancer cells in mice. Cell images were obtained by hematoxylin and eosin staining (H&E) and by detection of apoptotic DNA

I.A.Lavrinchenko, T.D.Moseev, M.V.Varaksin, V.N.Charushin, O.N.Chupakhin
Russ. Chem. Rev., 2024, **93** (10) RCR5130

13 of 34

(*a*) for **82a** (R^1 = Br): 4-[4-(2-butyloctyl)-5-(tributylstannyl)thiophen-2-yl]-*N,N*-bis(4-methoxy-phenyl)aniline, Pd(PPh$_3$)$_4$, PhMe;[50]

(*b*) for **82b,c** (R^1 = 2-bromo-2-thienyl): 4-(octyloxy)-*N*-[4-(octyloxy)phenyl]-*N*-[4-(4,4,5,5-tetramethyl-1,3,2-dioxaborolan-2-yl)phenyl]aniline; R^{3}B(OH)$_2$, K$_2$CO$_3$, Pd(PPh$_3$)$_4$, PhMe, N$_2$, 80 °C, 48 h (see[51])

Figure 13. Images of mice bearing 4T1 tumours under laser radiation at 660 nm for different time intervals after the injection of **82a** nanoparticles (*a*), temperature change in the 4T1 tumour-bearing mice after the intravenous injection of **82a** NPs and phosphate-buffered saline (PBS) under laser irradiation (λ = 660 nm, power of 0.5 W cm^{-2}) for 10 min (*b*), change in the relative tumour volume after different types of treatment (*c*), images of four groups of 4T1 tumour-bearing mice after 14 days of treatment (*d*); confocal laser microscopy images of H&E- and TUNEL-stained tumour tissues after different types of treatment (*e*). Reproduced from Tang and co-workers[50] with permission from the American Chemical Society.

Figure 14. Fluorescence imaging of mouse *in vivo* (*a*); NIR-II imaging (NIR-II is the near IR region) with intravenously injected **82b** nanoparticles and heartbeat and respiratory curves recorded by monitoring oscillations of the fluorescence signal from the heart (ROI-1 is the region of interest 1) and liver (ROI-2 is the region of interest 2) (*b*); and variation of NIR-II images with time after subcutaneous injection of the agent through the pad of the foot ($\lambda_{ex} = 730$ nm, 1100LP optical filter, $\tau = 10$ ms irradiation time) (*c*). Reproduced from Wu and co-workers [51] with permission from Wiley.

fragmentation (TUNEL method). These methods make it possible to evaluate the decrease in the number of cancer cells in the body after ph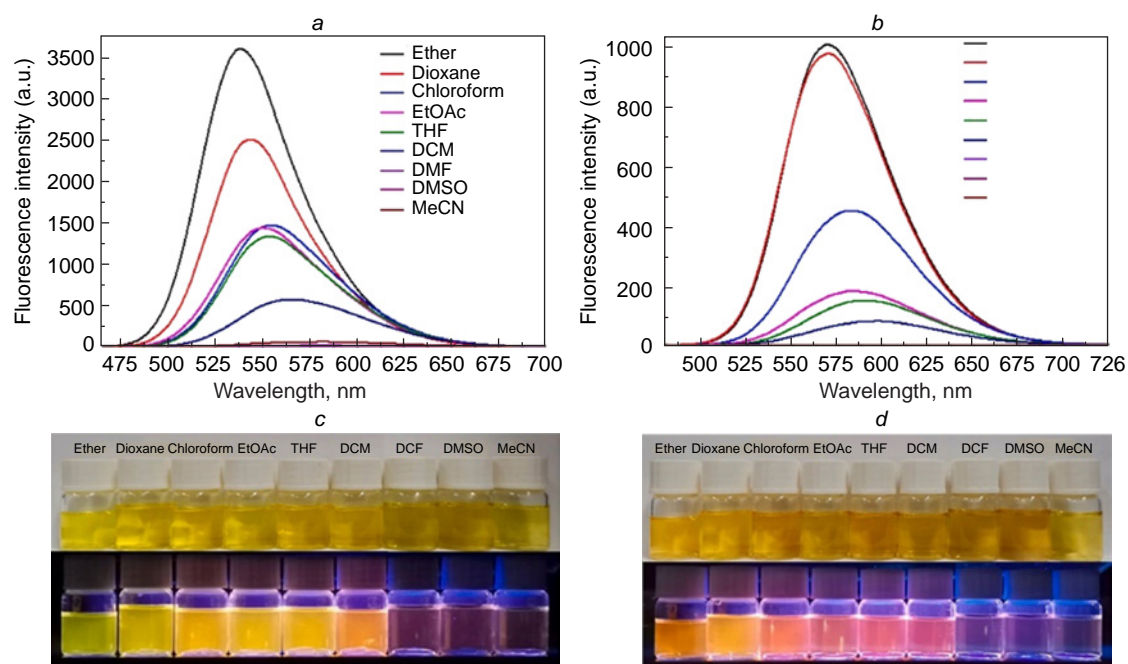otodynamic therapy (Fig. 13). Compound **82b** was used to monitor the heart rate (Fig. 14). A similar method is used to detect cardiac disorders and other pathological changes in the blood circulation system. In addition, these compounds proved to be effective for the detection of adipose bodies in a cell and, therefore, they can be used to diagnose hepatic steatosis.

Lu and co-workers [52] and Deng and co-workers [53] proposed similar methods for the synthesis of 4,7-disubstituted 2*H*-functionalized 1,2,3-benzotriazoles **84** in good yields by the Suzuki–Miyaura cross-coupling of substrates **83** with

Scheme 15

(a) for **84a**: $R^3B(OH)_2$, Pd(PPh$_3$)$_4$, Na$_2$CO$_3$, 12 h; or R^3BPin, KOPh, 48 h;[52]
(b) for **84b**: $R^3B(OH)_2$, K$_2$CO$_3$, Pd(PPh$_3$)$_4$, H$_2$O, THF [53]

83
R^1 = CF$_3$, H, F; R^2 = H, F

84 (75–83%, 4 examples)

Examples of products

R^1 = CF$_3$, R^2 = H,

(84a)
λ_{abs} (solution) = 404 nm;
λ_{em} (solution) = 531 nm;
QY (solution) = 25%;
λ_{abs} (film) = 422 nm;
λ_{em} (film) = 505 nm;
QY (film) = 19%

$R^1 = R^2$ = H,

(84b)
λ_{abs} = 446 nm;
λ_{em} = 554 nm;
QY = 74%

I.A.Lavrinchenko, T.D.Moseev, M.V.Varaksin, V.N.Charushin, O.N.Chupakhin
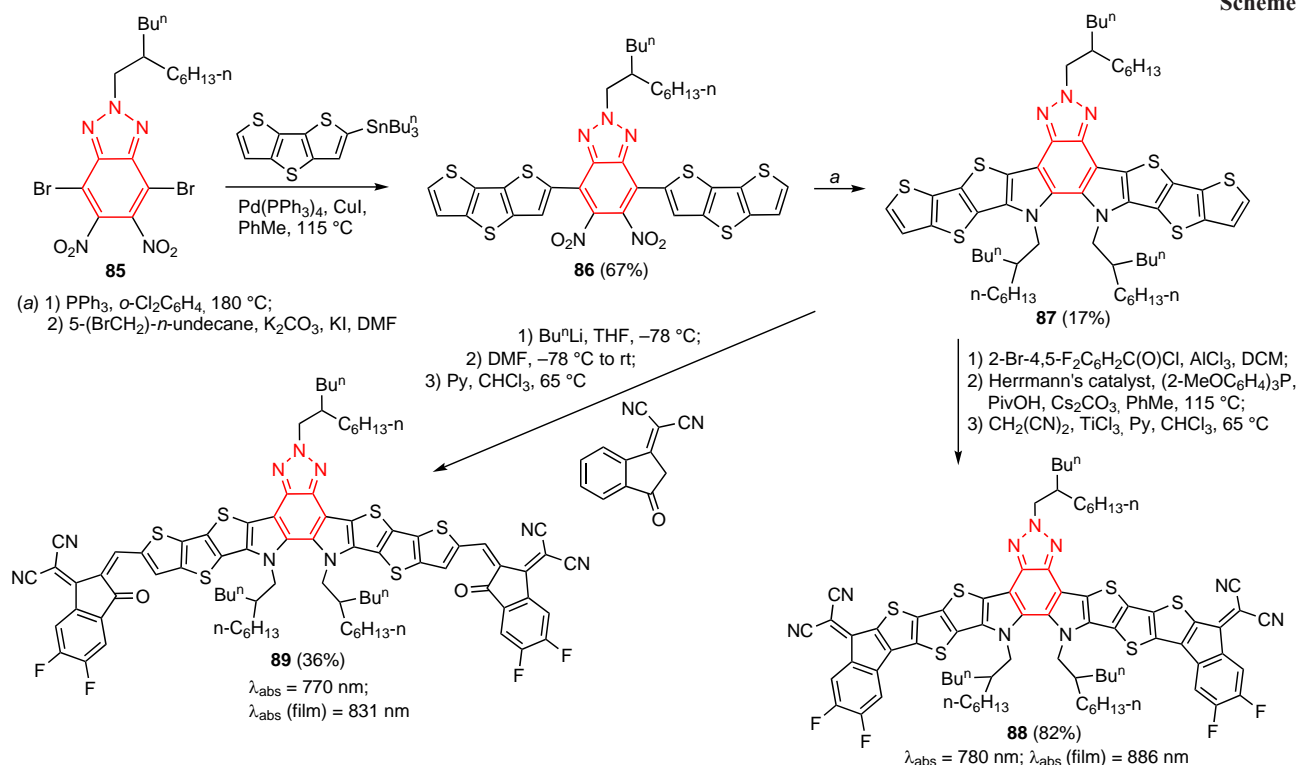*Russ. Chem. Rev.*, 2024, **93** (10) RCR5130

15 of 34

Figure 15. Emission spectra of compounds **84a** (*a*) and **84b** (*b*) in various solvents; photographs of solutions of **84a** (*c*) and **84b** (*d*) at room temperature (*above*) and under irradiation with UV lamp (λ_{ex} = 254 nm) (*below*). Reproduced from Deng and co-workers[53] with permission from Elsevier.
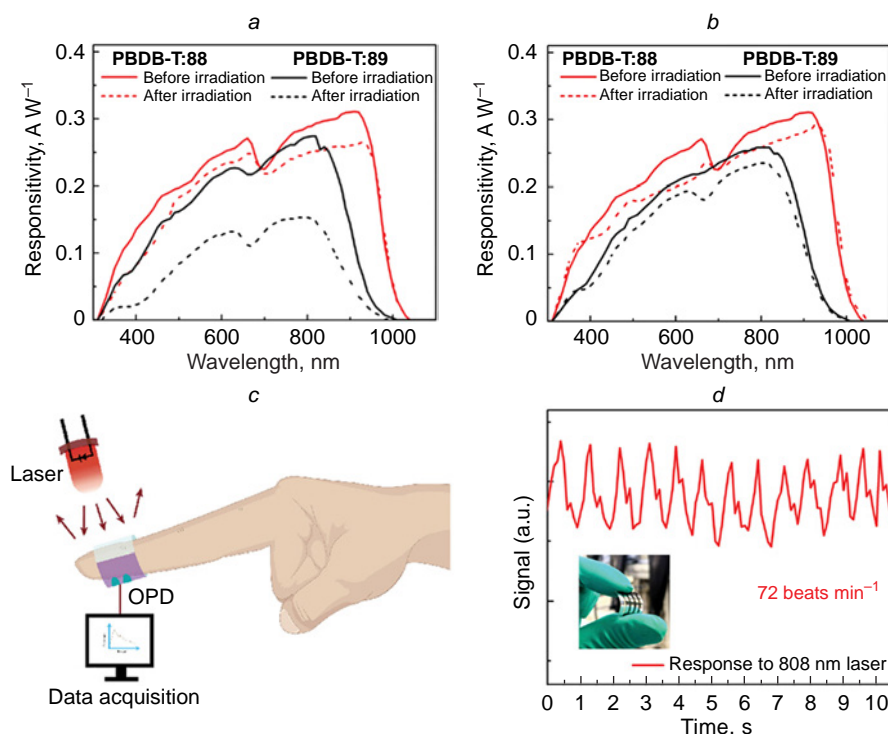
boronic acids or their pinacol esters (Scheme 15). These fluorophores emit at 455–590 nm [the molar absorption coefficient (ε) is > 22 000], with the quantum yields being up to 96%; they show positive solvatochromic effect and Stokes shift of up to 5530 cm^{-1}. Films based on benzotriazole **84a** were also prepared, and their photophysical properties proved to be similar to the properties of solutions. In addition, chemosensory properties for the detection of water in organic solvents were found; in the presence of water, the emission intensity decreased by a factor of eight. The limit of detection achieved using compound **84a** was 0.009% for THF and 0.024% for 1,4-dioxane relative to the solvent volume (Fig. 15).

A research group headed by Liu and Miao[54] reported the synthesis of dipyrrolobenzotriazole-based fluorophores consisting of several (hetero)aromatic rings (Scheme 16). The first step was the Stille reaction of benzotriazole **85** to give intermediate **86**, which was subjected to oxidative cyclization and alkylation to give compound **87**. Product **88** was obtained in high yield by electrophilic substitution at position 2 of the thiophene ring, intramolecular cyclization in the presence of Herrmann's catalyst, and condensation with malononitrile.

Scheme 16

85

86 (67%)

87 (17%)

(*a*) 1) PPh$_3$, *o*-Cl$_2$C$_6$H$_4$, 180 °C;
2) 5-(BrCH$_2$)-*n*-undecane, K$_2$CO$_3$, KI, DMF

1) Bu^{n}Li, THF, −78 °C;
2) DMF, −78 °C to rt;
3) Py, CHCl$_3$, 65 °C

1) 2-Br-4,5-F$_2$C$_6$H$_2$C(O)Cl, AlCl$_3$, DCM;
2) Herrmann's catalyst, (2-MeOC$_6$H$_4$)$_3$P, PivOH, Cs$_2$CO$_3$, PhMe, 115 °C;
3) CH$_2$(CN)$_2$, TiCl$_3$, Py, CHCl$_3$, 65 °C

89 (36%)
λ_{abs} = 770 nm;
λ_{abs} (film) = 831 nm

88 (82%)
λ_{abs} = 780 nm; λ_{abs} (film) = 886 nm

Herrmann's catalyst is *trans*-bis(acetato)bis[*o*-(di-*o*-tolylphosphino)benzyl]dipalladium(II)

Figure 16. Responsivity of organic photodetectors (OPD) with the active layer based on the thiophene-containing polymer **PBDB-T** and compounds **88** and **89** before and after 18 h irradiation at 100 mW cm^{-2} simulating solar light (*a*) and before and after storage under inert atmosphere (N$_2$) for 600 h (*b*); block diagram of operation of OPD devices (*c*) and pulse signal measured with a laser at $\lambda = 808$ nm through a fingertip (the inset shows the OPD image) (*d*). Reproduced from Wang and co-workers[54] with permission from Wiley.
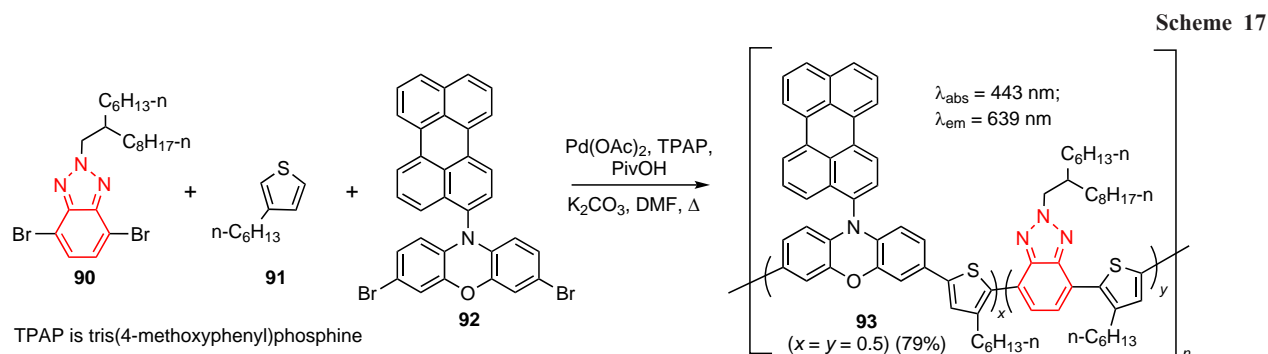
Another derivative **89** was synthesized in a moderate yield by successive formylation and reaction with malononitrile. The obtained products absorb light in the near-IR region: below 780 nm in solution and below 886 nm in films. They have been used as photodetectors with dark current density (J_d) of 2.01×10^{-10} A cm^{-2} at a voltage of 0 V (Fig. 16).

Nguyen and co-workers[55] described a palladium-catalyzed three-component reaction of polymer synthesis from benzotriazole **90** involving thiophene **91** and phenoxazine **92** derivatives (Scheme 17). The molecular mass of polymer **93** was 11 300 a.m.u., and the polymer absorption peaked at 443 nm, while emission occurred in the red spectral range at 639 nm. This fluorophore showed chemosensory properties for the detection of trinitrotoluene (TNT) with a high selectivity and LOD = 10^{-6} M. In addition, this chemosensor is characterized by a response in both the solid state and gaseous phase, which allows it to be used for the analysis of explosives in air and in soil. Using this compound, test strips for fast detection of TNT in various media were manufactured (Fig. 17).
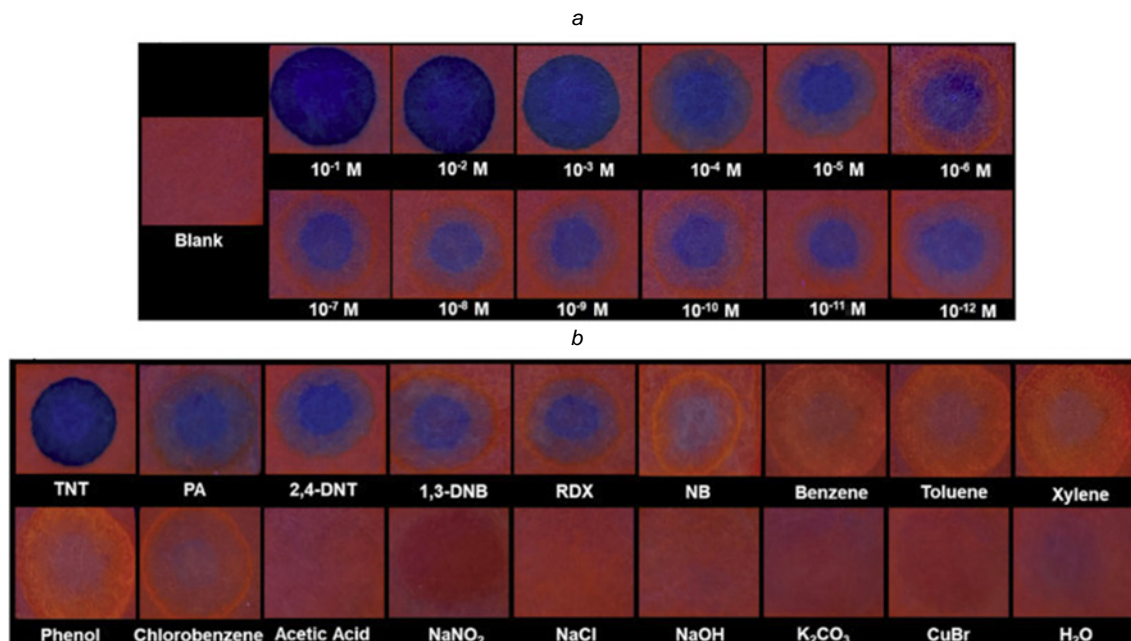
Toppare and co-workers[56] reported the synthesis of ambipolar polymers based on benzotriazole **72** (Scheme 18). In the first step, the starting benzotriazole is alkylated with dodecyl bromide (**94**) and brominated with molecular bromine to give compound

95; this is followed by the Stille reaction with thiophene derivative **96**. Intermediate **97** is again brominated with NBS, and then the Suzuki–Miyaura cross-coupling with boronic acid **98** or the Stille reaction with distannylthiophene **99** is carried out to furnish polymers **100** or **101** in moderate yields. The molecular weights of polymers **100** and **101** are 7000 and 10 000 a.m.u., respectively. These compounds exhibit emission in the range from 573 to 584 nm in solutions and in thin films. Their photophysical and electrochemical characteristics indicate that both polymers are applicable as the working elements of electrochromic indicators (Fig. 18).

Valiyaveettil's research group[57] proposed a method for the synthesis of fluorescent polymers, conjugates of benzotriazole and BF$_2$-dipyrromethene (BODIPY) (Scheme 19). The alkynyl BODIPY derivative **102** reacted with either 4,7-dibromo-2-dodecylbenzotriazole **95** or triazoloquinoxaline **103** to give products **104** or **105** in high yields. The molecular weights of polymers **104** and **105** range from 16 000 to 89 000 a.m.u., and emission occurs in the range of 650–750 nm in solutions and 740–920 nm in films, with the quantum yields reaching 15%. These compounds exhibit chemosensory properties suitable for the detection of benzene, toluene, and other volatile organic solvents.

Scheme 17

TPAP is tris(4-methoxyphenyl)phosphine

I.A.Lavrinchenko, T.D.Moseev, M.V.Varaksin, V.N.Charushin, O.N.Chupakhin
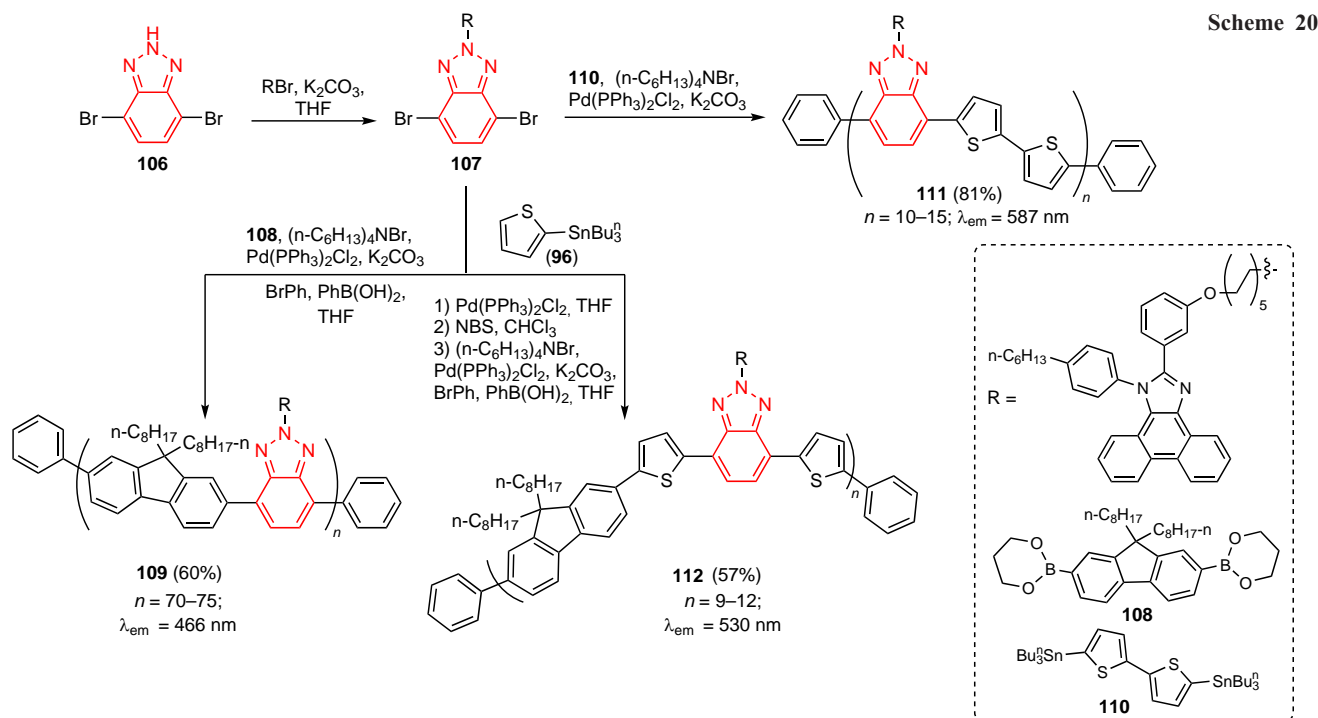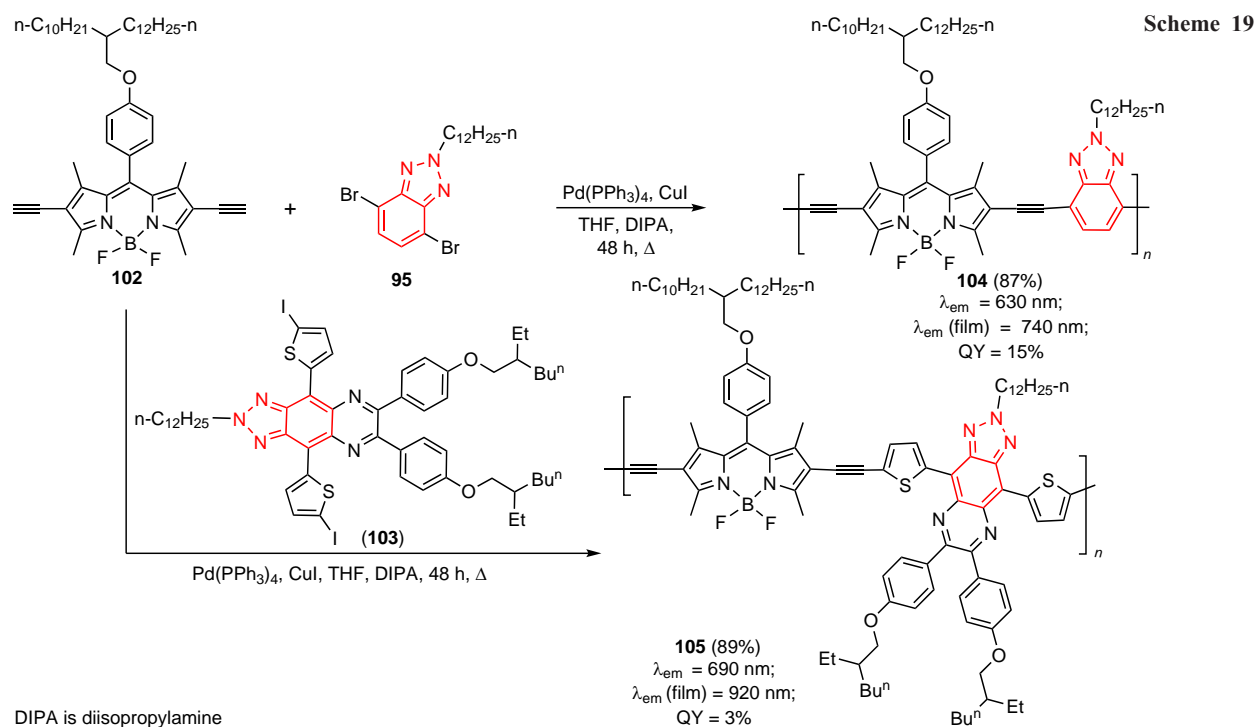*Russ. Chem. Rev.*, 2024, **93** (10) RCR5130

17 of 34

Figure 17. Photographs of paper test strips coated with compound **93** after adding TNT solution in different concentrations (*a*) and selectivity of TNT detection in the presence of other analytes (*b*). Reproduced from Nguyen and co-workers[55] with permission from Elsevier.

Scheme 18
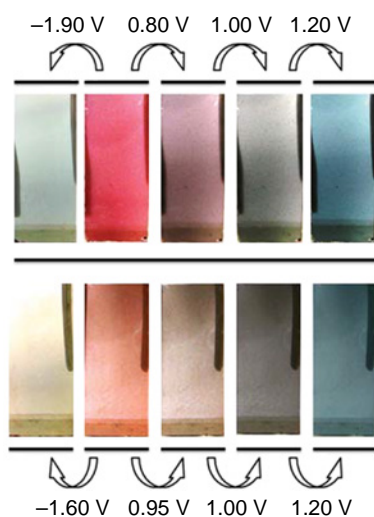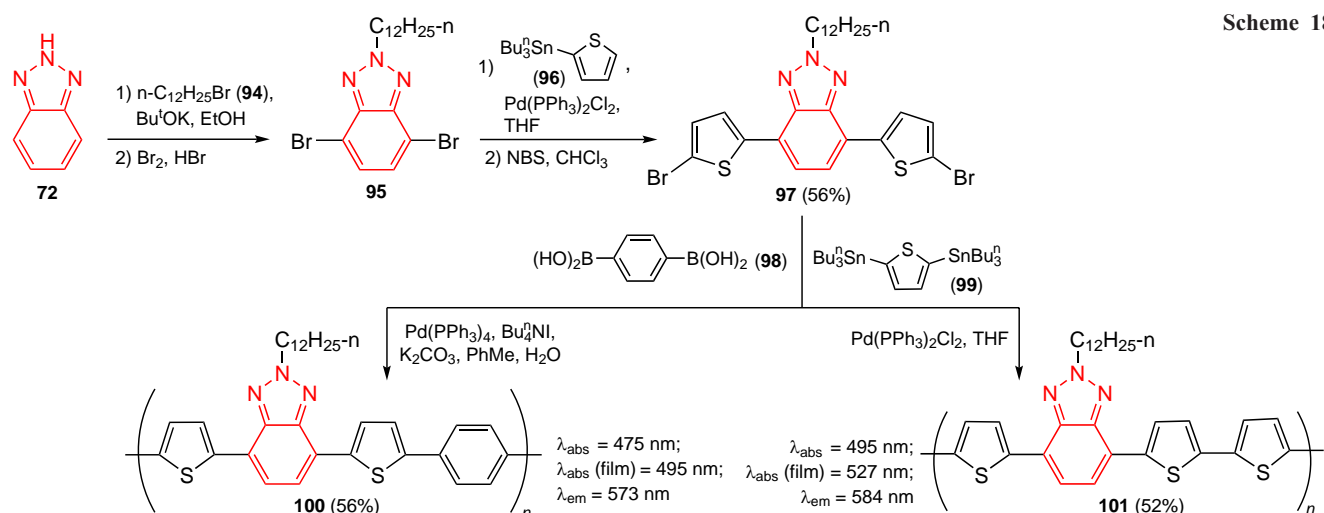
Figure 18. Colours of polymers **100** (*above*) and **101** (*below*) in neutral oxidized state. Reproduced from Toppare and co-workers[56] with permission from the Royal Society of Chemistry.

Toppare and Cirpan's research group[58] prepared three different polymers based on benzotriazole and phenanthroimidazole conjugate (Scheme 20). Initially, benzotriazole **106** reacted with imidazole to give intermediate **107**, which then underwent the Suzuki–Miyaura cross-coupling with diboronic ester **108** or Stille cross-coupling (with reagents **110** or **96**), giving rise to polymers **109**, **111**, and **112**, respectively, in up to 81% yields. The polymers emit light at 466, 530, and 587 nm in solutions, while in the spectra of their films, the bands are red-shifted by 15 to 67 nm. Polymers **109**, **111**, and **112** were found to exhibit electroluminescence, fast switching to the oxidized coloured form under the action of electrical current (switching time τ of 0.2 s), and contrast (*T*, meaning the ratio of the black to white level) of up to 64%, depending on the structure (Fig. 19). The authors proposed to use these polymers as working elements of organic light-emitting diodes.
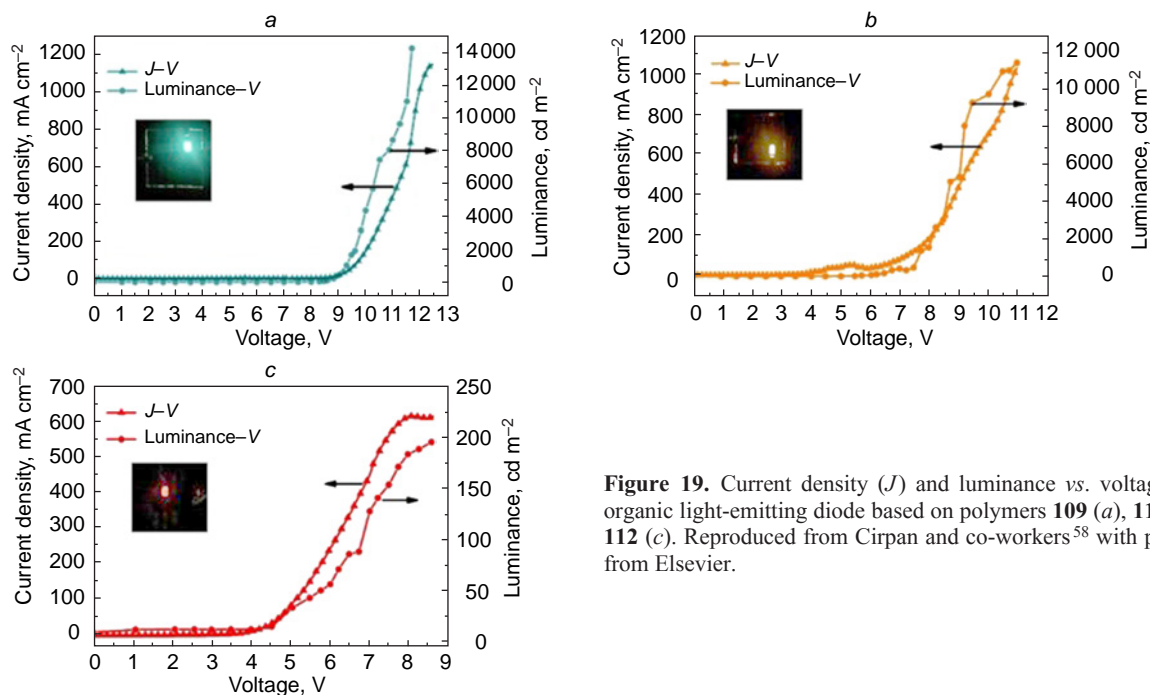
Quan and co-workers[59] developed a benzotriazole-containing fluorescent chemosensor for the determination of cyanide anions

18 of 34

I.A.Lavrinchenko, T.D.Moseev, M.V.Varaksin, V.N.Charushin, O.N.Chupakhin
Russ. Chem. Rev., 2024, **93** (10) RCR5130

Scheme 19

102 + **95** → **104** (87%)
λ_{em} = 630 nm;
λ_{em} (film) = 740 nm;
QY = 15%

103

Pd(PPh$_3$)$_4$, CuI, THF, DIPA, 48 h, Δ

105 (89%)
λ_{em} = 690 nm;
λ_{em} (film) = 920 nm;
QY = 3%

DIPA is diisopropylamine

Scheme 20

106 → **107** → **111** (81%)
n = 10–15; λ_{em} = 587 nm

108, (n-C$_6$H$_{13}$)$_4$NBr,
Pd(PPh$_3$)$_2$Cl$_2$, K$_2$CO$_3$
BrPh, PhB(OH)$_2$,
THF

109 (60%)
n = 70–75;
λ_{em} = 466 nm

112 (57%)
n = 9–12;
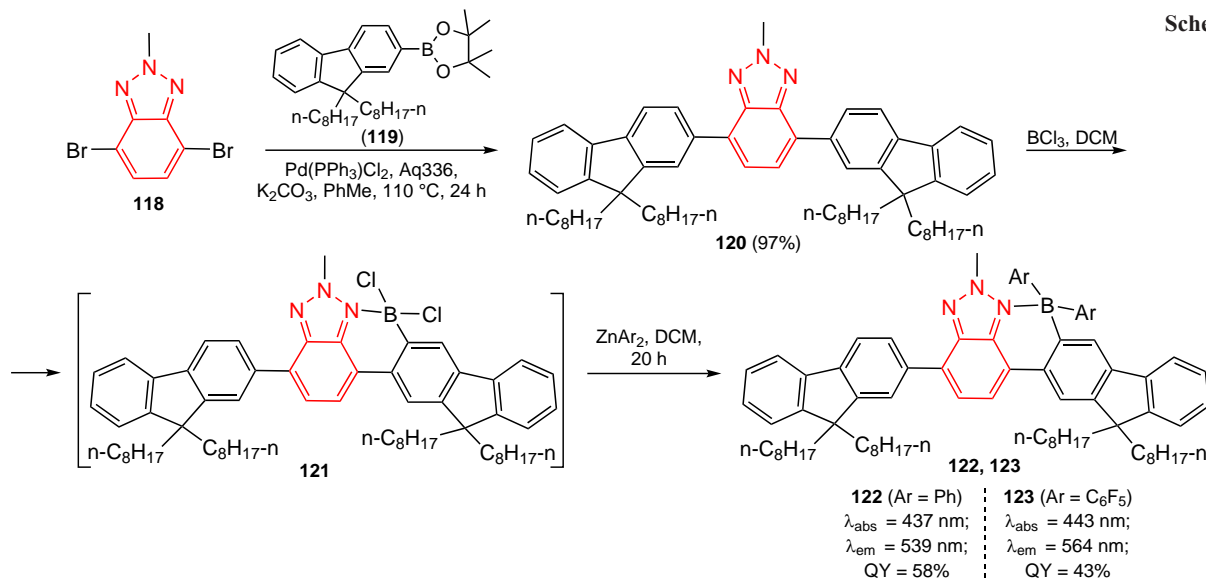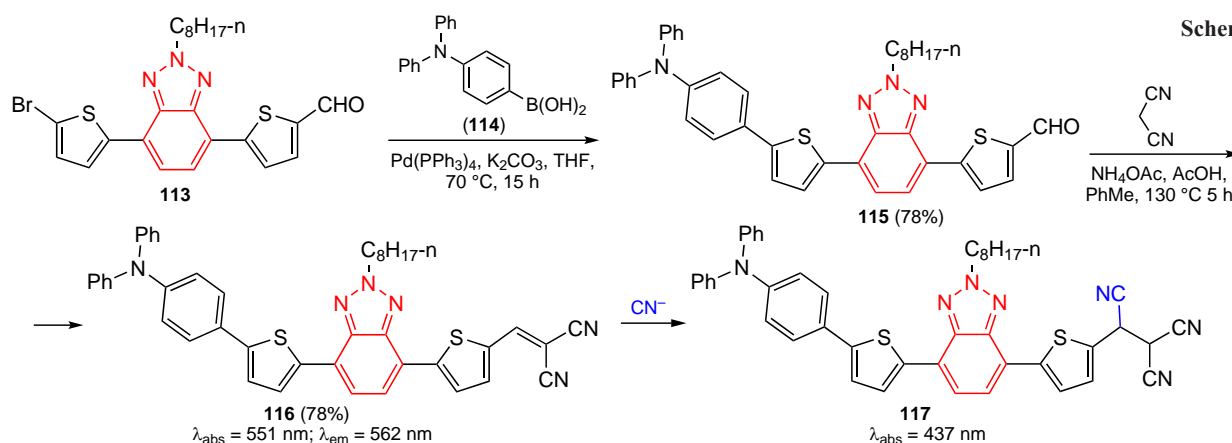λ_{em} = 530 nm

R =

108

110

(Scheme 21). The synthesis consisted of two successive steps; the first one was the Suzuki–Miyaura reaction of benzotriazole **113** with boronic acid **114**, while the subsequent Knoevenagel reaction of aldehyde **115** with malononitrile afforded the target compounds **116** in a high yields. This chemosensor showed high selectivity and sensitivity to CN⁻ ions present in a mixture with other cations and anions (Fig. 20). After the addition of an analytical sample, the cyanide adds to the double bond of compound **116**, and the absorption maximum of adduct **117** is blue-shifted from 551 to 437 nm, with its intensity increasing 17-fold. The limit of detection for this chemosensor is 10^{-8} M, which is much lower than the minimum concentration in

drinking water (1.9 µM) according to World Health Organization safety standards. In addition, it was found that this compound is applicable to detection of cyanide anions in pheochromocytoma cells (PC-12) (Fig. 21).

Turner and Ingleson's research group[60] proposed a method for the synthesis of new fluorophores based on benzotriazole boracycles (Scheme 22). First, benzotriazole **118** underwent the Suzuki–Miyaura reaction with arylboronic acid pinacol ester **119** to give intermediate **120**, which subsequently reacted with BCl$_3$, which resulted in C–H activation of the neighbouring aromatic ring and formation of fused unstable boracycle **121**. The final step was the reaction with diarylzinc

I.A.Lavrinchenko, T.D.Moseev, M.V.Varaksin, V.N.Charushin, O.N.Chupakhin
Russ. Chem. Rev., 2024, **93** (10) RCR5130

19 of 34

Figure 19. Current density (*J*) and luminance *vs.* voltage (*V*) for organic light-emitting diode based on polymers **109** (*a*), **111** (*b*), and **112** (*c*). Reproduced from Cirpan and co-workers[58] with permission from Elsevier.

Scheme 21

Scheme 22

20 of 34

I.A.Lavrinchenko, T.D.Moseev, M.V.Varaksin, V.N.Charushin, O.N.Chupakhin
Russ. Chem. Rev., 2024, **93** (10) RCR5130

Figure 20. Absorption (*a*) and emission (*b*) spectra of compound **116** (in 10 μM concentration) after the addition of CN^- and other anions; diagram of the change in the fluorescence intensity of compound **116** in THF in the presence of only CN^- (*1*), CN^- with Cl^- (*2*), CO_3^{2-} (*3*), ClO_4^- (*4*), HSO_4^- (*5*), Br^- (*6*), AcO^- (*7*), HPO_4^{2-} (*8*), $H_2PO_4^-$ (*9*), NO_3^- (*10*), I^- (*11*), or F^- (*12*) anions, and in the absence of any anions (*13*) (*c*); photographs of solutions of compound **116** with anions under daylight (*d*) and under irradiation with light at $\lambda_{ex} = 430$ nm (*e*). Reproduced from Quan and co-workers[59] with permission from Elsevier.

Figure 21. Confocal fluorescence microscopy images of PC12 cells: bright-field (*a*) and dark-field (*b*) images of cells incubated with compound **116** and merged image (*c*); bright-field (*d*) and dark-field (*e*) images of cells incubated with compound **116** and CN^- and merged image (*f*). $\lambda_{ex} = 488$ nm; $500-550$ nm detection range. Reproduced from Quan and co-workers[59] with permission from Elsevier.

to give two new fluorophores **122** and **123** in 91 and 86% yields. The resulting fluorophores have an absorption band in the range from 437 to 443 nm and an emission band in the range from 539 to 564 nm, with quantum yields being up to 58%.
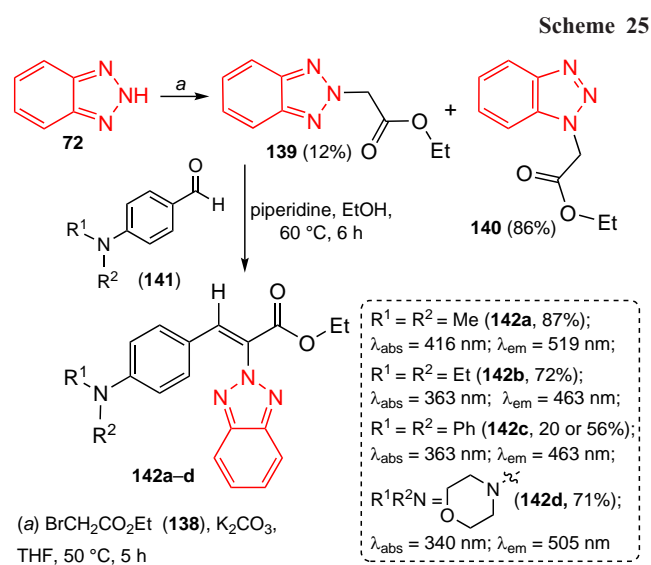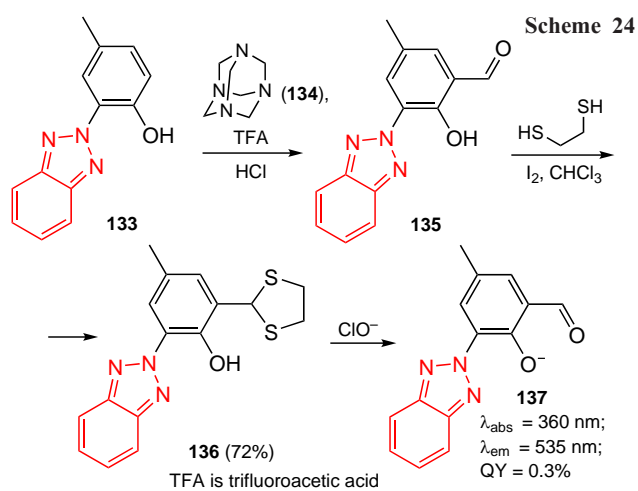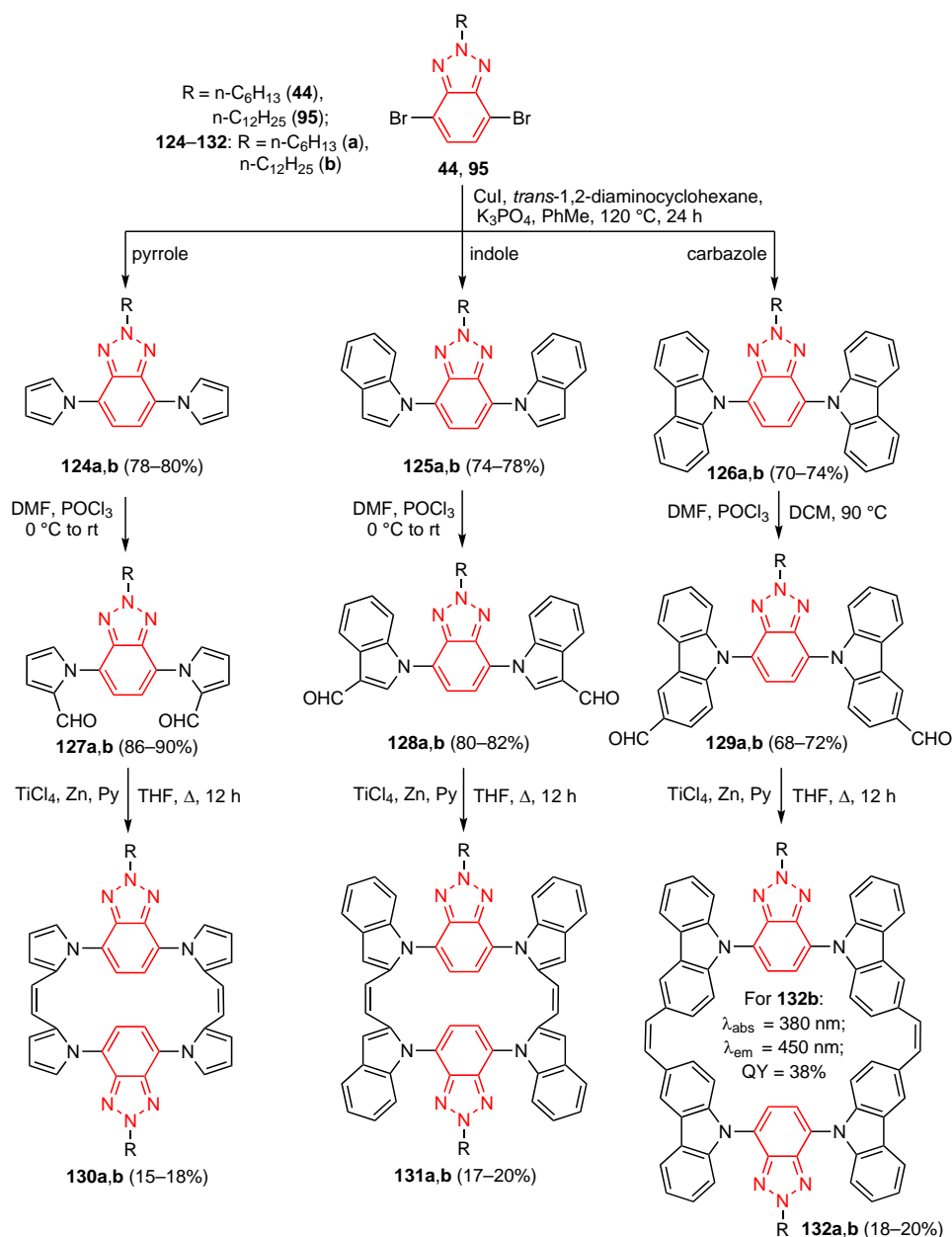
Rajakumar and co-workers[61] synthesized new benzotriazole-based cyclophanes containing a pyrrole, indole, or carbazole moiety (Scheme 23). In the first stage, benzotriazoles **44** and **95** underwent *N*-H-arylation with azaheterocycles in the presence of CuI to give intermediate compounds **124–126**. The subsequent reactions with $POCl_3$ furnished aldehydes **127–129**, which dimerized in the presence of $TiCl_4$ to give macrocycles **130–132** in relatively low yields. Among the obtained compounds, only cyclophane **132b** has luminescent properties with emission maximum at 450 nm and quantum yield of 38%. In addition, this fluorophore exhibits chemosensory properties
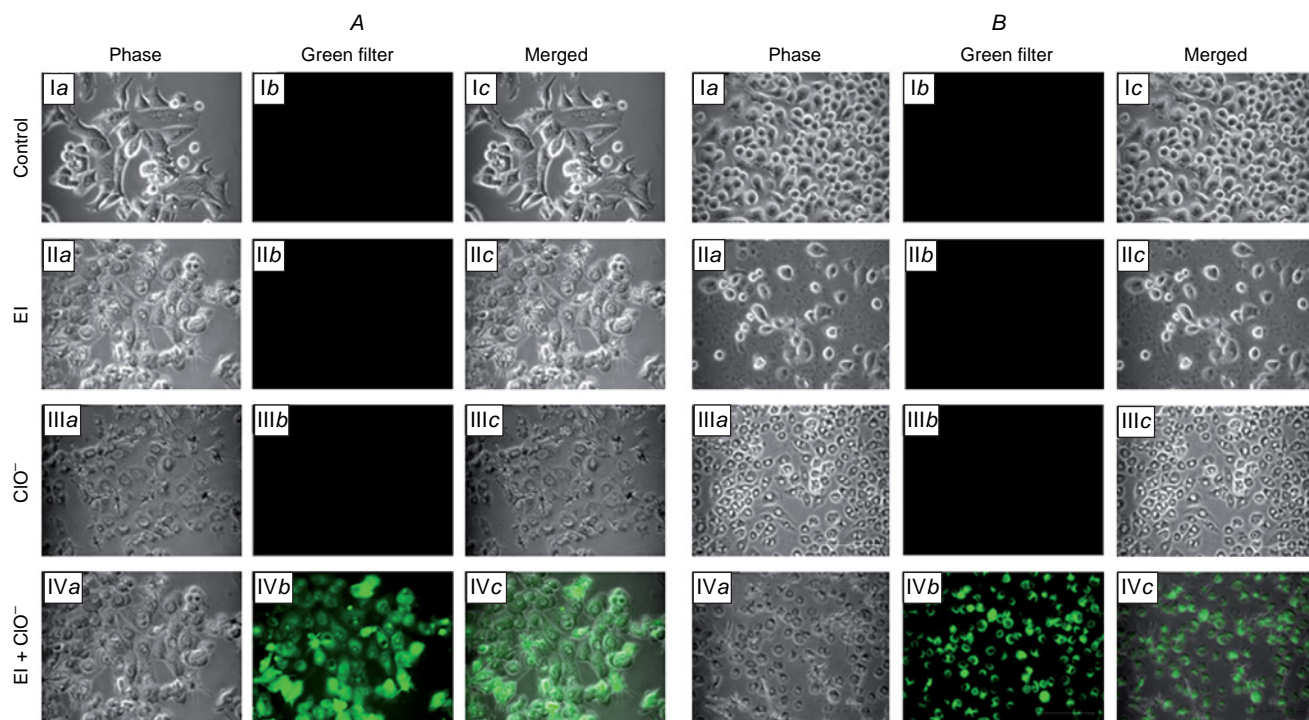
and can be used for the detection of picric acid (LOD = 10^{-6} ppm).

The research group headed by Chattopadhyay[62] developed a synthetic protocol towards benzotriazole-based fluorophores (Scheme 24). In the first step, the formylation of benzotriazole **133** in the presence of hexamethylenetetramine (**134**) gave derivative **135**, which then reacted with ethanedithiol to give the target product **136** in a moderate yield. The obtained fluorophore possesses an absorption maximum at 360 nm and an emission maximum at 535 nm, and exhibits chemosensory properties for the determination of hypochlorite ions (LOD = 10^{-10} M) in the pH range from 4 to 11. Upon the reaction with compound **136**, the 1,3-dithiolane moiety was converted to the carbonyl group giving rise to anion **137**, for which the luminescence quantum yield increased from 0.3 to 5%. In addition, benzotriazole **136** has low cytotoxicity; therefore, it can be used to detect hypochlorite in living cells, for example, during the development of breast cancer (Fig. 22). The authors also fabricated paper strips for the determination of hypochlorite ions in various media (Fig. 23).

Michaelis and Hernandez–Fernandez's research group[63] proposed a method for the synthesis of ethyl (*Z*)-benzotriazolylacrylates (Scheme 25). First, the authors alkylated benzotriazole **72** with ethyl bromoacetate in the presence of K_2CO_3, which afforded isomers **139** and **140** in various yields. Although 1*H*-substituted triazole **140** was formed as the major product, the authors prepared a luminescent system based on 2*H*-triazole. In the presence of piperidine under the action of microwave radiation (MW) or heating, benzotriazole **139** underwent the Knoevenagel reaction with *p*-amino-substituted aromatic aldehydes **141** to give products **142a–d**. In the reaction induced by heating, compound **142c** formed in the lowest yield (20%), which could be markedly increased by conducting MW-assisted reaction at 100 °C for 80 min. For all obtained fluorophores, the absorption peaks in the electronic spectra were located in the range from 340 to 416 nm, while the emission peaks were in the $460-520$ nm range. Compound **142a** was

I.A.Lavrinchenko, T.D.Moseev, M.V.Varaksin, V.N.Charushin, O.N.Chupakhin
Russ. Chem. Rev., 2024, **93** (10) RCR5130

21 of 34

R = n-C$_6$H$_{13}$ (**44**),
n-C$_{12}$H$_{25}$ (**95**);
124–132: R = n-C$_6$H$_{13}$ (**a**),
n-C$_{12}$H$_{25}$ (**b**)

44, **95**

CuI, *trans*-1,2-diaminocyclohexane,
K$_3$PO$_4$, PhMe, 120 °C, 24 h

pyrrole | indole | carbazole

124a,b (78–80%) | **125a,b** (74–78%) | **126a,b** (70–74%)

DMF, POCl$_3$
0 °C to rt | DMF, POCl$_3$
0 °C to rt | DMF, POCl$_3$ | DCM, 90 °C

127a,b (86–90%) | **128a,b** (80–82%) | **129a,b** (68–72%)

TiCl$_4$, Zn, Py | THF, Δ, 12 h | TiCl$_4$, Zn, Py | THF, Δ, 12 h | TiCl$_4$, Zn, Py | THF, Δ, 12 h

130a,b (15–18%) | **131a,b** (17–20%) | For **132b**:
λ$_{abs}$ = 380 nm;
λ$_{em}$ = 450 nm;
QY = 38%

132a,b (18–20%)

133

(**134**),
TFA
HCl

135

HS⁓SH
I$_2$, CHCl$_3$

136 (72%)
TFA is trifluoroacetic acid

ClO⁻

137
λ$_{abs}$ = 360 nm;
λ$_{em}$ = 535 nm;
QY = 0.3%

72 — *a* → **139** (12%) + **140** (86%)

piperidine, EtOH,
60 °C, 6 h

(**141**)

142a–d

R^1 = R^2 = Me (**142a**, 87%);
λ$_{abs}$ = 416 nm; λ$_{em}$ = 519 nm;
R^1 = R^2 = Et (**142b**, 72%);
λ$_{abs}$ = 363 nm; λ$_{em}$ = 463 nm;
R^1 = R^2 = Ph (**142c**, 20 or 56%);
λ$_{abs}$ = 363 nm; λ$_{em}$ = 463 nm;
R^{1}R^{2}N = (morpholine) (**142d**, 71%);
λ$_{abs}$ = 340 nm; λ$_{em}$ = 505 nm

(*a*) BrCH$_2$CO$_2$Et (**138**), K$_2$CO$_3$,
THF, 50 °C, 5 h

22 of 34

I.A.Lavrinchenko, T.D.Moseev, M.V.Varaksin, V.N.Charushin, O.N.Chupakhin
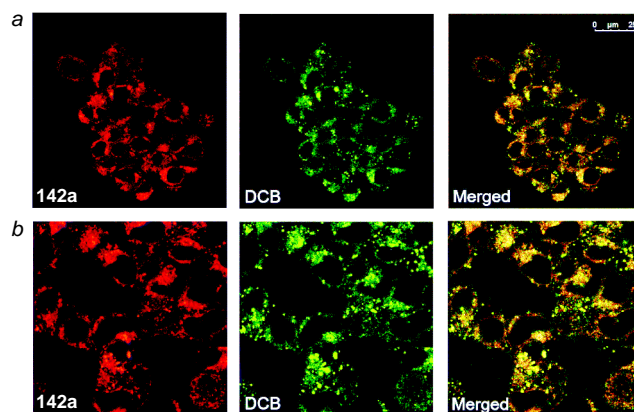*Russ. Chem. Rev.*, 2024, **93** (10) RCR5130

Figure 22. Confocal fluorescence microscopy images of MCF-7 (*A*) and J774A1 (*B*) cells: (I) control group; (II) cells incubated with compound **136**; (III) cells treated with ClO⁻ anions; (IV) cells treated with ClO⁻ anions and then with compound **136**; phase-contrast images (*a*) and fluorescence images (λ_{ex} = 480 nm, λ_{em} = 520 nm) (*b*), and merged image (*c*) are given. A DMi8 fluorescence microscope with a Plan Fluor objective (40X, NA 0.60), Leica Microsystems GmbH. Reproduced from Chattopadhyay and co-workers[62] with permission from the Royal Society of Chemistry.
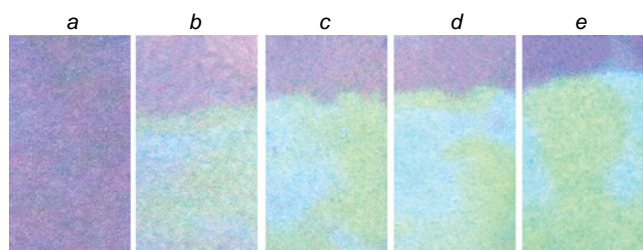
Figure 23. Photographs of the paper strips treated with compound **136** directly (*a*) and with addition of ClO⁻ in concentration of 50 (*b*), 100 (*c*), 200 (*d*), or 300 mM (*e*). Reproduced from Chattopadhyay and co-workers[62] with permission from the Royal Society of Chemistry.

Figure 24. Confocal fluorescence microscopy images of HEK293T cells incubated with compound **142a** and DCB (dextran–cascade blue) for 16 h (*a*) and for 20 h followed by incubation with compound **142a** alone in 10 μM concentration for 4 h (*b*). Reproduced from Michaelis and co-workers[63] with permission from the Royal Society of Chemistry.

found to possess low cytotoxicity against HEK293T cells (IC_{50} = 50 μM) and to be applicable as a fluorescent probe for bioimaging (Fig. 24).
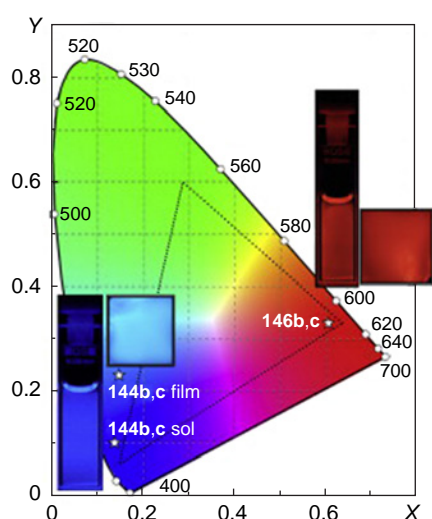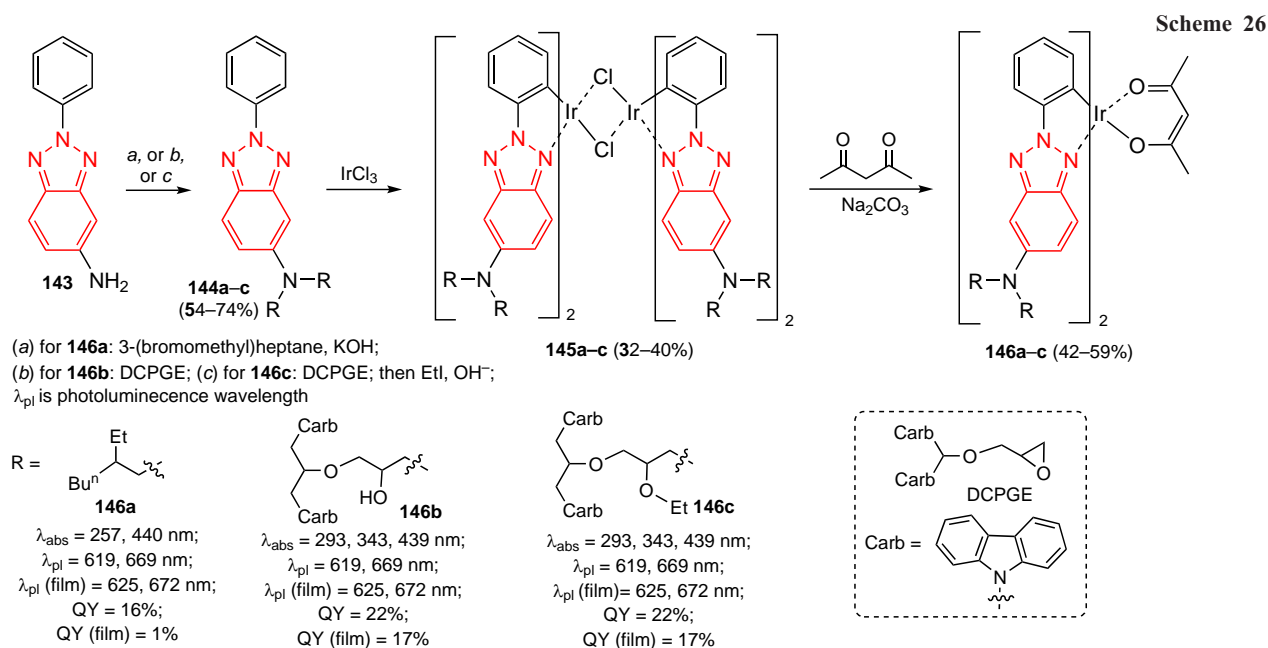
A few papers are devoted to luminescent iridium complexes in which a 2*H*-functionalized 1,2,3-benzotriazole moiety is present as a ligand. Getautis's research group[64] proposed a synthesis of these complexes from 2-phenyl-1,2,3-benzotriazoles containing carbazole moieties (Scheme 26). The desired ligand was obtained by alkylating the amino group in the starting benzotriazole **143**; and the target iridium(III) complex was obtained from products **144** *via* two steps. The first step was the synthesis of dimeric coordination compound L₄Ir₂Cl₂ (**145**), which was then treated with acetylacetone being thus converted to the metal complexes L₂Ir(acac) (acac is acetylacetonate) (**146a–c**). The resulting compounds are readily soluble (in organic solvents); they show red phosphorescence with an emission maximum at 650 nm, lifetime of 5.7 ms, and quantum yields of 22 and 17% for solutions and solid samples (films and

powders), respectively. Experimental red OLEDs with up to 22 V voltage at the maximum brightness and quantum efficiency of up to 1.8% were developed on the basis of these compounds (Fig. 25).

A method for the synthesis of iridium complexes based on isoquinolin-4-ylbenzotriazole with picolinic acid and its derivatives (Scheme 27) has been proposed.[65–67] The synthesis of the target ligand included the Suzuki–Miyaura reaction involving triarylamine type boronic acid **147** and dibromobenzotriazole **148**, the subsequent borylation of bromide

I.A.Lavrinchenko, T.D.Moseev, M.V.Varaksin, V.N.Charushin, O.N.Chupakhin
Russ. Chem. Rev., 2024, **93** (10) RCR5130

23 of 34

Scheme 26

(*a*) for **146a**: 3-(bromomethyl)heptane, KOH;
(*b*) for **146b**: DCPGE; (*c*) for **146c**: DCPGE; then EtI, OH⁻;
λ_{pl} is photoluminecence wavelength

R =

146a
λ_{abs} = 257, 440 nm;
λ_{pl} = 619, 669 nm;
λ_{pl} (film) = 625, 672 nm;
QY = 16%;
QY (film) = 1%

146b
λ_{abs} = 293, 343, 439 nm;
λ_{pl} = 619, 669 nm;
λ_{pl} (film) = 625, 672 nm;
QY = 22%;
QY (film) = 17%

146c
λ_{abs} = 293, 343, 439 nm;
λ_{pl} = 619, 669 nm;
λ_{pl} (film)= 625, 672 nm;
QY = 22%;
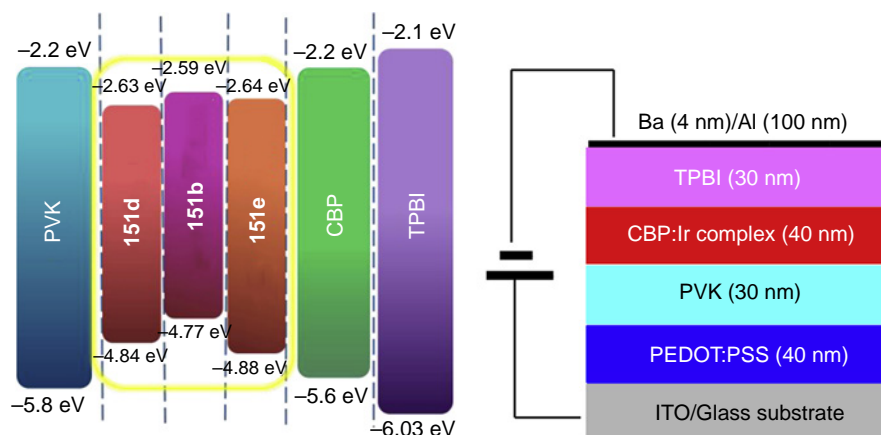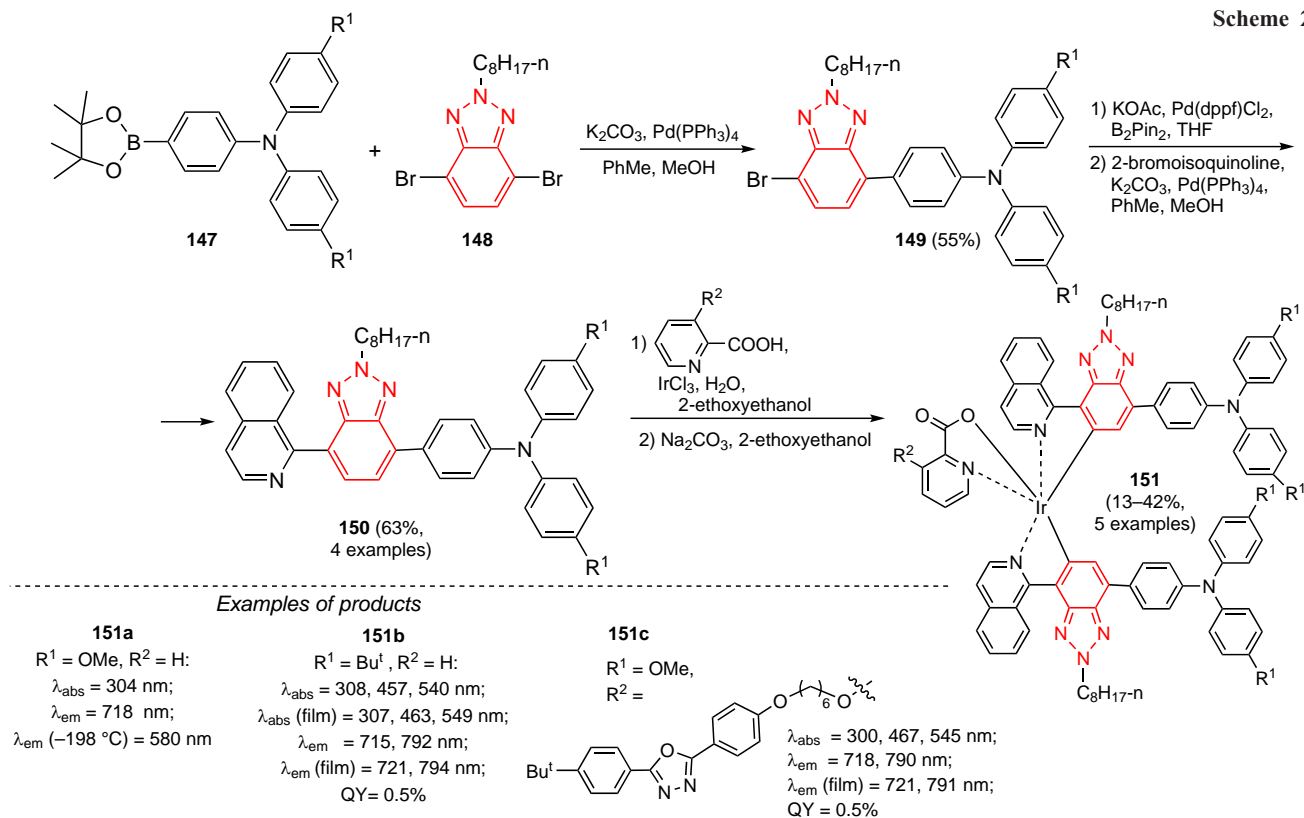QY (film) = 17%

DCPGE

Carb =

Figure 25. Chromaticity diagram of iridium complexes **146**. The vertices of the triangle indicate coordinates of the RGB primary colours specified by the HDTV standard. Reproduced from Getautis and co-workers[64] with permission from Elsevier.

149, and one more Suzuki–Miyaura reaction with 2-bromoisoquinoline to form product **150**. The complex is synthesized by a two-step procedure similar to that described in the above example; altogether five compounds **151** were isolated in moderate yields. The products showed emission in the electronic spectra up to 792 nm in solutions and up to 794 nm in films, with the fluorescence quantum yields for the films being 0.5%. OLED devices with quantum efficiency of 1.15% were fabricated on the basis of metal complexes **151** (Fig. 26). However, this quantum efficiency proved to be markedly lower than these values for known OLEDs (10–30%).[68] It should be noted that at –198 °C, the emission band of compound **151a** was blue-shifted to 580 nm. The fluorescence properties of thin films did not differ from those of solutions. Experimental red-emitting PLED devices with quantum efficiency of up to 0.4% were developed on the basis of these metal complexes (Figs 27, 28; OXD-7 is 1,3-bis[2-(4-*tert*-butylphenyl)-1,3,4-oxadiazol-5-yl] benzene, TPBI is 1,3,5-tris(1-phenyl-1*H*-benzimidazol-2-yl) benzene, ITO is indium tin oxide, PEDOT:PSS is poly(3,4-ethylenedioxythiophene)-poly(styrene sulfonate), PVK is poly(9-vinylcarbazole)).
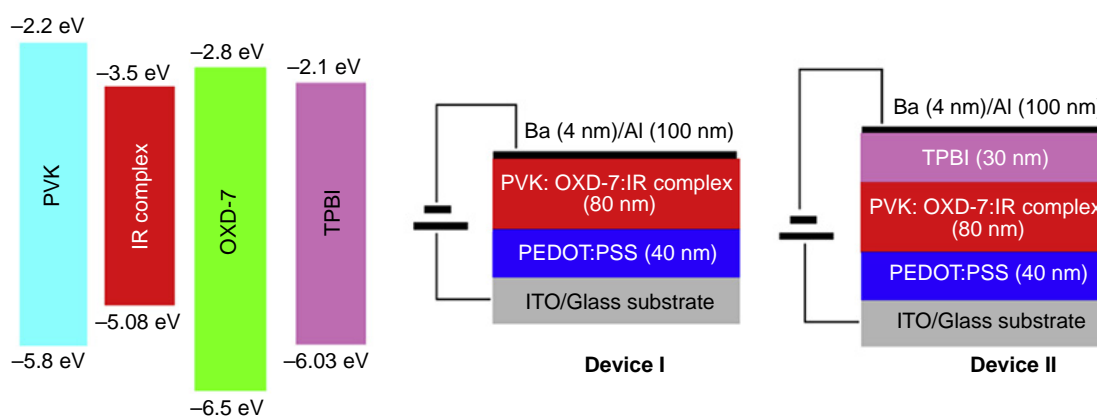

Figure 26. Energy level diagram (on the left) and structure of PLED device based on compound **151a**. Reproduced from Chattopadhyay and co-workers[62] with permission from Elsevier.

Scheme 27

Examples of products

151a
R^1 = OMe, R^2 = H:
λ_{abs} = 304 nm;
λ_{em} = 718 nm;
λ_{em} (−198 °C) = 580 nm

151b
R^1 = Bu^t, R^2 = H:
λ_{abs} = 308, 457, 540 nm;
λ_{abs} (film) = 307, 463, 549 nm;
λ_{em} = 715, 792 nm;
λ_{em} (film) = 721, 794 nm;
QY = 0.5%

151c
R^1 = OMe,
R^2 =
λ_{abs} = 300, 467, 545 nm;
λ_{em} = 718, 790 nm;
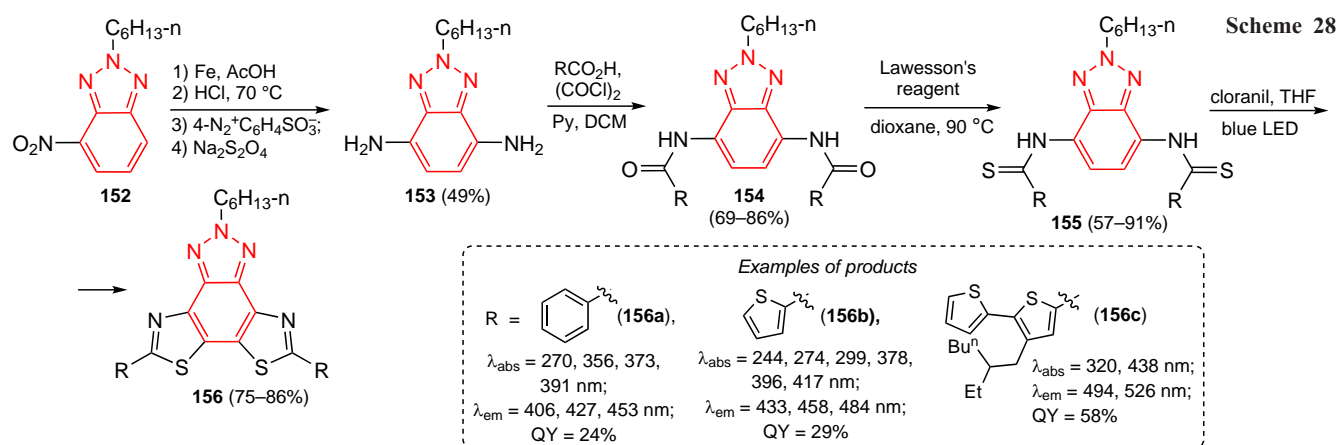λ_{em} (film) = 721, 791 nm;
QY = 0.5%

Figure 27. Energy level diagram (on the left) and structure of organic light-emitting diodes based on compounds **151b**, **151d** (R^1 = R^2 = H) and **151e** (R^1 = F, R^2 = H). Reproduced from Yu *et al.*[67] with permission from Elsevier.
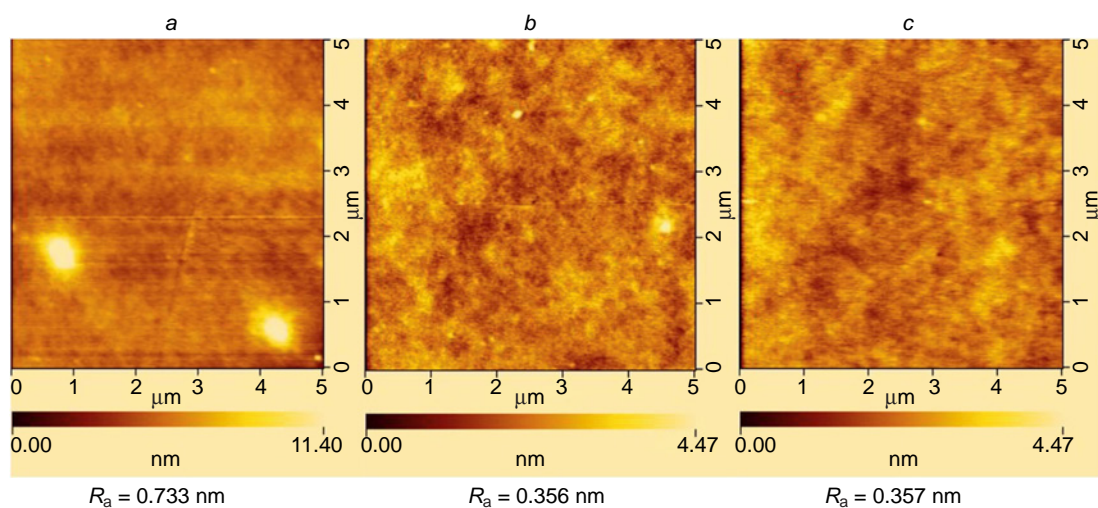
Figure 28. Atomic force microscopy images of 4,4′-bis(*N*-carbazolyl)-1,1′-biphenyl (CBP) films doped with compounds **151b,d,e** (*a−c*, respectively). R_a is the surface roughness. Reproduced from Yu *et al.*[67] with permission from Elsevier.

I.A.Lavrinchenko, T.D.Moseev, M.V.Varaksin, V.N.Charushin, O.N.Chupakhin
Russ. Chem. Rev., 2024, **93** (10) RCR5130

25 of 34

Scheme 28

Examples of products

R = phenyl (**156a**),
λ_{abs} = 270, 356, 373, 391 nm;
λ_{em} = 406, 427, 453 nm;
QY = 24%

thiophene (**156b**),
λ_{abs} = 244, 274, 299, 378, 396, 417 nm;
λ_{em} = 433, 458, 484 nm;
QY = 29%

(**156c**)
λ_{abs} = 320, 438 nm;
λ_{em} = 494, 526 nm;
QY = 58%

Fisyuk's research group[69] reported fluorophores based on bis(thiazolo)benzotriazole (Scheme 28). The target photoactive molecules were obtained from 2-hexyl-4-nitrobenzotriazole **152** by a six-step procedure. One amino group was formed upon the reduction of the nitro group with iron filings in acetic acid, while the other one resulted from the azo coupling reaction followed by reduction with sodium dithionite. The subsequent acylation of compound **153**, thionation of diamides **154** with Lawesson's reagent [2,4-bis(4-methoxyphenyl)-1,3,2,2,4-dithiadiphospho-phetane 2,4-disulfide], and intramolecular cyclization of thioamides **155** furnished products **156a – c**. These luminophores exhibit two to five absorption peaks in the electronic spectra between 244 and 448 nm, emission in the 406–526 nm range, and quantum yields of up to 58%. In addition, electro-polymerization of these compounds resulted in the formation of polymers exhibiting red to blue-green electroluminescence, characterized by high thermal stability, and applicable as electrochromic devices (Fig. 29).

Lee and co-workers[70] reported the synthesis and photophysical characteristics of 2*H*-functionalized bis(triazolo)-benzenes (Scheme 29). These fluorophores were prepared in 46 to 74% yields by azo-coupling of benzotriazole **157** with *para*-substituted anilines followed by cyclization of intermediates **158** to form heterocycles **159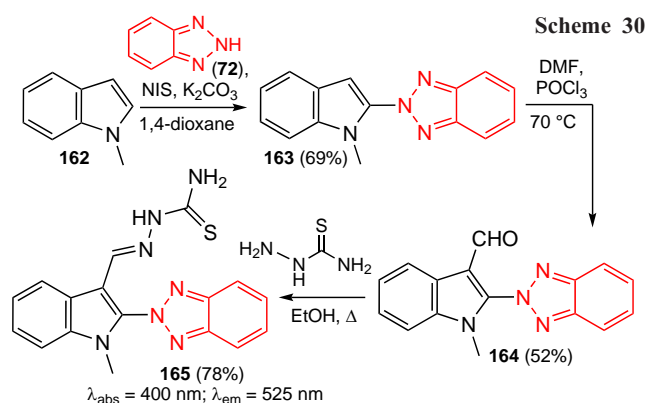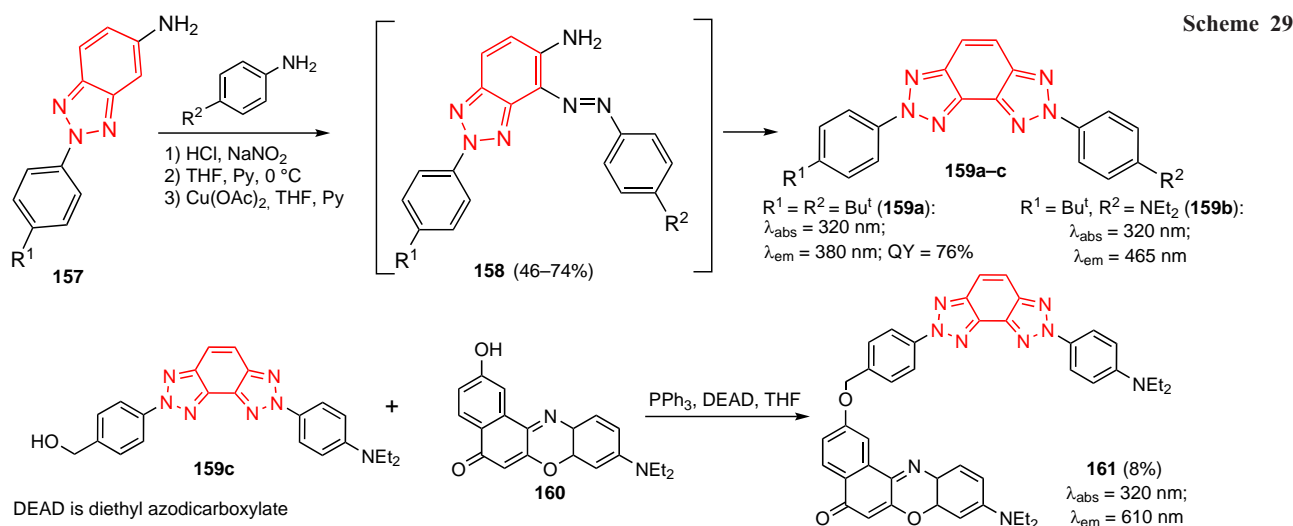**. The products emit in the blue and green regions of the visible spectrum with wavelengths ranging from 380 to 465 nm. Compound **159b** show response to the change in the pH of the medium: increase in the concentration of protons in solution induces a blue shift of the emission peaks from 465 to 385 nm. The reaction of derivative **159c** with phenoxazine **160** gives conjugate **161** with emission peak at >600 nm wavelength.

Lv *et al.*[71] developed a method for the synthesis of fluoro-phore based on 2-indolylbenzotriazole (Scheme 30). First, benzotriazole **72** was arylated with 1-methylindole (**162**) in the presence of *N*-iodosuccinimide; the subsequent Vilsmeier–Haack reaction of compound **163** resulted in the formation of aldehyde **164**, which reacted with thiosemicarbazide to give the target product **165**. The obtained luminophore has an absorption peak at 400 nm and emission in the range from 425 to 700 nm. This compound was found to exhibit chemosensory properties suitable for the detection of cations: for example, in the presence of Ag^+, the fluorescence intensity increases eight-fold. Conversely, in the presence of Hg^{2+} and Cu^{2+} ions, the fluorescence intensity decreases four-fold. A considerable drawback of the obtained chemosensors is that the simultaneous detection of any pair of the above ions is impossible.

A few research groups used a similar synthetic approach to prepare fluorophores based on 2-substituted naphtho[1,2-*d*]-
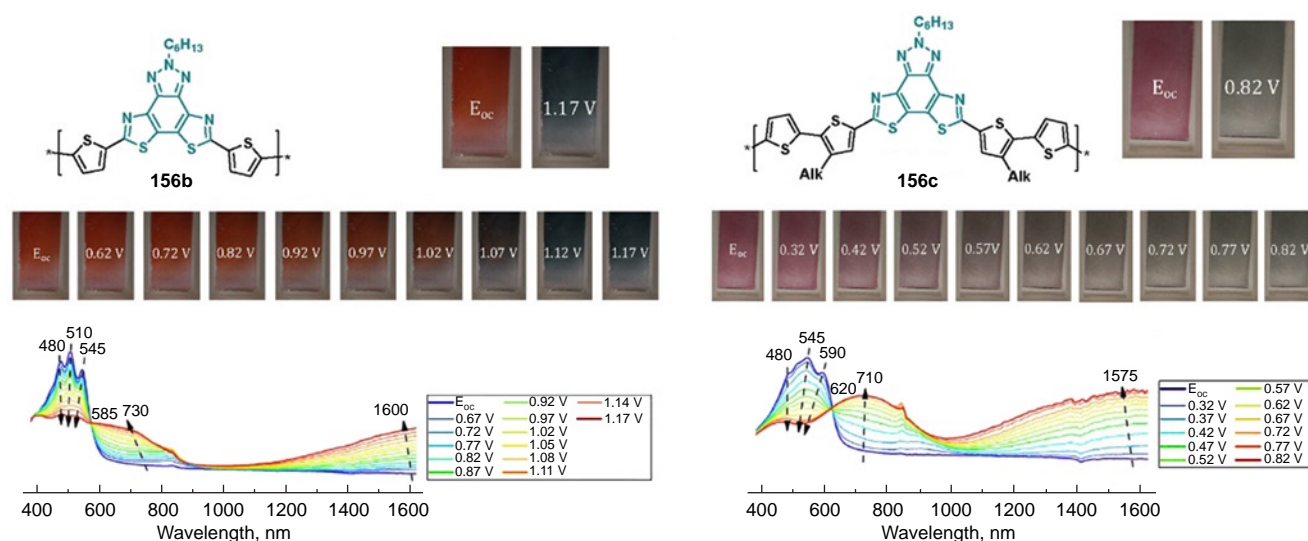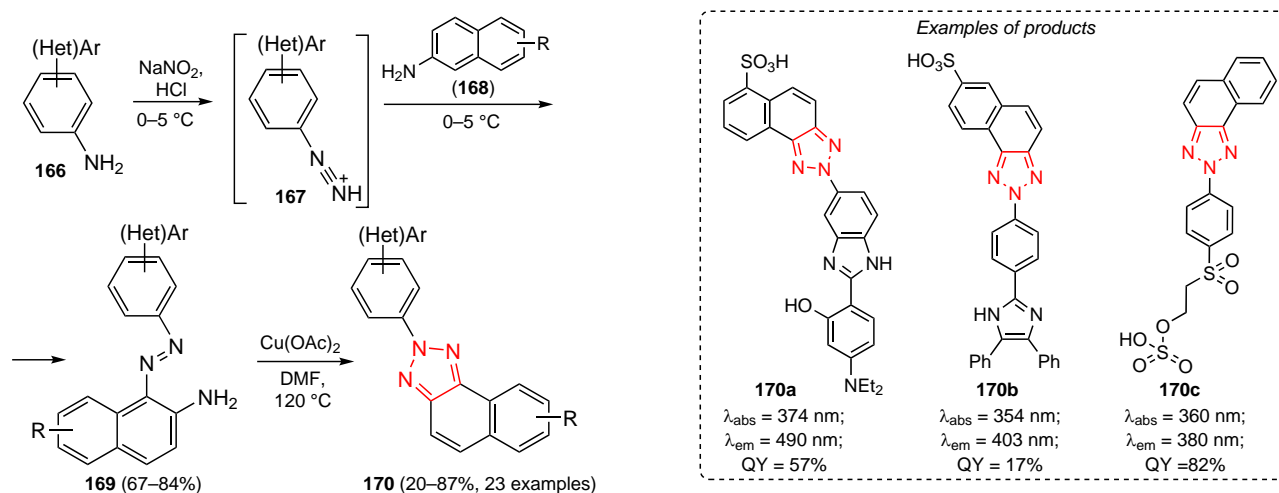

Figure 29. Absorption spectra of thin films of polymers **156b** (*above*) and **156c** (*below*) measured in the p-doping mode and photographs of films with voltage-dependent emission. Reproduced from Fisyuk and co-workers[69] with permission from the American Chemical Society.

Scheme 29

DEAD is diethyl azodicarboxylate

Scheme 30

obtained conjugates with imidazole in 79 to 87% yields. These fluorophores absorb in the 335–373 nm range and emit in the blue region (370 to 470 nm); the quantum yields are 14 to 19%. Under the supervision of Oliveira–Campos,[73] fluorescent compounds containing a naphthalene-fused triazole moiety (20 to 49% yield) were obtained. These fluorophores show emission in the 360–380 nm range, with the quantum yields being 83%.

Thus, this Section presents methods for the synthesis of 2*H*-1,2,3-benzotriazole derivatives that exhibit chemosensory properties and are used as agents for bioimaging, phototherapy and as components of light-emitting and electrochromic devices. The main approach to compounds of this class is cyclization of diazonium salts followed by functionalization, which involves either the nitrogen atom in position 2, being performed by (hetero)arylation, or the annulated ring, being usually performed by Suzuki–Miyaura or Stille cross-coupling reaction. The presence of several annulated rings enables modification of these molecules, which can be used for the targeted design of photoactive compounds with valuable properties. A promising but not yet fully elaborated lines of research are the synthesis of polymers meant for bioimaging of various intracellular processes or detection of pathologies at early stages and the synthesis of ligands for second- and third-generation organic light-emitting diodes based on transition metal complexes.
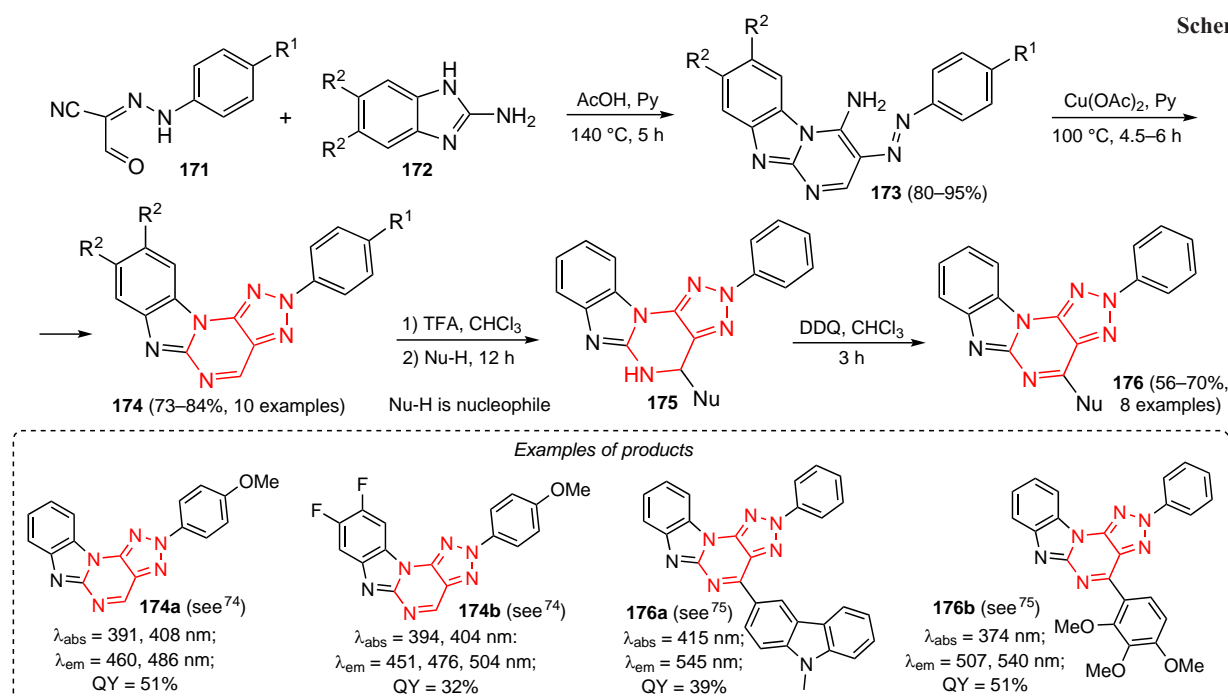
[1,2,3]triazoles. In the first step, arene **166**, containing an amino group, reacted with sodium nitrite and hydrochloric acid to give diazonium salt **167**; this product underwent azo coupling reaction with naphthalimines **168** to yield compounds **169**, which cyclized to the target products **170** (Scheme 31). In particular, Sekar's research group[72] proposed a method for the synthesis of benzimidazole and benzotriazole conjugates. The resulting fluorophores possess blue and green emission and are characterized by quantum yields of 20 to 57%. The same authors

Scheme 31

I.A.Lavrinchenko, T.D.Moseev, M.V.Varaksin, V.N.Charushin, O.N.Chupakhin
Russ. Chem. Rev., 2024, **93** (10) RCR5130

27 of 34

Scheme 32

Examples of products

174a (see [74])
λ_{abs} = 391, 408 nm;
λ_{em} = 460, 486 nm;
QY = 51%

174b (see [74])
λ_{abs} = 394, 404 nm:
λ_{em} = 451, 476, 504 nm;
QY = 32%

176a (see [75])
λ_{abs} = 415 nm;
λ_{em} = 545 nm;
QY = 39%

176b (see [75])
λ_{abs} = 374 nm;
λ_{em} = 507, 540 nm;
QY = 51%

5. Heteroannulated and miscellaneous derivatives of 2*H*-aryl-1,2,3-triazoles

This Section addresses the synthesis of 2*H*-1,2,3-triazole-based fluorophores containing a heterocyclic annulated moiety and derivatives that have not been described above. The key approaches to the preparation of these structures are intramolecular cyclization reactions.
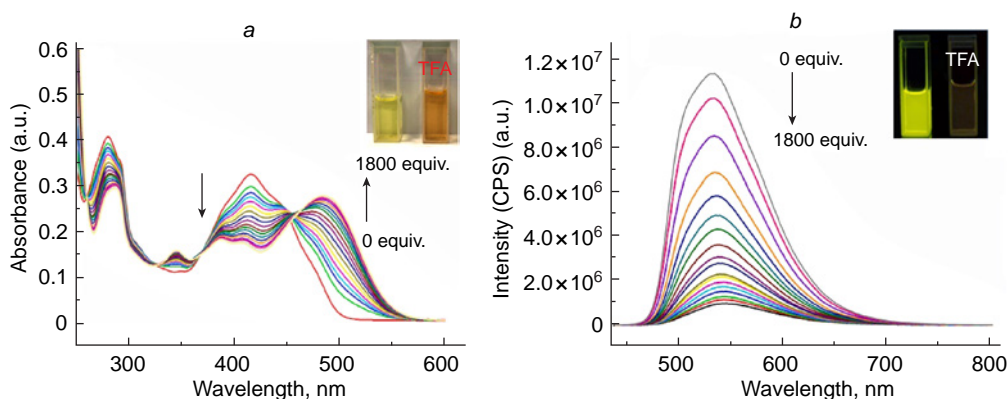
The research group of Fedotov and Belskaya [74] proposed an approach to the synthesis of new polycyclic 8-azapurines (Scheme 32) with a triazole ring. This approach includes the condensation of aminobenzoimidazoles **171** with 3-oxo-2-phenylazopropionitrile **172** and the subsequent oxidative cyclization of compounds **173** in the presence of copper(II) acetate to give products **174a**–**e** in moderate to high yields. The resulting fluorophores absorb in the 379–399 nm range, emit in the 471–505 nm range, and have lifetimes of up to 4.7 ns and quantum yields of up to 60%. Charushin and co-workers [75] showed that it is possible to perform further modification of compounds by nucleophilic substitution of hydrogen (S_N^H). The substitution at the H–C=N bond in the pyrimidine ring on treatment with various nucleophiles (thiophene, phenol, indole) affords stable σ-adducts **175**, which are then oxidized with

2,3-dichloro-5,6-dicyano-1,4-benzoquinone (DDQ). Functionalized compounds **176a,b** emit in the range from 507 to 570 nm, with the quantum yields being up to 60%. In addition, the obtained luminophores were found to exhibit acidochromism and AIE effect. In the former case, the emission intensity considerably decreases when protons are present in the system, while the formation of aggregates induces a blue shift of the emission (Figs 30 and 31).

Verbitsky *et al.*[76] synthesized triazoles with an annulated triazolopyridine ring containing electron-donating groups in the molecules (Scheme 33). The first step is the reaction of **177** with isobutyl bromide, which affords 2*H*-substituted compound **178**. The subsequent nucleophilic substitution under the action of thiophene, bromination, oxidation of intermediate **179**, and the Suzuki–Miyaura reaction involving bromide **180** and arylboronic acid picolinate **181** lead to target products **182** in 20–49% yields. The fluorophores prepared in this way emit in the 562–619 nm range with quantum yields of up to 12%. The authors found chemosensory properties for detection of nitroaromatic compounds such as DNT (2,4-dinitrotoluene), 2,4-dinitroanisole, picric acid, trinitroresorcinol, 1,3,5-triethoxy-2,4,6-trinitrobenzene, 2,4,6-trinitrotoluene, and nitrobenzene. The limits of
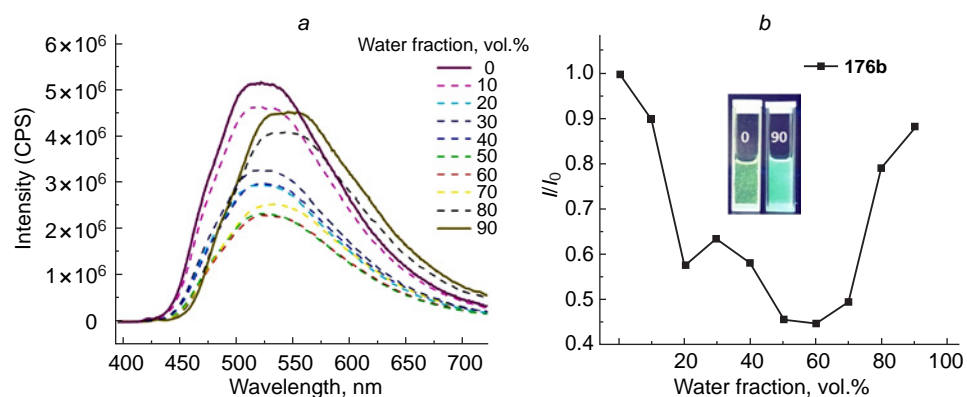
Figure 30. Emission spectra of compounds **176b** in a MeOH–water solution with different component contents (vol.%) (*a*) and I/I_0 ratio (I_0 is the fluorescence intensity in pure MeOH) *vs.* the fraction of water (vol.%) (*b*); the inset shows photographs of the emission for solutions of compound **176b** (10^{-5} M) in methanol (0) and in water with 10% MeOH under UV irradiation (λ_{ex} = 365 nm). Reproduced from Charushin and co-workers [75] with permission from Elsevier.

I.A.Lavrinchenko, T.D.Moseev, M.V.Varaksin, V.N.Charushin, O.N.Chupakhin
*Russ. Chem. Rev.*, 2024, **93** (10) RCR5130

Figure 31. Absorption (*a*) and emission (*b*) spectra of compound **176a** upon the addition of TFA. The inserts show the photographs of solutions of compound **176a** alone (*on the left*) and in the presence of TFA (*on the right*). Reproduced from Charushin and co-workers[75] with permission from Elsevier.
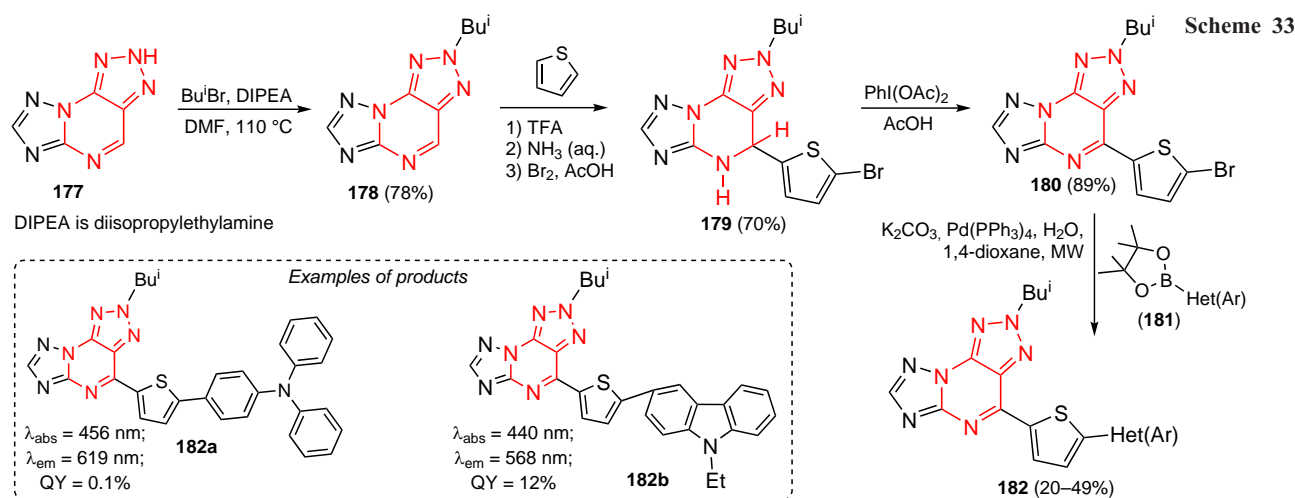
Scheme 33

detection vary in the range from 10^{-1} to 10^{-5} mol L^{-1}, depending on the analyte (Fig. 32).

Nenajdenko's research group[77] described a three-step synthesis of a 1,2,3-triazole-based heterocyclic system (Scheme 34). First, *N*-substituted hydrazones **185** were obtained by condensation of carbonylacetylenes **183** with arylhydrazines **184**. The subsequent alkyl halogenation (intermediate **186**),
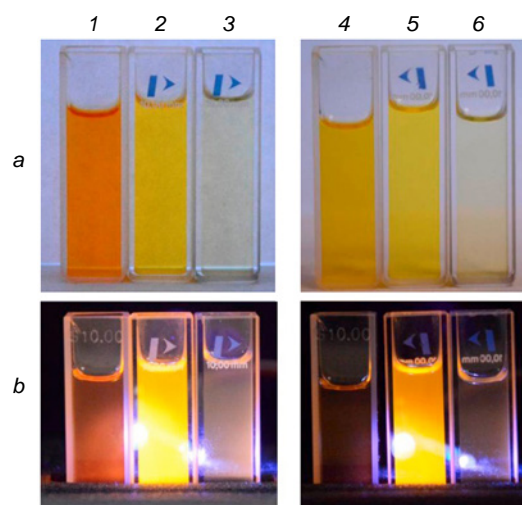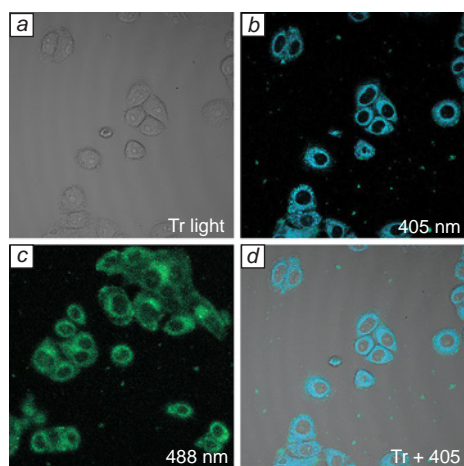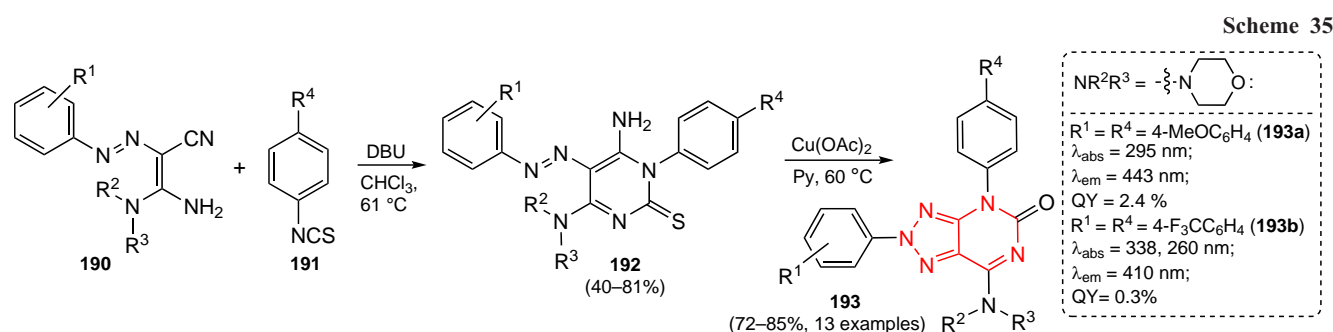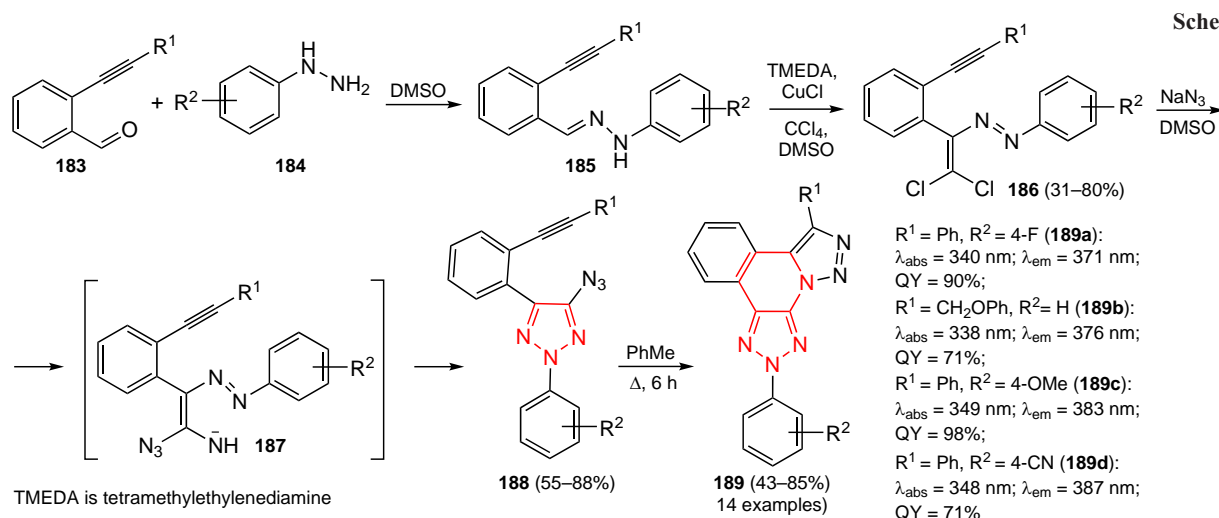

Figure 32. Photographs of the fluorescence of compounds **182** in MeCN (*1 – 3*) and in MeCN containing DNT (*4 – 6*) under daylight (*a*) and after light irradiation at $\lambda_{ex} = 376$ nm (*b*). Reproduced from Verbitsky *et al*.[76] with permission from the Royal Society of Chemistry.

azidation (**187**), and intramolecular cyclization of azide **188** afforded the target bitriazoles **189** in 43 – 85% yield. Heterocyclic compounds of this series have two triazole rings in the molecule. These fluorophores absorb in the 312 – 348 nm range and emit in the blue region from 370 to 390 nm; the quantum yields are up to 98%.

Belskaya, Benassi, and co-workers[78] developed a two-step method for the synthesis of triazolopyrimidines (Scheme 35). Pyrimidines **192** were prepared by the reaction of compounds **190** with isothiocyanates **191** in the presence of 1,8-diazabicyclo[5.4.0]undec-7-ene (DBU) on heating. The subsequent cyclization in the presence of copper acetate gave compounds **193a–l** in up to 85% yields. Note that the reaction was accompanied by hydrolysis of the thiocarbonyl group to carbonyl group. The resulting fluorophores **193** showed emission in the blue spectral region (from 400 to 443 nm) and a Stokes shift of up to 26015 cm^{-1}; the quantum yields reached 39%. According to the next study,[79] these compounds exhibit acidochromism and chemosensory properties for the detection of HCl vapour. In addition, they were found to stain all cell organelles except the nucleus and, hence, they can be considered as fluorescent dyes for bioimaging (Fig. 33).

The research group headed by Yu and Lu[80] reported a synthesis of triazolopyridines (Scheme 36). The key intermediate **195** was prepared by cyclization of compound **194** induced by sodium nitrite in acetic acid. This intermediate then reacted with various alkyl halides in the presence of potassium carbonate to form 2*H*-functionalized triazolopyridines **196**, which were subjected to the Stille reaction with stannane **197** to give products **198** in moderate to high yields. Fluorophores **198** have quantum yields of 80 to 89% in solutions and 26% in powders.

I.A.Lavrinchenko, T.D.Moseev, M.V.Varaksin, V.N.Charushin, O.N.Chupakhin
Russ. Chem. Rev., 2024, **93** (10) RCR5130

29 of 34

Scheme 34

R[1] = Ph, R[2] = 4-F (**189a**):
λ_{abs} = 340 nm; λ_{em} = 371 nm;
QY = 90%;
R[1] = CH$_2$OPh, R[2]= H (**189b**):
λ_{abs} = 338 nm; λ_{em} = 376 nm;
QY = 71%;
R[1] = Ph, R[2] = 4-OMe (**189c**):
λ_{abs} = 349 nm; λ_{em} = 383 nm;
QY = 98%;
R[1] = Ph, R[2] = 4-CN (**189d**):
λ_{abs} = 348 nm; λ_{em} = 387 nm;
QY = 71%

TMEDA is tetramethylethylenediamine

188 (55–88%)

189 (43–85%)
14 examples

Scheme 35

NR[2]R[3] = morpholine:

R[1] = R[4] = 4-MeOC$_6$H$_4$ (**193a**)
λ_{abs} = 295 nm;
λ_{em} = 443 nm;
QY = 2.4 %
R[1] = R[4] = 4-F$_3$CC$_6$H$_4$ (**193b**)
λ_{abs} = 338, 260 nm;
λ_{em} = 410 nm;
QY= 0.3%

192
(40–81%)

193
(72–85%, 13 examples)

Figure 33. Confocal fluorescence microscopy images of HeLa cells incubated with compound **193a** in PBS at 37 °C for 0.5 h: light-field image (*a*); at λ_{ex} = 405 nm with a 405–430 nm filter (*b*); at λ_{ex} = 488 nm with a 488–600 nm filter (*c*); overlay of images (*d*). Reproduced from Belskaya and co-workers[79] with permission from Wiley.
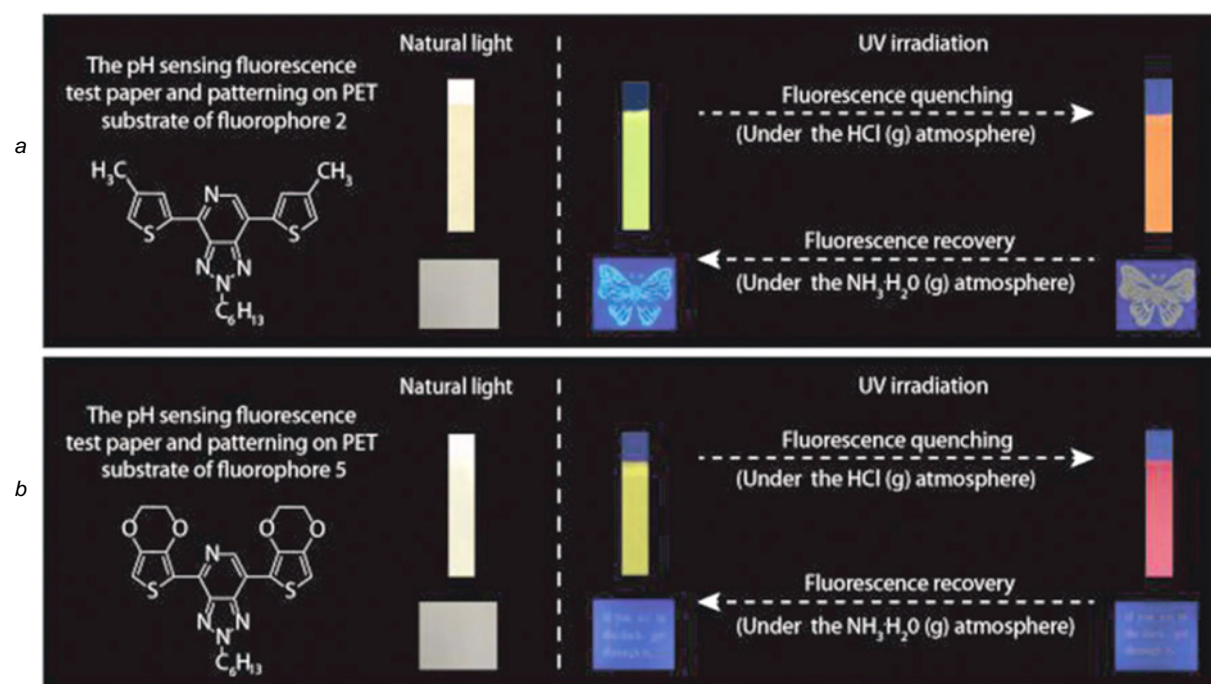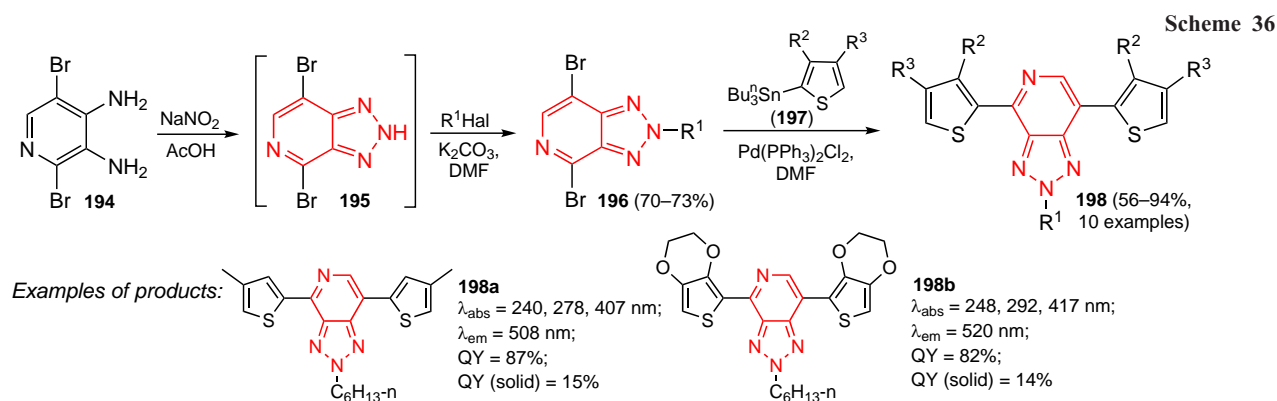
Their chemosensory properties for pH determination from 4 to 7 were found: in particular, in acidic solutions, a blue shift of emission is observed in the electronic spectra, while in alkaline solutions, a red shift takes place. The authors manufactured paper strips for pH measurement that can be used to analyze the quality of water or the content of hydrogen chloride in air (Fig. 34).

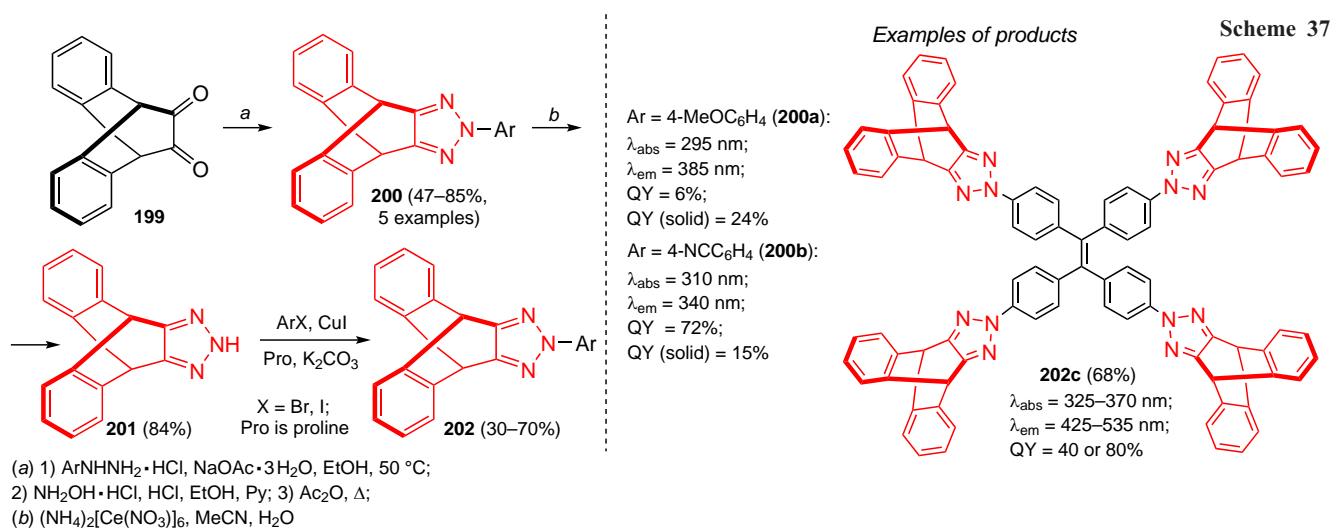Lee and co-workers[81] obtained fluorophores combining the 1,2,3-triazole moieties and an iptycene cage in the molecule (Scheme 37). The iptycene type dicarbonyl starting compound **199** was allowed to react, first, with arylhydrazine and then with hydroxylamine and acetic anhydride to give triazoles **200**. To study the effect of various substituents at the N(2) atom, the authors dearylated triazole **201** by the oxidation with cerium(IV) ammonium nitrate (CAN) in high yield and conducted the copper(I)-catalyzed reaction with aryl halides. Products **202** showed absorption up to 280 nm in the spectrum; the emission intensity peaked in the range from 340 to 495 nm, while the quantum yields reached 72% in solution and 24% in the solid state. Kim *et al.*[82] synthesized tetrasubstituted iptycene triazole derivative **202c**, containing a tetraphenylethylene moiety that absorbed photons in the 325–370 nm range and exhibited mechanoluminescence in the 425–535 nm range. The quantum yields were above 40% in the usual state and 80% after the mechanical treatment (Fig. 35).
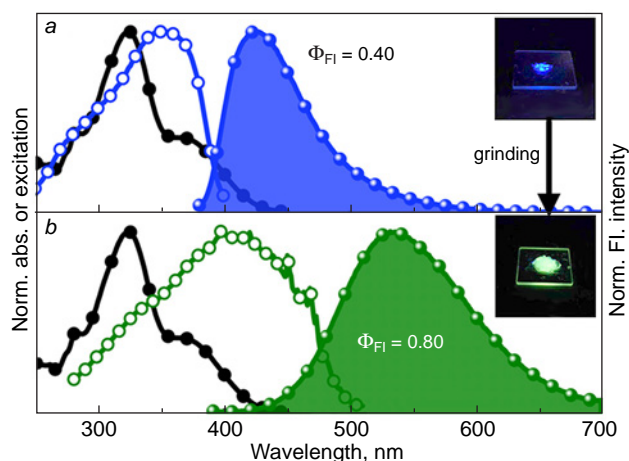
The research group headed by Aprahamian[83] proposed a method for the synthesis of a chemosensor based on pyridine-fused 1,2,3-triazole (Scheme 38). The first step was the preparation of the diazonium salt from *para*-methoxyaniline **203**, the azo coupling of which with pyridine derivative **204** gave intermediate **205**. The subsequent oxidative cyclization resulted in triazole **206** in a moderate yield. This compound absorbs at 365 nm and emits at 400 nm. In the presence of cyanide anions, the emission intensity of product **206** sharply increases, and an additional peak at 504 nm appears in the emission spectrum due to ring opening and formation of 2-functionalized 1,2,3-triazole **207**.

The research group of Shi and Li[84] synthesized fluorophores based on triazapentalene zwitter-ions (Scheme 39). The synthesis was based on gold-catalyzed intramolecular condensation of triazoles **208** containing a triple bond in the side

Scheme 36

Examples of products:

198a
λ_{abs} = 240, 278, 407 nm;
λ_{em} = 508 nm;
QY = 87%;
QY (solid) = 15%

198b
λ_{abs} = 248, 292, 417 nm;
λ_{em} = 520 nm;
QY = 82%;
QY (solid) = 14%

Figure 34. Fluorescent paper strips for the detection of acids in the presence of compounds **198a** (*a*) and **198b** (*b*). Reproduced from Lu and co-workers[80] with permission from the Royal Society of Chemistry.

Scheme 37

Examples of products

Ar = 4-MeOC$_6$H$_4$ (**200a**):
λ_{abs} = 295 nm;
λ_{em} = 385 nm;
QY = 6%;
QY (solid) = 24%

Ar = 4-NCC$_6$H$_4$ (**200b**):
λ_{abs} = 310 nm;
λ_{em} = 340 nm;
QY = 72%;
QY (solid) = 15%

202c (68%)
λ_{abs} = 325–370 nm;
λ_{em} = 425–535 nm;
QY = 40 or 80%

199

200 (47–85%, 5 examples)

201 (84%)

ArX, CuI
Pro, K$_2$CO$_3$

X = Br, I;
Pro is proline

202 (30–70%)

(*a*) 1) ArNHNH$_2$·HCl, NaOAc·3H$_2$O, EtOH, 50 °C;
2) NH$_2$OH·HCl, HCl, EtOH, Py; 3) Ac$_2$O, Δ;
(*b*) (NH$_4$)$_2$[Ce(NO$_3$)]$_6$, MeCN, H$_2$O

I.A.Lavrinchenko, T.D.Moseev, M.V.Varaksin, V.N.Charushin, O.N.Chupakhin
Russ. Chem. Rev., 2024, **93** (10) RCR5130

31 of 34

Figure 35. Normalized absorption spectra (black curve with black circles) in $CHCl_3$ ($C = 10$ mM), excitation spectra for the powders (blue curve with light circles), and fluorescence spectra (green curve with filled circles) for compound **202c** in the usual state (*a*) and after mechanical treatment (*b*). $\lambda_{ex} = 370$ nm. Reproduced from Kim *et al.*[82] with permission from the Royal Society of Chemistry.

Scheme 38

Scheme 39
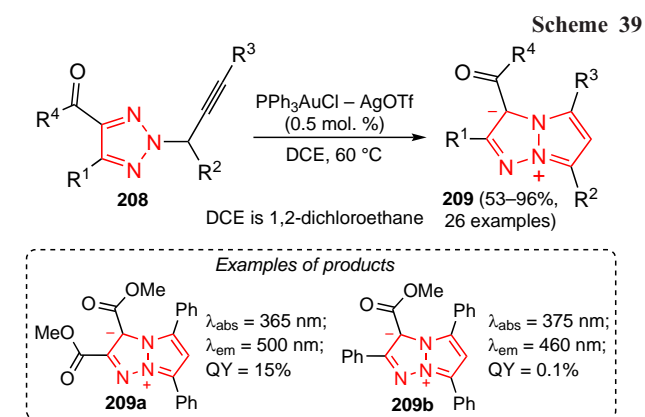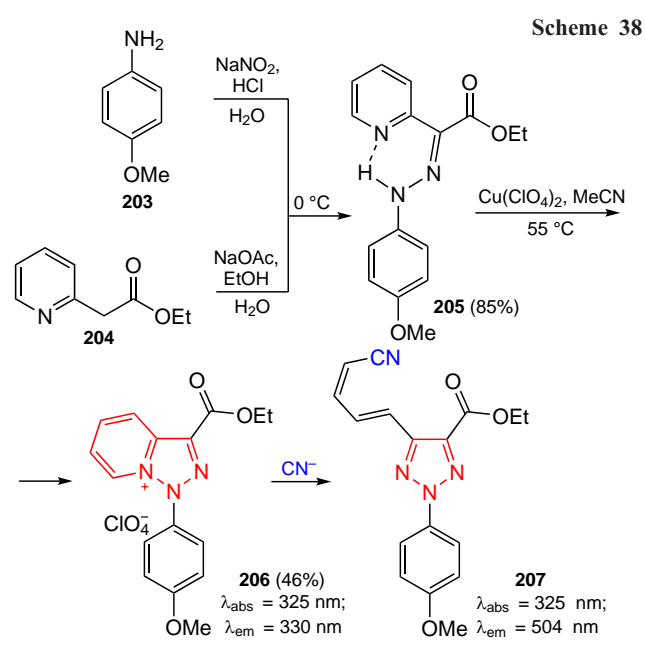
chain. The target products **209** were formed in moderate to almost quantitative yields. These fluorophores show emission in the $450 - 500$ nm range; the quantum yields of materials with two ester groups reach 15%, while in the case of one ester group, they do not exceed 1%.

Thus, this Section addresses methods for the synthesis and luminescent properties of heteroanullated and miscellaneous 2*H*-1,2,3-triazole derivatives. The synthesized compounds can be used as chemosensors for pH determination, detection of nitroaromatic compounds and acids, as well as dyes for bioimaging applications. A relatively small number of methods for the synthesis of compounds of this class have been reported in the literature; therefore, their practically useful properties have not been adequately studied and, hence, further studies are needed to find new applications for these derivatives.

6. Conclusion

This literature review describes and systematizes methods for the synthesis of 2*H*-functionalized 1,2,3-triazoles and their (hetero)annulated analogues, as well as photophysical characteristics of these compounds and discusses their possible practical applications. The photoactive molecules of this class find applications as chemosensors, organic light-emitting diodes, compounds for bioimaging, and agents for photodynamic therapy.

Among the title compounds, benzannulated 1,2,3-triazoles have been studied most comprehensively. Most often, they are synthesized using a combined approach consisting of the assembly of the benzannulated ring and further functionalization *via* cross-coupling reactions of various types. Quite a few functional polymers have been obtained on the basis of these compounds and prototypes of molecular electronic devices have been designed. It is worth noting that the use of only these derivatives as ligands for second-generation phosphorescent organic light-emitting diodes is known to date.

Meanwhile, 2*H*-functionalized 1,2,3-triazoles and their heteroannulated analogues have not been comprehensively studied. The emission of these triazoles extends up to the red spectral region and the quantum yields are high; however, there are only a few examples of their application as working elements of various devices. Non-fused 1,2,3-triazoles are prepared using two major methods: azide – alkyne cycloaddition followed by functionalization *via* cross-coupling reactions of various types and assembly of the heterocyclic nucleus *via* cyclization. The heteroannulated derivatives are prepared, most often, by oxidative cyclization of the corresponding molecular ensembles.

Thus, 2*H*-functionalized 1,2,3-triazoles represent a promising platform for the design of optical functional materials. Certain advances in this field have been made in recent years and active research is in progress. In the future, one can expect that these compounds would underlie the design of new organic semiconductors, rectifiers, and other components of the existing and future organic electronics, as well as dyes for bioimaging, probes, and chemosensors for the environmental monitoring and for detection of various analytes in bio-objects (cell organelles and biological fluids).

7. List of abbreviations and symbols

The following abbreviations and symbols were used in the review:

ε — molar absorption coefficient;
λ_{abs} — absorption wavelength;
λ_{em} — emission wavelength;
λ_{ex} — excitation wavelength;
λ_{pl} — photoluminescence wavelength;
τ — switching time to another form;
F — fluorescence intensity;
f_w — fraction of water in the mixture;
J — current density;
J_d — dark current density;
T_{dec} — decomposition temperature;
T — contrast ratio;
V — voltage;
V_{oc} — open circuit voltage;
A — electron-withdrawing moiety;
acac — acetylacetonate;
AcH — 9,9-dimethyl-9,10-dihydroacridine;
AIE — aggregation-induced emission;
All — allyl;
Aq336 — methyltrioctylammonium chloride;
BODIPY — BF$_2$ dipyrromethene;
B$_2$Pin$_2$ — bis(pinacolato)diboron;
CAN — cerium(IV) ammonium nitrate;
CBP — 4,4′-bis(*N*-carbazolyl)-1,1′-biphenyl;
Cy — cyclohexyl;
D — electron-donating moiety;
DBU — 1,8-diazabicyclo[5.4.0]undec-7-ene;
DCE — dichloroethane;
DCM — dichloromethane;
DDQ — 2,3-dichloro-5,6-dicyano-1,4-benzoquinone;
DEAD — diethyl azodicarboxylate;
DIPA — diisopropylamine;
DIPEA — diisopropylethylamine;
DMA — dimethylacetamide;
DNT — 2,4-dinitrotoluene;
dppf — 1,1′-bis(diphenylphosphino)ferrocene;
EQE — external quantum efficiency;
HBTU — benzotriazol-2-yltetramethyluronium hexafluorophosphate;
H&E — eosin;
Herrmann's catalyst — *trans*-di(acetate)bis[*o*-(di-*o*-tolylphosphino)benzyl]dipalladium(II);
ICG — indocyanine green;
Lawesson's reagent — 2,4-bis(4-methoxyphenyl)-1,3,2,4-dithiadiphosphetane 2,4-disulfide;
LDA — lithium diisopropylamide;
LOD — limit of detection;
MW — microwave radiation;
NBS — *N*-bromosuccinimide;
NIR-II — near-IR range;
NIS — *N*-iodosuccinimide;
NPs — nanoparticles;
NuH — nucleophile;
OFET — organic field-effect transistor,
OLED — organic light-emitting diode;
OPD — organic photodetectors;
PBS — phosphate-buffered saline;
PCC — pyridinium chlorochromate;
PCE — power conversion efficiency;
PEA — phenylethylamine;

POH — phenoxazine;
PIDA — phenyliodine(III) diacetate, di(acetoxy)-iodobenzene;
Piv — pivaloyl;
PLED — polymer light-emitting diodes;
PV$_{fill\ factor}$ — fill factor for organic photovoltaics;
Pro — proline;
PTC — phase transfer catalyst;
Py — pyridine;
QY — quantum yield;
rt — room temperature;
tAcH — 2,7-di-*tert*-butyl-9,9-dimethyl-9,10-dihydroacridine;
TBS — *tert*-butyldimethylsilyl;
TEA — triethylamine;
TFA — trifluoroacetic acid;
TMEDA — tetramethylethylenediamine;
TMS — trimethylsilyl;
TNT — trinitrotoluene;
TPAP — tris(4-methoxyphenyl)phosphine;
Tris — tris(hydroxymethyl)aminomethane;
TUNEL — terminal deoxynucleotidyl transferase dUTP nick end labelling.

8. References

1. V.S.Padalkar, S.K.Lanke, S.B.Chemate, N.Sekar. *J. Fluoresc.*, **25**, 985 (2015); https://doi.org/10.1007/s10895-015-1580-7
2. Q.Shen, S.Wang, N.-D.Yang, C.Zhang, Q.Wu, C.Yu. *J. Luminesc.*, **225**, 117338 (2020); https://doi.org/10.1016/j.jlumin.2020.117338
3. Q.Zheng, M.F.Juette, S.Jockusch, M.R.Wasserman, Z.Zhou, R.B.Altman, S.C.Blanchard. *Chem. Soc. Rev.*, **43**, 1044 (2014); https://doi.org/10.1039/C3CS60237K
4. Y.Yang, F.Gao, Y.Wang, H.Li, J.Zhang, Z.Sun, Y.Jiang. *Molecules*, **27**, 8421 (2022); https://doi.org/10.3390/molecules27238421
5. S.-J.Zou, Y.Shen, F.-M.Xie, J.-D.Chen, Y.-Q.Li, J.-X.Tang. *Mater. Chem. Front.*, **4**, 788 (2020); https://doi.org/10.1039/C9QM00716D
6. V.I.Martynov, A.A.Pakhomov. *Russ. Chem. Rev.*, **90**, 1213 (2021); https://doi.org/10.1070/RCR4985
7. R.Misra, S.P.Bhattacharyya. In *Intramolecular Charge Transfer: Theory and Applications*. (Weinheim: Wiley-VCH, 2018). P. 243; https://doi.org/10.1002/9783527801916
8. S.A.Khan, M.J.Akhtar, U.Gogoi, D.U.Meenakshi, A.Das. *Pharmaceuticals*, **16**, 179 (2023); https://doi.org/10.3390/ph16020179
9. S.Rachwal, A.R.Katritzky. In *Comprehensive Heterocyclic Chemistry III*. (Amsterdam: Elsevier, 2008). P. 1; https://doi.org/10.1016/B978-008044992-0.00501-0
10. M.P.Schmidt, A.Hagenbocker. *Ber. Dtsch. Chem. Ges., Ser. B*, **54**, 2191 (1921); https://doi.org/10.1002/cber.19210540903
11. M.Watkinson. In *Click Triazoles*. (Ed. J.Košmrlj). (*Ser. Topics in Heterocyclic Chemistry*. Vol. 28). (Berlin, Heidelberg: Springer, 2012). P. 109; https://doi.org/10.1007/7081_2011_69
12. B.Schulze, U.S.Schubert. *Chem. Soc. Rev.*, **43**, 2522 (2014); https://doi.org/10.1039/C3CS60386E
13. C.Kok, C.Doyranli, B.Canimkurbey, S.P.Mucur, S.Koyuncu. *RSC Adv.*, **10**, 18639 (2020); https://doi.org/10.1039/D0RA02527E
14. N.Ma, Y.Wang, B.Zhao, W.Ye, S.Jiang. *Drug Des. Devel. Ther.*, **1585** (2015); https://doi.org/10.2147/DDDT.S56038
15. F.de Carvalho da Silva, M.F.do C.Cardoso, P.G.Ferreira, V.F.Ferreira. In *Chemistry of 1,2,3-Triazoles*. (Eds W.Dehaen, V.Bakulev). (*Ser. Topics in Heterocyclic Chemistry*. Vol. 40). (Cham: Springer, 2014). P. 117; https://doi.org/10.1007/7081_2014_124

I.A.Lavrinchenko, T.D.Moseev, M.V.Varaksin, V.N.Charushin, O.N.Chupakhin
Russ. Chem. Rev., 2024, **93** (10) RCR5130

33 of 34

16. R.O.M.A.D.Souza, L.S.D.M.E.Miranda. *An. Acad. Bras. Cienc.*, **91**, e20180751 (2019); https://doi.org/10.1590/0001-3765201820180751

17. J.Dai, S.Tian, X.Yang, Z.Liu. *Front. Chem.*, **10** (2022); https://doi.org/10.3389/fchem.2022.891484

18. M.J.Vaishnani, S.Bijani, M.Rahamathulla, L.Baldaniya, V.Jain, K.Y.Thajudeen, M.M.Ahmed, S.A.Farhana, I.Pasha. *Green Chem. Lett. Rev.*, **17** (2024); https://doi.org/10.1080/17518253.2024.2307989

19. J.S.S.Neto, G.Zeni. *Coord. Chem. Rev.*, **409**, 213217 (2020); https://doi.org/10.1016/j.ccr.2020.213217

20. S.Kumar, S.L.Khokra, A.Yadav. *Fut. J. Pharm. Sci.*, **7**, 106, (2021); https://doi.org/10.1186/s43094-021-00241-3

21. H.Sachdeva, M.Saquib, K.Tanwar. *Anticancer Agents Med. Chem.*, **22**, 3269 (2022); https://doi.org/10.2174/1871520622666220412133112

22. V.Ram, A.Sethi, M.Nath, R.Pratap. In *Chemistry of Heterocycles: Nomenclature and Chemistry of Three-to-Five Membered Heterocycles*. (Amsterdam: Elsevier, 2019). 489 p.; https://doi.org/10.1016/C2015-0-05990-1

23. A.R.Katritzky, C.W.Rees. In *Comprehensive Heterocyclic Chemistry Reference Work*. (New York: Pergamon, 1984). 731 p.; https://doi.org/10.1016/B978-008096519-2.00001-1

24. K.D.Gavlik, E.S.Sukhorukova, Y.M.Shafran, P.A.Slepukhin, E.Benassi, N.P.Belskaya. *Dyes Pigments*, **136**, 229 (2017); https://doi.org/10.1016/j.dyepig.2016.08.015

25. N.E.Safronov, T.O.Fomin, A.S.Minin, L.Todorov, I.Kostova, E.Benassi, N.P.Belskaya. *Dyes Pigments*, **178**, 108343 (2020); https://doi.org/10.1016/j.dyepig.2020.108343

26. N.E.Safronov, I.P.Kostova, M.A.Palafox, N.P.Belskaya. *Int. J. Mol. Sci.*, **24**, 8947 (2023); https://doi.org/10.3390/ijms24108947

27. N.E.Safronov, A.S.Minin, P.A.Slepukhin, I.P.Kostova, E.Benassi, N.P.Belskaya. *Spectrochim. Acta Part A*, **292**, 122419 (2023); https://doi.org/10.1016/j.saa.2023.122419

28. H.Kim, Y.Lee, H.Lee, J.-I.Hong, D.Lee. *ACS Appl. Mater. Interfaces*, **13**, 12286 (2021); https://doi.org/10.1021/acsami.1c00278

29. Q.Lai, Q.Liu, K.Zhao, C.Shan, L.Wojtas, Q.Zheng, X.Shi, Z.Song. *Chem. Commun.*, **55**, 4603 (2019); https://doi.org/10.1039/C9CC00262F

30. Q.Lai, Q.Liu, Y.He, K.Zhao, C.Wei, L.Wojtas, X.Shi, Z.Song. *Org. Biomol. Chem.*, **16**, 7801 (2018); https://doi.org/10.1039/C8OB02482K

31. W.Yan, Q.Wang, Q.Lin, M.Li, J.L.Petersen, X.Shi. *Chem. – Eur. J.*, **17**, 5011 (2011); https://doi.org/10.1002/chem.201002937

32. V.A.Motornov, A.A.Tabolin, R.A.Novikov, N.E.Shepel, V.G.Nenajdenko, S.L.Ioffe. *Tetrahedron*, **74**, 3897 (2018); https://doi.org/10.1016/j.tet.2018.05.071

33. B.Szemenyei, M.Malmosi, D.Pál, P.Baranyai, L.Drahos, I.Móczár, P.Huszthy. *New J. Chem.*, **45**, 22639 (2021); https://doi.org/10.1039/D1NJ04173H

34. Y.-C.Zhang, R.Jin, L.-Y.Li, Z.Chen, L.-M.Fu. *Molecules*, **22**, 1380 (2017); https://doi.org/10.3390/molecules22091380

35. J.Li, G.Ding, Y.Niu, L.Wu, H.Feng, W.He. *Spectrochim. Acta, Part A*, **200**, 127 (2018); https://doi.org/10.1016/j.saa.2018.04.009

36. I.A.Lavrinchenko, T.D.Moseev, Y.A.Seleznev, M.V.Varaksin, A.N.Tsmokaluk, V.N.Charushin, O.N.Chupakhin. *Asian J. Org. Chem.*, **12**, e202300008 (2023); https://doi.org/10.1002/ajoc.202300008

37. I.A.Lavrinchenko, T.D.Moseev, M.V.Varaksin, Y.A.Seleznev, L.K.Sadieva, G.V.Zyryanov, A.N.Tsmokaluk, V.N.Charushin, O.N.Chupakhin. *Dokl. Chem.*, **512**, 232 (2023); https://doi.org/10.1134/S0012500823600682

38. M.Ichikawa, S.Mochizuki, H.-G.Jeon, S.Hayashi, N.Yokoyama, Y.Taniguchi. *J. Mater. Chem.*, **21**, 11791 (2011); https://doi.org/10.1039/C1JM10901D

39. V.B.Bojinov, I.P.Panova. *Dyes Pigments*, **80**, 61 (2009); https://doi.org/10.1016/j.dyepig.2008.05.007

40. V.B.Bojinov, I.K.Grabchev. *J. Photochem. Photobiol. A: Chem.*, **172**, 308 (2005); https://doi.org/10.1016/j.jphotochem.2004.12.020

41. V.B.Bojinov, I.P.Panova, J.-M.Chovelon. *Sens. Actuators B: Chem.*, **135**, 172 (2008); https://doi.org/10.1016/j.snb.2008.08.016

42. T.Uesaka, T.Ishitani, T.Shimeno, N.Suzuki, S.Yagi, T.Maeda. *RSC Adv.*, **12**, 17350 (2022); https://doi.org/10.1039/D2RA02028A

43. M.-H.Liu, T.-C.Chen, J.R.Vicente, C.-N.Yao, Y.-C.Yang, C.-P.Chen, P.-W.Lin, Y.-C.Ho, J.Chen, S.-Y.Lin, Y.-H.Chan. *ACS Appl. Bio Mater.*, **3**, 3846 (2020); https://doi.org/10.1021/acsabm.0c00417

44. G.T.Dempsey, J.C.Vaughan, K.H.Chen, M.Bates, X.Zhuang. *Nat. Methods*, **8**, 1027 (2011); https://doi.org/10.1038/nmeth.1768

45. J.L.Banal, J.Subbiah, H.Graham, J.-K.Lee, K.P.Ghiggino, W.W.H.Wong. *Polym. Chem.*, 1077 (2013); https://doi.org/10.1039/C2PY20850D

46. F.Pan, C.Sun, H.Bin, I.Angunawela, W.Lai, L.Meng, H.Ade, Y.Li. *Org. Electron.*, **78**, 105603 (2020); https://doi.org/10.1016/j.orgel.2019.105603

47. D.Han, J.Li, Q.Zhang, Z.He, Z.Wu, J.Chu, Y.Lu. *Polymers*, **13**, 254 (2021); https://doi.org/10.3390/polym13020254

48. L.Gao, J.Xu, H.Luo, H.Lei, X.Chen, J.Wan, J.Feng, K.Liu. *J. Fluoresc.*, **33**, 1577 (2023); https://doi.org/10.1007/s10895-023-03164-9

49. H.Luo, J.Xu, X.Chen, J.Wan, H.Lei, Y.Chen, J.Feng, K.Liu. *J. Polym. Sci.*, **62**, 200 (2024); https://doi.org/10.1002/pol.20230552

50. H.Xie, Z.Bi, J.Yin, Z.Li, L.Hu, C.Zhang, J.Zhang, J.W.Y.Lam, P.Zhang, R.T.K.Kwok, K.Li, B.Z.Tang. *ACS Nano*, **17**, 4591 (2023); https://doi.org/10.1021/acsnano.2c10661

51. X.Zhou, K.Zhang, C.Yang, Y.Pei, L.Zhao, X.Kang, Z.Li, F.Li, Y.Qin, L.Wu. *Adv. Funct. Mater.*, **32**, 2109929 (2022); https://doi.org/10.1002/adfm.202109929

52. Z.Wang, X.Wu, H.Li, J.Yu, Y.Wang, P.Lu. *Chem. – Asian J.*, **18**, e202201230 (2023); https://doi.org/10.1002/asia.202201230

53. F.Hou, X.Liu, X.Hao, G.Li, F.Lu, Q.Deng. *Dyes Pigments*, **195**, 109667 (2021); https://doi.org/10.1016/j.dyepig.2021.109667

54. Y.Zhang, Y.Yu, X.Liu, J.Miao, Y.Han, J.Liu, L.Wang. *Adv. Mater.*, **35**, (2023); https://doi.org/10.1002/adma.202211714

55. C.H.T.Nguyen, T.H.Nguyen, T.P.L.Nguyen, H.Le Tran, T.H.Luu, C.D.Tran, Q.-T.Nguyen, L.-T.T.Nguyen, T.Yokozawa, H.T.Nguyen. *Dyes Pigments*, **219**, 111613 (2023); https://doi.org/10.1016/j.dyepig.2023.111613

56. G.Hızalan, A.Balan, D.Baran, L.Toppare. *J. Mater. Chem.*, **21**, 1804 (2011); https://doi.org/10.1039/C0JM03000G

57. C.P.Sen, R.G.Shrestha, L.K.Shrestha, K.Ariga, S.Valiyaveettil. *Chem. – Eur. J.*, **21**, 17344 (2015); https://doi.org/10.1002/chem.201502939

58. Ş.C.Cevher, D.Keles, G.Hizalan, L.Toppare, A.Cirpan. *Synth. Met.*, **244**, 1 (2018); https://doi.org/10.1016/j.synthmet.2018.06.007

59. Q.Li, Z.Wang, W.Song, H.Ma, J.Dong, Y.-Y.Quan, X.Ye, Z.-S.Huang. *Dyes Pigments*, **161**, 389 (2019); https://doi.org/10.1016/j.dyepig.2018.09.074

60. B.P.Dash, I.Hamilton, D.J.Tate, D.L.Crossley, J.-S.Kim, M.J.Ingleson, M.L.Turner. *J. Mater. Chem. C*, **7**, 718 (2019); https://doi.org/10.1039/C8TC05131C

61. N.Venkatesan, V.Singh, P.Rajakumar, A.-k.Mishra. *RSC Adv.*, **4**, 53484 (2014); https://doi.org/10.1039/C4RA06320A

62. E.Ahmmed, S.Lohar, S.Ghatak, S.K.Hira, P.P.Manna, P.Chattopadhyay. *Anal. Methods*, **11**, 2415 (2019); https://doi.org/10.1039/C9AY00325H

63. A.S.Ortega-Villarreal, E.Hernández-Fernández, C.Jensen, G.A.Valdivia-Berroeta, S.Garrard, I.López, S.J.Smith, K.A.Christensen, M.A.Reyes-González, D.J.Michaelis.

34 of 34

I.A.Lavrinchenko, T.D.Moseev, M.V.Varaksin, V.N.Charushin, O.N.Chupakhin
Russ. Chem. Rev., 2024, **93** (10) RCR5130

RSC Adv., **9**, 8759 (2019);
https://doi.org/10.1039/C9RA00108E

64. T.Malinauskas, M.Daskeviciene, K.Kazlauskas, H.-C.Su,
J.V.Grazulevicius, S.Jursenas, C.-C.Wu, V.Getautis.
Tetrahedron, **67**, 1852 (2011);
https://doi.org/10.1016/j.tet.2011.01.026

65. J.Yu, M.Li, C.Xu, F.Meng, J.Cao, H.Tan, W.Zhu. *Dalton
Trans.*, **49**, 8785 (2020); https://doi.org/10.1039/D0DT01415J

66. J.Yu, H.Tan, F.Meng, K.Lv, W.Zhu, S.Su. *Dyes Pigments*,
131, 231 (2016); https://doi.org/10.1016/j.dyepig.2016.04.021

67. J.Yu, C.Xu, F.Meng, H.Tan, M.Li, W.Zhu. *Dyes Pigments*,
166, 307 (2019); https://doi.org/10.1016/j.dyepig.2019.03.047

68. J.M.Ha, S.H.Hur, A.Pathak, J.-E.Jeong, H.Y.Woo. *NPG Asia
Mater.*, **13**, 53 (2021);
https://doi.org/10.1038/s41427-021-00318-8

69. A.S.Kostyuchenko, E.B.Uliankin, A.J.Stasyuk,
T.Y.Zheleznova, A.S.Fisyuk. *J. Org. Chem.*, **88**, 5875 (2023);
https://doi.org/10.1021/acs.joc.3c00286

70. B.G.Park, D.H.Hong, H.Y.Lee, M.Lee, D.Lee. *Chem. – Eur. J.*,
22, 6610 (2016); https://doi.org/10.1002/chem.201600318

71. Y.Lv, L.Zhu, H.Liu, Y.Wu, Z.Chen, H.Fu, Z.Tian. *Anal. Chim.
Acta*, **839**, 74 (2014); https://doi.org/10.1016/j.aca.2014.06.010

72. V.S.Padalkar, S.B.Chemate, S.K.Lanke, N.Sekar. *J. Luminesc.*,
168, 114 (2015); https://doi.org/10.1016/j.jlumin.2015.07.051

73. A.M.F.Oliveira-Campos, L.M.Rodrigues, A.P.Esteves,
M.E.Silva, A.Sivasubramanian, R.Hrdina, G.M.B.Soares,
T.A.D.Pinto, O.Machalicky. *Dyes Pigments*, **87**, 188 (2010);
https://doi.org/10.1016/j.dyepig.2010.03.025

74. V.V.Fedotov, E.N.Ulomsky, N.P.Belskaya, A.K.Eltyshev,
K.V.Savateev, E.K.Voinkov, D.N.Lyapustin, V.L.Rusinov.
J. Org. Chem., **86**, 8319 (2021);
https://doi.org/10.1021/acs.joc.1c00760

75. O.S.Taniya, V.V.Fedotov, A.S.Novikov, L.K.Sadieva,
A.P.Krinochkin, I.S.Kovalev, D.S.Kopchuk, G.V.Zyryanov,
Y.Liu, E.N.Ulomsky, V.L.Rusinov, V.N.Charushin.
Dyes Pigments, **204**, 110405 (2022);
https://doi.org/10.1016/j.dyepig.2022.110405

76. E.V.Verbitskiy, E.B.Gorbunov, A.A.Baranova, K.I.Lugovik,
K.O.Khokhlov, E.M.Cheprakova, G.A.Kim, G.L.Rusinov,
O.N.Chupakhin, V.N.Charushin. *Tetrahedron*, **72**, 4954
(2016); https://doi.org/10.1016/j.tet.2016.06.071

77. B.Tsyrenova, V.Khrustalev, V.Nenajdenko. *J. Org. Chem.*, **85**,
7024 (2020); https://doi.org/10.1021/acs.joc.0c00263

78. A.K.Eltyshev, P.O.Suntsova, K.D.Karmatskaia, O.S.Taniya,
P.A.Slepukhin, E.Benassi, N.P.Belskaya. *Org. Biomol. Chem.*,
16, 9420 (2018); https://doi.org/10.1039/C8OB02644K

79. A.K.Eltyshev, A.S.Minin, L.T.Smoliuk, E.Benassi,
N.P.Belskaya. *Eur. J. Org. Chem.*, 316 (2020);
https://doi.org/10.1002/ejoc.201901582

80. N.Jian, K.Qu, H.Gu, L.Zou, X.Liu, F.Hu, J.Xu, Y.Yu, B.Lu.
Phys. Chem. Chem. Phys., **21**, 7174 (2019);
https://doi.org/10.1039/C9CP00672A

81. T.Kang, H.Kim, D.Lee. *Org. Lett.*, **19**, 6380 (2017);
https://doi.org/10.1021/acs.orglett.7b03239

82. H.Kim, H.Yoo, J.Y.Kim, D.Lee. *J. Mater. Chem. C*, **11**, 12933
(2023); https://doi.org/10.1039/D3TC01826A

83. T.F.Robbins, H.Qian, X.Su, R.P.Hughes, I.Aprahamian. *Org.
Lett.*, **15**, 2386 (2013); https://doi.org/10.1021/ol4008298

84. R.Cai, D.Wang, Y.Chen, W.Yan, N.R.Geise, S.Sharma, H.Li,
J.L.Petersen, M.Li, X.Shi. *Chem. Commun.*, **50**, 7303 (2014);
https://doi.org/10.1039/C4CC03175J